Thesis for the Degree of Doctor of Philosophy

# Drug metabolism system associated with the exposure of benzo[a]pyrene and trichlorfon in rockfish (*Sebastes schlegelii*)



by

Soo Ji Woo

Department of Aquatic Life Medicine

The Graduate School

Pukyong National University

February, 2019

# Drug metabolism system associated with the exposure of benzo[a]pyrene and trichlorfon in rockfish (*Sebastes schlegelii*)

# (Benzo[a]pyrene 과 trichlorfon 노출을 통한 조피볼락의 약물대사 특성 연구)

Advisor: Prof. Joon Ki Chung

by

Soo Ji Woo

A thesis submitted in partial fulfillment of the requirements

for the degree of

Doctor of Philosophy

in Department of Aquatic Life Medicine, The Graduate School,

Pukyong National University

February 2019

Drug metabolism system associated with the exposure of benzo[a]pyrene and trichlorfon in rockfish (*Sebastes schlegelii*)

A dissertation

by

Soo Ji Woo

Approved by:


_____

(Chairman) Hyung Ho Lee

_____ _____

(Member) Kim Do Hyung (Member) Kwan Ha Park

_____ _____

(Member) Sung Hee Jung (Member) Joon Ki Chung

February 22, 2019

# CONTENTS

# CHAPTER III

## Evaluation of pharmacokinetic effect in trichlorfon from *Sebastes schlegelii* ---------- 78

# Benzo[a]pyrene 과 trichlorfon 노출을 통한 조피볼락의 약물대사 특성 연구

우 수 지

부 경 대 학 교 대 학 원 수 산 생 명 의 학 과

## 요 약

Cytochrome P450 (CYP)는 대부분의 약물이나 환경물질들 등의 다양한 외인성 물질 또는 스테로이드나 지질 등의 내인성 물질에 대해 Phase I 산화적 대사 작용을 하는 햄단백질 (Hemeprotein) 로 약물대사학적으로 중요한 효소이다. 본 연구에서는 조피볼락에 존재하는 CYP1 family (CYP1A, CYP1B, CYP1C1, CYP1C2)의 서열을 밝히고 benzo[a]pyrene과 trichlorfon 노출을 통한 조피볼락의 약물대사 특성을 분석하고자 하였다. CYP1A는 간, 심장, 신장에서 주로 발현되고, CYP1B는 아가미에서, CYP1C1는 근육, 아가미, 비장, CYP1C2는 근육, 심장, 생식소, 뇌에서 특징적으로 발현되었다. 또한 AhR agonist 안 B[a]P 농도 별 노출 시, 아가미, 간, 신장, 비장의 CYP1A, CYP1B, CYP1C1, CYP1C2 발현이 대부분 증가하였다. 그 중에서 CYP1A의 ELISA법과 EROD assay를 분석한 결과, B[a]P 노출 농도가 높아짐에 따라 CYP1A의 발현 정도가 증가하였으며 이는 조직면역염색(IHC) 결과를 뒷받침하였다. 이로써 B[a]P 노출시 조피볼락의 CYP1 family의 유전자 발현을 증가시키고, 특히 간 내 CYP1A의 단백질 발현을 크게 유도시킴을 알렸다.

양식산업의 급속한 성장으로 수산생물의 생산량 증가와 함께 양식생물의 질병 발생 피해도 증가하였다. 그 중 기생충에 의한 피해는 상당한 수준일 뿐만 아니라, 이에 대한 대책으로 현재 국내에서 5종 정도의 구충제가 허가되어 사용되고 있다. Trichlorfon (TCF)는 흡충, 조충, 선충, 구두충 등 기생충성 질병 치료에 가장 빈번하게 사용되고 있는 유기인계 구충제이다. 하지만 TCF는 잔류허용기준(MRL)이 설정되어 있지 않은 채 국내 제조 및 수입사에서 제조 판매되고 있는 상황이다. 따라서 정확한 용법과 용량 설정을 위한 기초데이터 확보를 위해 TCF를 조피볼락 (체중 100±5 g) 에 30, 150 mg/kg bw 농도로 15℃

및 25℃에 약욕시킨 후, 경시적 (0, 0.5, 1, 3,6,12, 24, 48, 96, 192, 336 시간)으로 혈청, 근육, 간 내 TCF의 잔류량을 LC-MS/MS로 분석하였다. TCF 약욕에 따른 조피볼락 체내 약물 잔류 농도 측정 결과를 바탕으로 JECFA tool 를 사용하여 임시적 MRL과 WT 1.4 를 사용하여 withdrawal period를 계산하였다. 그리고 Non-compartment model로 PK Solver를 이용하여 TCF의 흡수, 배설, 반감기 등 약물동태학적 매개변수(parameter)를 조사하였다. 또한 TCF 노출에 따른 어류의 항산화, 코티솔, 신경독성, 약물대사 Phase Ⅰ, Phase Ⅱ 를 분석해 조피볼락의 약물대사특성을 연구하였다. 수온 및 농도에 따른 전체적인 실험 결과, 15℃에 TCF 150 mg/kg bw 약욕 후 0.01mg/kg 의 MRL 과 약 24일의 휴약기간을 제안하였다. 본 연구는 조피볼락의 CYP1 family의 역할과 B[a]P와 TCF 노출에 따른 획기적인 어류 약물대사 시스템을 알리고, TCF에 대한 조피볼락의 체내 생화학적 변화, 조직 별 잔류농도, MRL, 휴약기간을 제시한 점에서 해수어종에 대한 수산용의약품 확대 사용 가능성을 처음으로 알리고 조피볼락의 약물동태학적 및 약물대사 특성 연구의 새로운 가능성을 제시한다.

# CHAPTER I

## Molecular characterization of Cytochrome P450 1A, 1B, 1C1 and 1C2 and effects of Benzo[a]prene on their hepatic expression in *Sebastes schlegelii*

**Abstract**

Knowledge of the complement of cytochrome P450 (CYP) genes is essential to understand detoxification and bioactivation mechanisms for many contaminants. In this study, we cloned four new CYP1 genes, *CYP1A*, *CYP1B*, *CYP1C1*, and *CYP1C2* from black rockfish (*Sebastes schlegelii*), an important model organism used in environmental toxicology. Quantitative PCR analysis of *CYP1* gene transcription in 11 organs revealed tissue-specific expression patterns. Furthermore, exposure to an aryl hydrocarbon receptor (AHR) agonist benzo[a]pyrene (B[a]P) at 2, 20, and 200 mg/kg body weight deregulated *CYP1A*, *CYP1B*, *CYP1C1*, and *CYP1C2* expression in the gills, liver, kidneys, and spleen. Thus, mRNA levels of *CYP1A* and *CYP1B* were upregulated by 450- and 17-fold, respectively, in the spleen and that of *CYP1C1* was increased 45-fold in the gills, whereas *CYP1C2* was decreased in the liver and gills, indicating differential effects of polycyclic aromatic hydrocarbons on fish organs. Furthermore, B[a]P induced CYP1A protein expression and 7-ethoxyresorufin O-deethylase activity in hepatic microsomes. The results suggest that the expression profiles of inducible CYP1 enzymes in *S. schlegelii* may be used as biomarkers in assessing aquatic contamination by AHR agonists. Determination of basal and induced expression levels and substrate specificity of the four CYP1 enzymes should contribute to better understand of their roles in metabolization of xenobiotics and drugs.

## 1.1 Introduction

Cytochrome P450 (CYP) comprises a superfamily of enzymes involved in the biotransformation of endogenous compounds, environmental pollutants and many drugs. CYPs have a broad range of substrates such as halogenated hydrocarbons, polycyclic aromatic hydrocarbons (PAH), pesticides and herbicides, result in metabolization and elimination from the body. Drug metabolism serves as detoxification as the metabolites formed are less biologically active than the parent compound. However, in some cases, the drug is converted to a highly reactive metabolite that increase risks of cancer and toxic effects (Nebert and Karp, 2008). Expression of fish CYP1As can be induced strongly by PAH, planar polychlorinated biphenyl (PCB), halogenated aromatic hydrocarbons (HAHs), dibenzo-p-dioxin (PCDD), and dibenzofuran (PCDF) congeners, and some natural products, via activation of aryl hydrocarbon receptor (AHR) (Hankinson, 1995; Arkoosh et al., 2001; Reynaud & Deschaux, 2006). Many studies have documented that the induction of CYP1A can provide an early warning biomarker to assess the exposure to important classes of AHR agonists (Goksøyr, 1995; Nebert & Karp, 2008). PAHs are hydrocarbons organic compounds, nonpolar and lipophilic. PAHs are abundant in the universe, primarily produced by the incomplete combustion of fossil fuels. PAH concentrations in the sediment may reach up to 50 μg $g^{-1}$ dry weight (dw) in an area relatively contaminated from the Europe (El Nemr et al., 2007). Many of the toxic effects of PAHs including mutagenicity and carcinogenicity are not caused by the parent compounds but by the metabolites. PAH biotransformation is initiated by cytochrome P450-dependent mono-oxygenases (Xue and Warshawsky, 2005). The monooxygenases metabolize PAH parent compounds into dihydrodiols, phenolics, and epoxide intermediates, which then are further catalyzed and eventually excreted (Shimada, 2006).

The prototypic PAH, benzo(a)pyrene [B(a)P] is genotoxic, mutagenic to aquatic organisms (Scott et al., 2011). And they can also decrease the development and morphology by environmental levels as low as 0.1ng ml-1 (Hose et al., 1982). Also, the main site for PAH metabolism is the liver, many studies reported the in situ metabolism of PAHs is causatively involved in toxicity from the liver (Granberg et al.,2000; Galván et al., 2005).

Most fish have only one CYP1A gene, one CYP1B1 gene and two CYP1Cs, the paralogous CYP1C1

and CYP1C2 (Godard et al., 2005). CYP1A, CYP1B1, and the CYP1Cs mRNA and protein are induced to varying degrees by AHR agonists in several fish species (Hawkins et al., 2002; Wang et al., 2010; Bugiak & Weber 2009).

Recently, zebrafish (*Danio rerio*) and killifish (*Fundulus heteroclitus*) have CYP1D1 which does not appear to be transcriptionally induced by typical AHR agonists (i.e., PCB126, TCDD, and FICZ) (Glodstone et al., 2009; Jönsson et al., 2009; Zanette et al., 2009)

Sensitive response to the effects of pollutants, the expression patterns of the CYP1A, CYP1B, and CYP1C genes in fish could become the available biomarkers in environmental impact assessments. To date, all five CYP1s have been reported specifically in zebrafish. EROD activity and CYP1A expression have been applied in several biomonitoring studies with zebrafish (Jönsson et al., 2009). We have been questioned that black rockfish, *Sebastes schlegelii*, also have the similar regulation and similar full suite of CYP1 genes. This species is one of the most abundant marine fish aquaculture in Korea. They are mainly found along the coastal line where possess shallow and rocky shores around the Korea, Japan, and China (Bai et al., 2001). Biological and ecological features, i.e., tolerance to lower water temperature, fast growth, and a high survival rate, and adaptation to high levels of contaminants have interest in this species as an aquatic alternative vertebrate model species (Lee et al., 2002).

Information on mRNA expression of other CYP1 isoforms than CYP1A is lacking in *Sebastes schlegelii*. The objective of the present study was therefore to identify all CYP1 genes, CYP1A, CYP1B, CYP1C1, and CYP1C2 expressed in *Sebastes schlegelii*, and determine their degree of inducibility by different concentration of B[a]P (0, 2, 20, and 200 μg/g B.W) in four different organs (liver, gill, kidney, and intestine). Another aim was to compare hepatic CYP1A protein expression and enzyme activity with B[a]P exposure. The results provide evidence of fundamental differences in the regulation of CYP1 isoforms by exogenous inducers and utility for hazard assessment of PAH contamination in aquatic ecosystems.

## 1.2 Material and Methods

### 1.2.1 Animals

Healthy black rockfish, *Sebastes schlegelii*, (mean length, 20 ±2 cm; mean weight, 120±10 g) were purchased from a commercial farm in Tongyeong, Korea. They were acclimatized to the laboratory conditions for two weeks in 400L aquarium tanks filled with aerated water 18±1 (Table 1.1). During the acclimation period, the fish were fed a commercial diet twice daily (Woosungfeed, Daejeon City, Korea), maintained on a photoperiod of 12 h light/ 12 h dark and constant condition at all times (Table 1). The experiments of the current study were approved by the Institutional Animal Care and Use Committee of Pukyong National University (Busan, South Korea).

### 1.2.2 RNA isolation and first-strand cDNA synthesis

Brain, gill, liver, kidney, spleen, and intestine were dissected from one randomly selected untreated healthy fish. Total RNA was extracted from the pooled tissue samples using QIAzol® (Qiagen), as per the vendor's protocol. Purified RNA was quantified based on its OD at 260/280 nm using a UV spectrophotometer (Ultrospec 6300 pro; Amersham Biosciences, Piscataway, NJ, USA). The absorbance ratios for all samples ranged from 1.80 to 2.00, indicating a satisfactory purity of the RNA samples. cDNA was synthesized from 2 μg of total RNA using a cDNA synthesis kit (EnzoLife Sciences Inc., Farmingdale, NY, USA). The synthesized cDNA was then diluted 20-fold in nuclease-free water and stored at -80 °C until use.

Table 1.1 The chemical components of seawater and experimental condition used in the experiments

| Components | Value |
|---|---|
| Temperature (  ) | 18 ± 1.0 |
| pH | 8.2 ± 0.5 |
| Salinity (‰) | 33.1±0.5 |
| Dissolved oxygen (mg/L) | 7.3 ± 0.2 |
| Chemical oxygen demand (mg/L) | 1.2 ± 0.1 |
| Ammonia (μg/L) | 11.3 ± 0.5 |
| Nitrite (μg/L) | 1.5 ± 0.2 |
| Nitrate (μg/L) | 10.1 ± 1.0 |

Table 1.2 Oligonucleotide primers used for quantitative real-time PCR.

| Primer name | 5'-3' sequence | Product size (bp) |
|---|---|---|
| Ssβ-Actin-F | CCTCGGTATGGAGTCTTGCGG | 111 |
| Ssβ-Actin-R | GTACCGCCAGACAGCACAGTG | |
| SsCYP1A-F | GACACCTGCGTCTTCATCAATCA | 118 |
| SsCYP1A-R | GCTTGATGACTTCGGTGCCATC | |
| SsCYP1B-F | GCACCATCAGGGACATGACA | 133 |
| SsCYP1B-R | AGTGTGTCTTGACTTGCTCCAA | |
| SsCYP1C1-F | CGCGCTTCCTGGATGGAAAC | 111 |
| SsCYP1C1-R | CTTCCACCTTGGCGATCTGG | |
| SsCYP1C2-F | GGCTCCCTAGACAAGGATCTCA | 126 |
| SsCYP1C2-R | GCATTGGTGGAGTAGAATCGCG | |

### 1.2.3 Cloning of SsCYP1A, SsCYP1B, SsCYP1C1, SsCYP1C2

To clone the four CYP1 genes from *Sebastes schlegelii*, we analyzed the liver tissue using the Next-generation sequencing (NGS) technology as the genomic and transcriptomic resource. NGS data were used to design gene specific primers and to confirm identity of cloned cDNAs (Table 1.2). For each putative transcript, four primers were designed: one pair targeting the untranslated regions of the transcript, and one pair targeting part of the coding region. SsCYP1A, SsCYP1B, SsCYP1C1, SsCYP1C2 cDNA were amplified by PCR using the gene specific primers with ExTaq™ DNA polymerase (Takara, Japan). The PCR products were separated on a 1% agarose gel, cloned into a pGEM®-T Easy vector (Promega, Wisconsin, USA) and subsequently custom sequenced by Macrogen Inc. (Seoul, South Korea).

Table 1.3 GenBank accession number used in the experiments

| Tree name | Species | Accession number |
|---|---|---|
| DANIO_17A1 | *Danio rerio* | NP_997971.2 |
| DANIO_1A | *Danio rerio* | BAB90841.1 |
| DANIO_1B1 | *Danio rerio* | NP_001038721.1 |
| DANIO_1C1 | *Danio rerio* | NP_001018446.2 |
| DANIO_1C2 | *Danio rerio* | NP_001108321.1 |
| DANIO_1D1 | *Danio rerio* | NP_001007311.1 |
| MEDAKA 1A1 | *Oryzias latipes* | NP_001098557.1 |
| MEDAKA 1B | | AEH05672.1 |
| MEDAKA 1C1 | | ABQ44509.1 c |
| MEDAKA 1C2 | | AGN04281.1 |
| SALMO_1A | *Salmo salar* | AAM00254.1 |
| SALMO_1B1_part | *Salmo salar* | EG855910.1, DY700468.1 |
| SALMO_1C2_EST | *Salmo salar* | EG933863.1,EG806773.1, EG762705.1, GO061841.1 |
| SALMO_1C3 | *Salmo salar* | ACI33284.1 |
| STENOT_1C1 | *Stenotomus chrysops* | AAL78297.1 |
| STENOT_1C2 | *Stenotomus chrysops* | AAL78299.1 |
| HUMAN_1A1 | *Homo sapiens* | NP_000490.1 |
| HUMAN_1A2 | *Homo sapiens* | NP_000752.2 |
| HUMAN_1B1 | *Homo sapiens* | NP_000095.2 |
| MOUSE_1A1 | *Mus musculus* | NP_034122.1 |
| MOUSE_1A2 | *Mus musculus* | NP_034123.1 |
| MOUSE_1B1 | *Mus musculus* | NP_034124.1 |
| TROUT_1A1 | *Oncorhynchus mykiss* | AAB69383.1 |
| TROUT_1A3 | *Oncorhynchus mykiss* | AAD45966.1 |
| TROUT_1B1 | *Oncorhynchus mykiss* | ADD51159.1 |
| TROUT_1C1 | *Oncorhynchus mykiss* | ADD51160.1 |
| TROUT_1C2 | *Oncorhynchus mykiss* | ADD51162.1 |
| TROUT_1C3 | *Oncorhynchus mykiss* | ADD51161.1 |

### 1.2.4 Identification and sequence analysis of CYP1 isoforms

Full-length cDNA sequences of *Sebastes schlegelii* CYP1A, CYP1B, CYP1C1, and CYP1C2 (SsCYP1A, SsCYP1B, SsCYP1C1, and SsCYP1C2, respectively) were identified from the *Sebastes schlegelii* transcriptome database established in our laboratory. The Basic Local Alignment Tool (BLAST), in the National Center for Biotechnology Information (NCBI) web based query system (http://www.ncbi.nlm.nih.gov/BLAST) with the default algorithm parameters was used to affirm the identified sequences. The open reading frame (ORF) and amino acid sequence of the putative proteins were analyzed using DNAssist software (version 2.2). Matrix Global Alignment Tool (MatGAT) v2.01was used to analyze the similarities of the relevant proteins with their orthologs. Multiple sequence alignment was carried out with the help of ClustalW2 (http://www.ebi.ac.uk/Tools/clustalw2/index.html) and color align conservation (http://www.bioinformatics.org/sms2/color_align_cons.html) web based software. ExPASy prosite (http://prosite.expasy.org) was used to find the conserved domains, while BioEdit was used to compared with homologous sequences in zebrafish by sequence identity analysis (Hall, 1999). while SignalP 4.1 server (http://www.cbs.dtu.dk/services/SignalP) was used to find the signal peptide sequence (Table 1.3). Substrate recognition regions (SRS) of the CYP1 proteins were located based on the prediction by Lewis et al. (2003). MEGA 6 software (Tamura et al., 2013) was used to analyze the evolutionary distances between CYP1 isoforms orthologs and paralogs, by constructing a phylogenetic tree using the neighbor-joining (NJ) method, with the bootstrap support of 1000 replicates.

### 1.2.5 Exposures

Twenty male fish were acclimated for two weeks in filtered and aerated water in four 400L aquarium tanks (5 fish per tank) at 18±1 . After acclimation the fish were weighed and each of five fish were intraperitoneally (I.P) injected with benzo(a)pyrene [B(a)P] dissolved in DMSO at the dose of 2, 20, 200 μg/g BW. Five fish were also injected with an equivalent volume of DMSO alone. Previous studies using Japanese medaka (*Oryzias latipes*), showed that injection of this B[a]P dose caused high-level induction in gene expression and catalytic function EROD assay of CYP1A with absence of mortality

(Carlson et al., 2004). At 48h after injection, control and B[a]P treated fish were anesthetized for 2 min in buffered 3-aminobenzoic acid ethyl ester (MS-222, Sandoz LTD, Basel, Switzerland). Kim et al (2008) reported 48h exposure can induced higher induction of CYP1A gene expression in river pufferfish (*Takifugu obscurus*) exposed to AHR agonists by various of exposure time tests. Liver, gill, kidney and spleen of individual fish were dissected and immediately placed in RNA later (Ambion). For biochemical analyses, tissue specimens were shock-frozen in liquid nitrogen before storage at -80 . For immunohistochemical analyses, tissues were fixed in Bouin's solution (without glacial acetic acid). After 24 h of fixation at room temperature, tissues were transferred into 70% ethanol and stored at 4 before routine processing for paraffin embedding and sectioning.

**1.2.6 Quantification of SsCYP1A, SsCYP1B, SsCYP1C1, SsCYP1C2**

Total RNA isolation and first-strand cDNA synthesis were carried out as described above. Gene-specific primers for the *Sebastes schlegelii* CYP1A, CYP1B, CYP1C1, CYP1C2 (SsCYP1A, SsCYP1B, SsCYP1C1, and SsCYP1C2, respectively) and β-actin designed with the aid of NCBI Primer-Blast Tool (http://www.ncbi.nlm.nih.gov/tools/primer-blast/). Quantitative real-time polymerase chain reaction (PCR) was performed to assess SsCYP1A, SsCYP1B, SsCYP1C1, and SsCYP1C2 gene expression using gene specific primers (Table 1.2). Real-time PCR assays were carried out in a quantitative thermal cycler (LightCycler® 480 II; Roche Diagnostics Ltd., Rotkreuz, Switzerland) in a final volume of 20 μL containing 10 μL of 2× Master Mix (LightCycler® 480 SYBR Green I Master, Roche Diagnostics) and 1 μL cDNA mix. HSP70 gene-specific primers were used to evaluate the mRNA levels of HSP70 in liver samples. β-Actin reference gene from *Sebastes schlegelii* was used as the internal control. The reaction cycling conditions were as follows: 5 min at 95 °C followed by 45 cycles of denaturation for 10 s at 95 °C, annealing for 10 s at 58 °C, and extension for 10 s at 72 °C. Melt curve analysis was performed on the PCR product was amplified. Relative quantitative values were expressed in accordance with CT methods ($2^{-\Delta\Delta CT}$ method) to analyze mRNA expression levels between different organs.

### 1.2.7 Preparation of tissue microsomes

Microsomes were obtained from individual fish liver following exposure to B[a]P different concentration using the method of Nilsen et al. (1998). Tissue was placed in a glass or glass tissue homogenizer with 1 ml of microsomal homogenization buffer (0.1 M sodium phosphate, 0.015 M potassium chloride, 1mM EDTA, and 1mM Dithiothreitol (DTT), pH 7.4) completely disrupted by 20 strokes each of the tight and loose fitting pestles, and transferred into 1.5ml microcentrifuge tubes. The homogenates were centrifuged at 12,000 g at 4 for 20min. The supernatants were carefully placed in pre-chilled at -20 ultracentrifuge polycarbonate tube (355647, Beckman) and centrifuged for 1h at 100,000 g at 4 with Optima Max-XP ultracentrifuge (Beckman Coulter). The supernatant (i.e., cytosol fraction) was discarded and the pellet containing the microsomal fraction resuspended in 200 µl of resuspension buffer (0.1 M sodium phosphate, 0.015 M potassium chloride, 1mM EDTA, and 1mM Dithiothreitol (DTT), and 20% [v/v] glycerol, pH 7.4) Microsomal fractions were aliquoted (10–20 µl/tube) into 0.5 ml microcentrifuge tubes and stored at -80ntil analyzed. The microsomes were used for EROD assay as well as ELISA. Total protein levels in the microsomal samples were determined using the BCA protein Assay kit (Thermo Scientific, Rockford, IL), measuring absorbance at 562 nm.

### 1.2.8 Western blot

CYP1A protein expression levels were determined from hepatic microsomal by Western blot analysis as described previously by Rahman and Thomas (2012). Briefly, protein samples were solubilized in loading buffer by boiling, resolved on SDS PAGE gels and transferred onto immunoblot nitrocellulose membranes (Bio Rad). Membranes were blocked with 3% bovine serum albumin in TBS T buffer for 1 h at room temperature and probed with CYP1A (Biosense AS, Bergen, Norway) primary antibodies (dilution: 1:200) overnight at 4°C. The mouse CYP1A monoclonal antibody was generated against a highly conserved amino acid sequence in rainbow trout CYP1A gene (Rice et al., 1998), which is 83% identical to the corresponding region of amino acid sequence in *S. schlegelii* CYP1A gene using by ClustalW (Hall, 1999). Membranes were then incubated with a horseradish peroxidase-conjugated secondary goat anti mouse antibody (1:500; Cell Signaling, Danvers, MA) for CYP1A. The

immunoreactive (IR) signals of CYP1A bands were visualized by the addition of chemiluminescent substrate ECL (GE Healthcare), photographed on FujiFilm LAS-4000 mini luminescent image analyzer (GE Life Sciences, Piscataway, NJ) and calculated by ImageJ software (National Institutes of Health, Bethesda, MD).

**1.2.9 Liver 7-Ethoxyresorufin O-deethylase (EROD) assay**

CYP1A enzyme activity in liver microsome was determined using an 7-Ethoxyresorufin O-deethylase (EROD) assay (Schloz et al., 1997). EROD assay were determined in a microplate format assay using a fluorometer plate reader (Fluostar, SLT-Tecan). Microsomal samples were diluted to a concentration of 10μg per 30 μl of TN buffer (Tris-NaCl buffer; 50mM Tris-NaCl, pH 7.4). 30 μl of diluted microsomal samples were added to 96-well microtiter plate. 250 μl of EROD buffer containing 47 μM β-NADPH (Sigma, USA) in PBS and 0.5 μM ethoxyresorufin (Sigma, USA) were added with the diluted microsomal samples. The amount of resorufin produced during 3 min at 21 was determined at the excitation wavelength of 544nm and at the emission wavelength of 590 nm. Each sample concentrations were optimized in preliminary experiments and was analyzed at triple. The mean value was used for following calculations. The reaction velocity was calculated from the linear portion of the reaction curve and resorufin standard curve was established by determining the fluorescence of serial resorufin (Sigma, USA) concentrations 30 – 500 nM. EROD assay was expressed as pmol/min/mg of protein.

**1.2.10 CYP1A ELISA**

The amount of CYP1A protein in microsomal samples was estimated semi quantitatively by an enzyme-linked immunosorbent assay (ELISA) (Carlson et al., 2002). The microsome samples were diluted to 10 μg protein/100 μl in coating buffer (50mM Na-bicarbonate, pH 9.5) and added in duplicate to Immunolon 96-well microtiter plate (Dynatech; Chantilly, Virginia) and incubated overnight at 4 . After 18-24h, wells were washed thoroughly with TPBS, blocked with 2% [w/v] BSA in PBS, and rewashed. 100 μl of primary antibody solution (monoclonal antibody C10-7 generated against a

polypeptide sequence 277-294 of rainbow trout, *Oncorhynchus mykiss*, Biosense AS, Bergen, Norway) diluted 1:500 in 1% BSA in PBS was then added to each well before overnight incubation at 4 . The following day, wells were washed with TPBS, incubated with secondary antibody solution (goat anti-mouse IgG Horseradish peroxidase conjugate diluted 1:2000 in 1% [W/V] BSA/PBS), and washed again with TPBS.

Staining was performed using 3,3′,5,5′-Tetramethylbenzidine (TMB, T-5525, Sigma) as substrate. And then after 3–5 min, the reaction was stopped by adding 100 µl 0.1M H2SO4. The peroxidase reaction product was measured as optical density in a spectrophotometer (Pharmacia, Freiburg, Germany) at 450 nm; controls (non-specific binding, blank) were included.

### 1.2.11 Histology and immunohistochemistry (*IHC*)

Organs to be processed for hematoxylin-eosin (H&E) and immunohistochemical (IHC) localization of CYP1A were fixed in 10% phosphate-buffered formalin immediately following fish sacrifice. Formalin-fixed samples (embedded in paraffin wax) were sectioned at a thickness of 5 µm and placed on Colorfrost/Plus microscope slides (Fisher Scientific).

The relative amount of CYP1A protein present within each individual cell/tissue type was assessed by IHC using a modification of the protocol (Stegman et al., 1989). Briefly, tissue sections were heated at 60 for 2 h and then incubated in two consecutive xylene baths to clear residual paraffin. Sections were sequentially soaked twice in absolute, 90%, and 70% ethanol (3 min each) before gentle rinsing in tap water. Following rehydration, tissues were allowed to equilibrate for at least 1 h in 0.01 M PBS (pH 7.4). One hundred microliters of blocking buffer (10% [v/v] normal goat serum in PBS) was added to each slide (completely covering each tissue section) and then incubated for 1 h. Slides were rinsed with PBS (to remove blocking buffer) and 100 µl primary antibody solution was added; monoclonal antibody C10-7 generated against a polypeptide sequence 277-294 of rainbow trout, *Oncorhynchus mykiss*, Biosense AS, Bergen, Norway. Control slides were incubated with nonspecific mouse IgG in 1% BSA/PBS. All slides were incubated overnight at 4 with primary antibody solution.

Following incubation, slides were washed with PBS, blotted dry, and the sections stained using ExtraAvidin alkaline phosphatase staining kit and Fast Red TR/naphthol AS-MX substrate solution (according to the manufacturer's instructions). Staining was terminated before generalized background staining became evident (~30 min) by gentle rinsing in distilled water. In some instances, sections were counterstained with Mayer's hematoxylin to stain cell nuclei. All slides were mounted with an aqueous PBS–glycerol solution (1:1). Tissue were viewed under a Nikon FX Photomicroscope (Nikon, Tokyo, Japan) by two different observers blinded to the study conditions.

**1.2.12 Statistics**

The experiment was conducted for 2 weeks and performed in triplicate. Statistical analysis of data was performed using the SPSS/PC+ statistical package (SPSS Inc., Chicago, IL, USA) and GraphPad Prism 5.0 (GraphPad Software Inc., San Diego, CA). All data were presented as the mean ± S.E. Significant differences between groups were identified using one-way ANOVA followed by Duncan's test for multiple comparisons (Duncan, 1995). The significance level was set at $P<0.05$.

## 1.3 Results

### 1.3.1 Cloning of *S. schlegelii* SYP1A, CYP1B, CYP1C1, and CYP1C2

Using NGS data based on CYP1 in healthy *S. schlegelii* liver, we were get full-length cDNAs of SsCYP1A, SsCYP1B, SsCYP1C1, and SsCYP1C2. We used specific primers targeting predicted untranslated and coding regions. SsCYP1A cDNA has a 1566bp open reading frame (ORF) that encodes 522 amino acid residues with a predicted molecular mass of 51.4 kDa. SsCYP1B cDNA has a 1599 ORF encodes 533 amino acid residues with a predicted molecular mass of 51.6 kDa. SsCYP1C1 cDNA has a 1571 ORF encodes 524 amino acid residues with a predicted molecular mass of 51.3 kDa while SsCYP1C2 cDNA has a 1566 ORF encodes 522 amino acid residues with a predicted molecular mass of 51.1 kDa. The C-terminal sequences in 3-'untranslated region of SsCYP1A, SsCYP1B, SsCYP1C1, and SsCYP1C2 included poly $(A)^+$ tail preceded by a polyadenylation signal sequence (AATAA). The start codon (ATG) was recognized by comparing Kozak sequences of SsCYP1A, SsCYP1B, SsCYP1C1, and SsCYP1C2 with corresponding homologue genes from other species.

### 1.3.2 Comparison of amino acid sequences

Deduced amino acid sequences of SsCYP1A, SsCYP1B, SsCYP1C1, and SsCYP1C2 were compared with CYP1 family amino acid sequences of *Danio rerio* (Table 1.4). 10-20 amino acids longer than the corresponding Danio CYP1A, 1B1, and 1C1, respectively. Interestingly, SsCYP1C2 have more 67 amino acids than Danio 1C2. The full-length *S. schlegelii* sequences display 74% and 81% pair-wise identity to CYP1A and CYP1C1 of zebrafish. According to Nelson et al (1996), our annotation of these subfamilies and genes is in agreement with the CYP classification based on the amino acid sequence percent identities when the identities are higher than 55% for the equal subfamily.

Table 1.4 Identities between *Sebastes schlegelii* (SEBASTES) and *Danio rerio* (DANRE) CYP1 sequences. Values for amino acid identities are presented in the right-top and nucleotide identities in the left-bottom of the table. Regions of ambiguously aligned sequences were masked

| | SEBASTES _1A | DANIO _1A | SEBASTES _1B | DANIO_1B | SEBASTES _1C1 | DANIO_1C1 | SEBASTES _1C2 | DANIO_1C2 |
|---|---|---|---|---|---|---|---|---|
| SEBASTES_1A | | 0.74 | 0.06 | 0.07 | 0.10 | 0.10 | 0.06 | 0.08 |
| DANIO_1A | 0.69 | | 0.07 | 0.07 | 0.09 | 0.10 | 0.07 | 0.07 |
| SEBASTES _1B | 0.28 | 0.26 | | 0.07 | 0.04 | 0.05 | 0.07 | 0.05 |
| DANIO_1B | 0.29 | 0.27 | 0.28 | | 0.05 | 0.05 | 0.05 | 0.06 |
| SEBASTES _1C1 | 0.31 | 0.29 | 0.25 | 0.256 | | 0.81 | 0.06 | 0.04 |
| DANIO_1C1 | 0.30 | 0.29 | 0.24 | 0.26 | 0.75 | | 0.06 | 0.04 |
| SEBASTES _1C2 | 0.29 | 0.07 | 0.28 | 0.27 | 0.29 | 0.28 | | 0.04 |
| DANIO_1C2 | 0.25 | 0.24 | 0.22 | 0.24 | 0.22 | 0.22 | 0.22 | |

### 1.3.3 Phylogentic tree analysis

A phylogentic tree was constructed from multiple alignments of the full-length amino acid sequences of SsCYP1A, SsCYP1B, SsCYP1C1, and SsCYP1C2 and other vertebrate species, using the neighbor-joining method (Fig 1.1). The amino acid sequences of CYP1 family isozymes were aligned using ClustalW analysis. The phylogentic analysis showed SsCYP1A, SsCYP1B, SsCYP1C1, and SsCYP1C2 belong to teleost CYP1A, 1B, 1C1, and 1C2 clades, respectively. SsCYP1A and SsCYP1B clustered most closely with the predicted CYP1A and CYP1B orthologues of medaka (*Oryzias latipes*) while SsCYP1C1 and SsCYP1C2 appeared with 1Cs orthologues of scup (*Stenotomus chrysops*). In previous analyses (Goldstone et al., 2009), Danio (*Danio rerio*) CYP1C1 and 1C2, Trout (*Oncorhynchus mykiss*) CYP1C1, 1C2 and 1C3 clustered together rather than with their respective orthologues. It might be due to gene conversion, as previously reported in avian CYP1As (Goldstone and Stegeman, 2006).

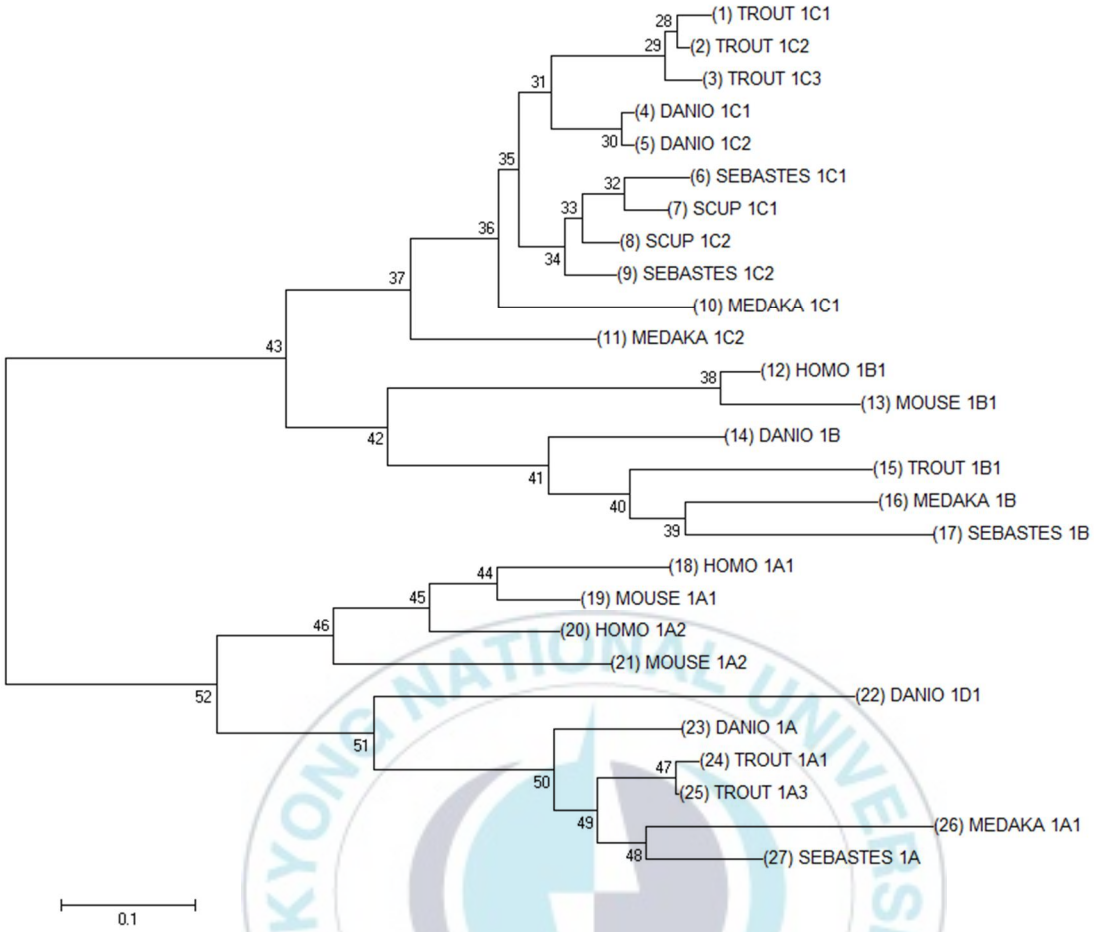


Fig 1.1 Phylogenetic anlaysis of full-length amino acid sequences of *Sebastes schlegelii* 1A, 1B, 1C1, and 1C2, and other vertebrate CYP1 family. The amino acid sequences of CYP1 family were aligned using Clustal W analysis. A phylogenetic tress of CYP1 family was generated by the neighbor-joining method using MEGA 7.1 program. Bootstrap values based upon 1000 sampling are shown in each branch.

### 1.3.4. Characteristic structural features of *S. schlegelii* CYP1 protein

#### 1.3.4.1 Substrate recognition sites (SRS)

Sequence alignment of *S. schlegelii* CYP1 protein (SsCYP1A, SsCYP1B, SsCYP1C1, and SsCYP1C2) and *D. rerio* CYP1 protein (DrCYP1A, DrCYP1B, DrCYP1C1, and DrCYP1C2) contain six separate substrate recognition sites (SRSs) (Fig 1.2). Location and amino acids sequences of the SRSs according to (Jönsson et al., 2007) are indicated as follows (Fig 1.2). The six SRS may differ in their relative importance among CYPs but are likely to correspond to regions containing substrate closely related residues in most CYP genes.

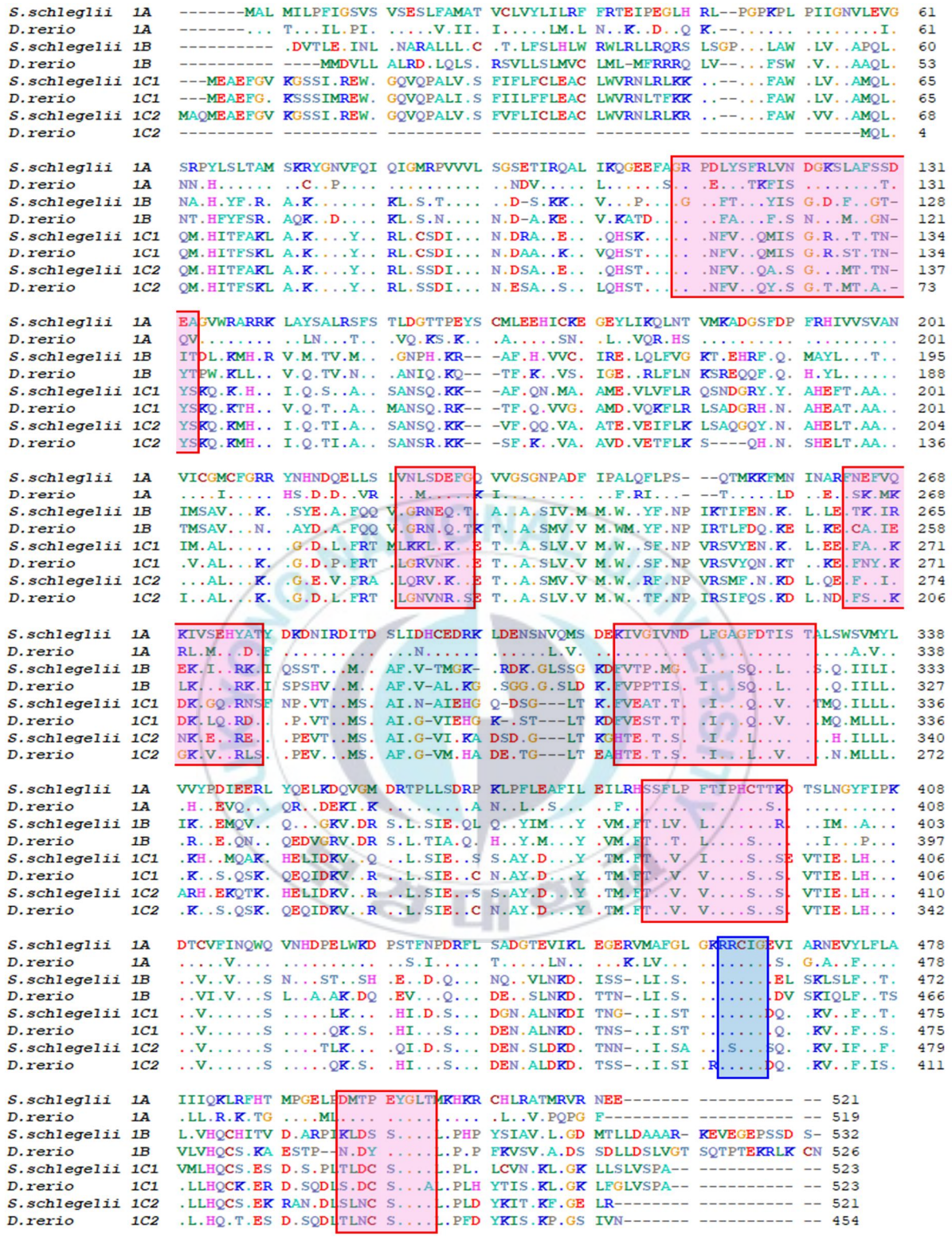

Fig 1.2 Alignment of *Sebastes schlegelii* and *Danio rerio* CYP1 family genes. The location for the heme binding site (blue) and the substrate recognition sites (SRS 1-6) (red) from (Jönsson et al., 2007) of the proposed enzymes are indicated by shading. Residues that are identical to SsCYP1A sequence are indicated by a dot. Accession numbers are available in the supplemental information.

### 1.3.4.2 Highest structural conserved regions

Deduced amino acid sequence of *S. schlegelii* CYP1 gene family possesses all major functional domains characteristics (Fig 1.3). The overall structure of CYP450 is generally conserved and six substrate recognition sites (SRS1-6) have identified to be necessary in the active site. SRS1-6 regions are very important role in the binding and the subsequent enzymatic conversion of the substrate.

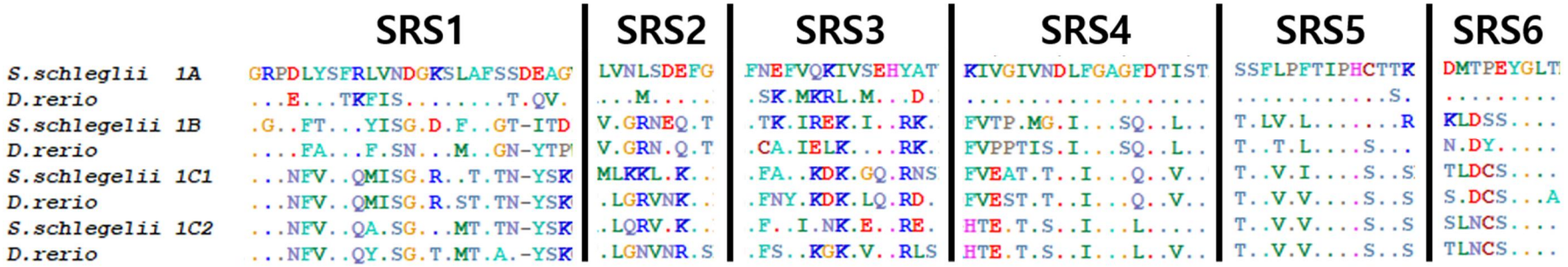


Fig 1.3 Alignment of substrate recognition sites (SRS 1-6) of *Sebastes schlegelii* and *Danio rerio* CYP1. Residues that are identical SsCYP1A sequence are indicated by a dot

### 1.3.5 Specific tissue expression in CYP1 mRNA level

Fig 1.4 - 7 shows the relative transcript levels of the four CYP1s measured by real time PCR using 2△△CT method. We sampled from healthy fish tissue; Brain, eye, gill, heart, stomach, phyloric ceca, liver, kidney, spleen, intestine, muscle and gonad. We chose the β-actin for comparing the tissue expression correction. CYP1A showed the highest expressed in liver, heart, kidney and muscle tissue. In liver, CYP1A was 33 times higher than CYP1B, 530 times higher than CYP1C1, and 7 times higher than CYP1C2. Levels of CYP1B transcript were high in gill, muscle, heart. In gill, CYP1B was most highly expressed transcripts. CYP1B was 9,138 and 885 times higher than 1A, 1C1, and 1C2, respectively. CYP1C1 and CYP1C2 showed generally similar patterns of expression levels among tissues, especially, the muscle is the highly expressed transcripts among CYP1C1 and CYP1C2. And CYP1C1 was expressed at the lowest levels among the four CYP1genes in most of the tissue.

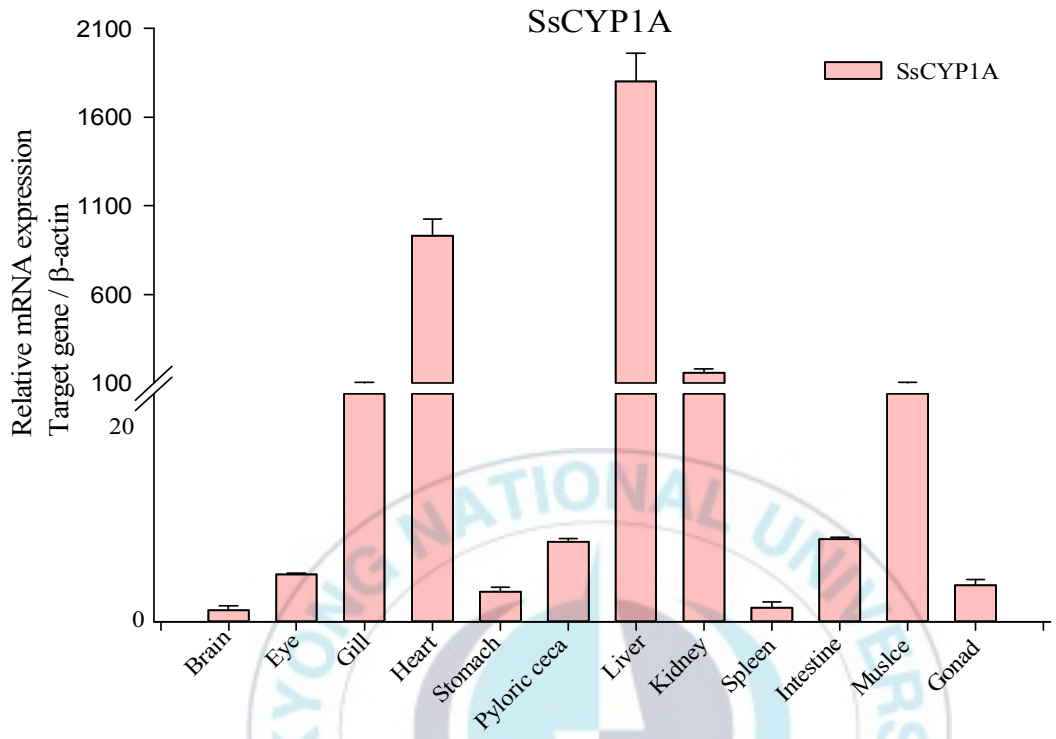


Fig 1.4 Organ-specific expression of CYP1A in *Sebastes schlegelii*. β-actin gene expression was determined by real-time PCR. Gene expression is presented as relative levels.

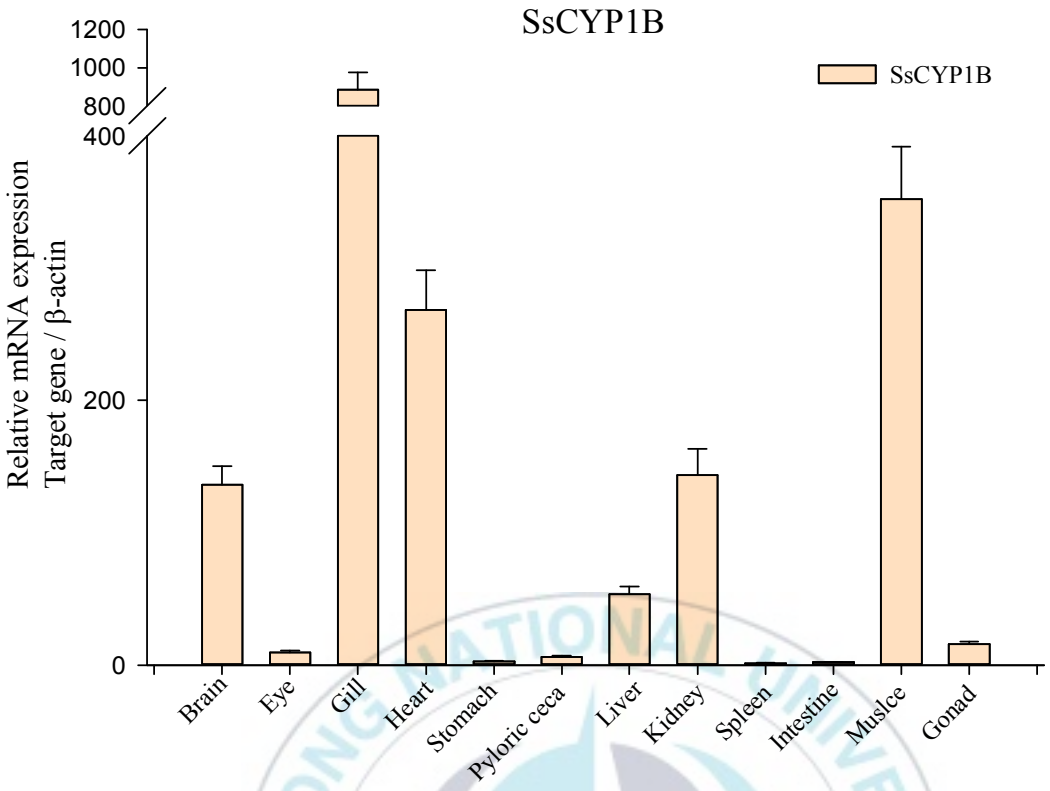


Fig 1.5 Organ-specific expression of CYP1B in *Sebastes schlegelii*. β-actin gene expression was determined by real-time PCR. Gene expression is presented as relative levels.

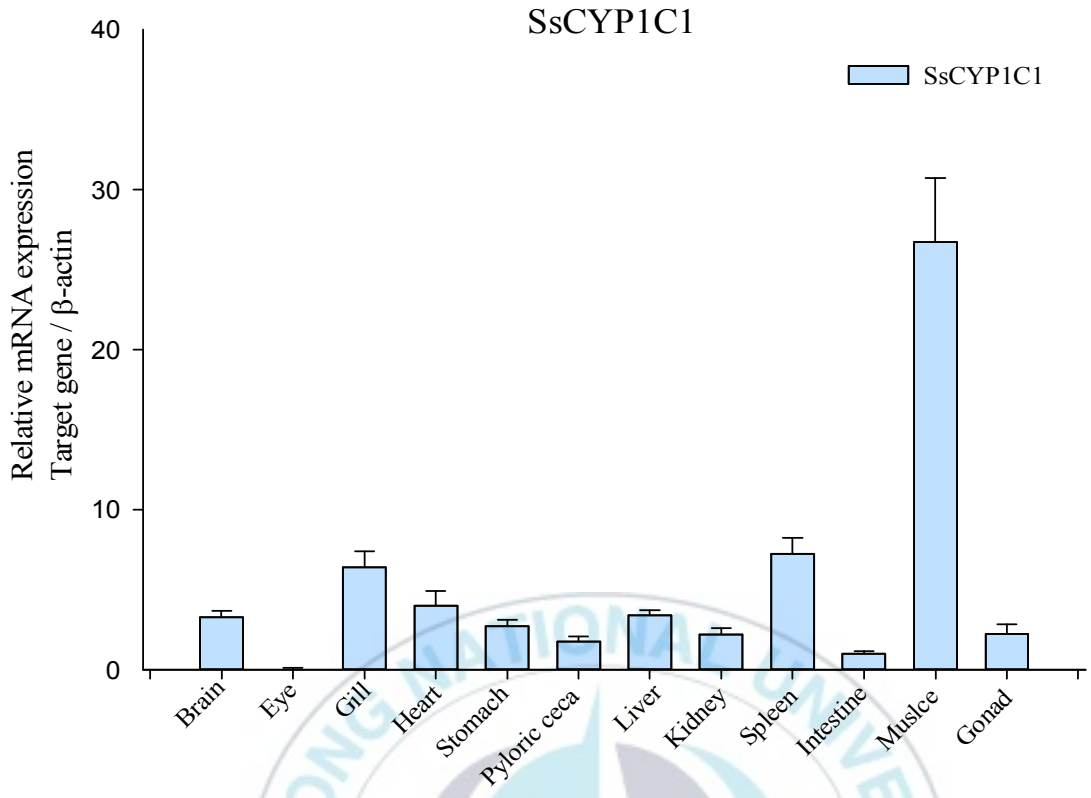


Fig 1.6 Organ-specific expression of CYP1C1 in *Sebastes schlegelii*. β-actin gene expression was determined by real-time PCR. Gene expression is presented as relative levels.

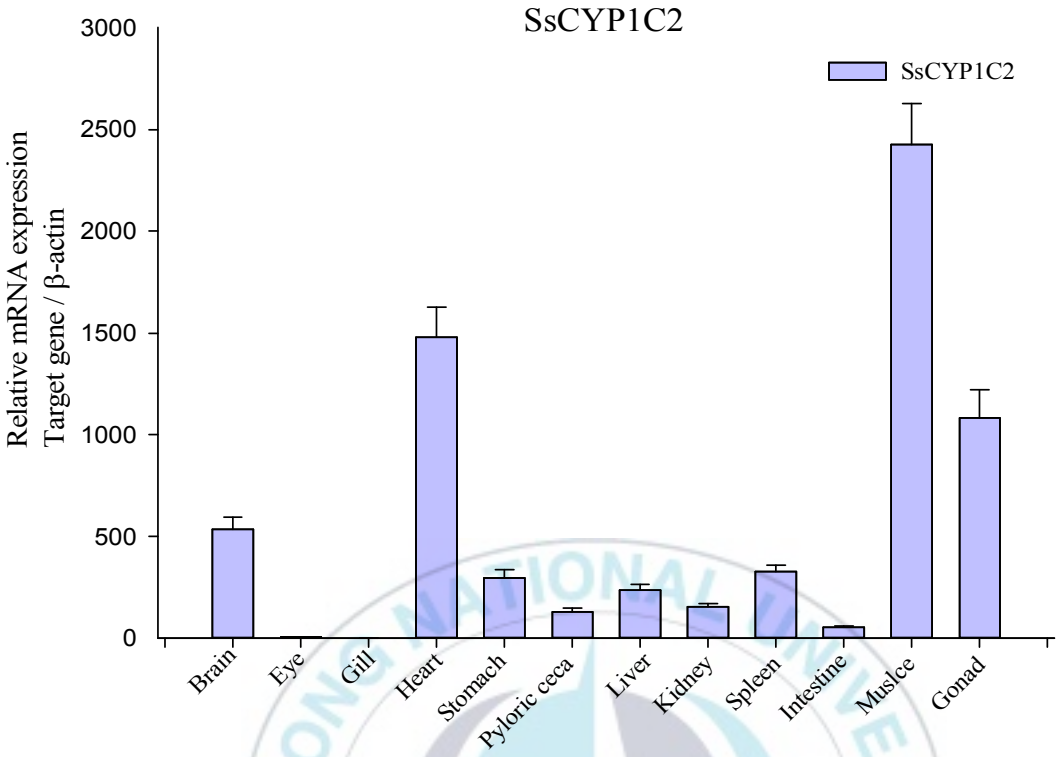


Fig 1.7 Organ-specific expression of CYP1C2 in *Sebastes schlegelii*. β-actin gene expression was determined by real-time PCR. Gene expression is presented as relative levels.

### 1.3.6 CYP1 mRNA level in different tissues of B[a]P treated fish

No mortality was observed in *S. schlegelii* injected B[a]P 2, 20, 200 μg/g bw or the control (DMSO). B[a]P induced the expression of CYP1A, CYP1B, CYP1C1 and CYP1C2 in all 4 tissues (gill, liver, kidney, and spleen) (Fig 1.8-11). The most significant changes in CYP1 expression in response to B[a]P 200mg/kg bw were in spleen, where CYP1A was induced 450 fold and CYP1B 17 fold, and in gill, where CYP1C1 was induced 45 fold. CYP1B in liver and spleen, CYP1C2 in kidney also were induced strongly.

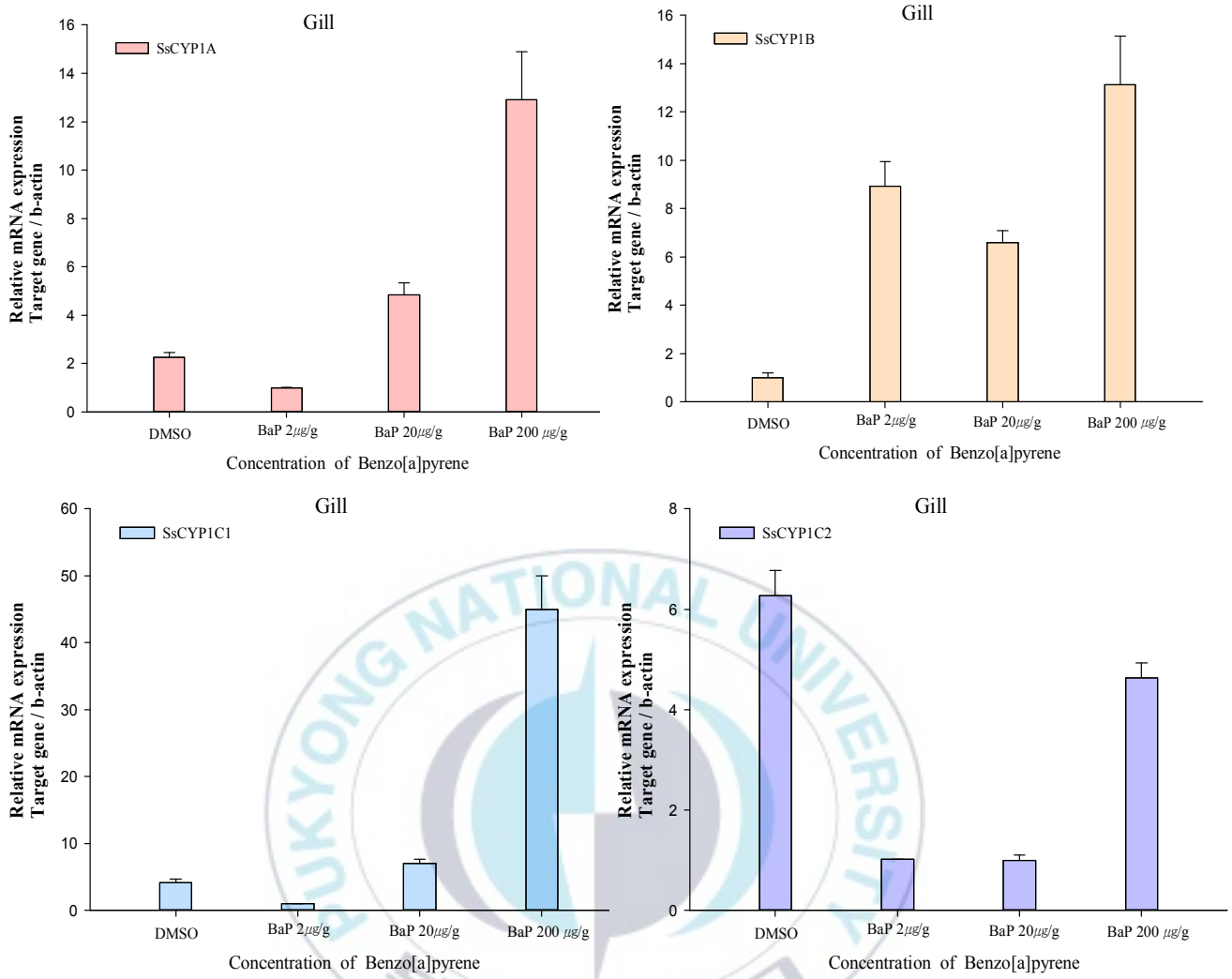


Fig 1.8 Relative transcriptional induction of SsCYP1A, 1B, 1C1, 1C2 in gill of B[a]P 0, 2, 20, 200 ug/g exposed *Sebastes schlegelii*. β-actin gene expression was determined by real-time PCR. Gene expression is presented as relative levels.

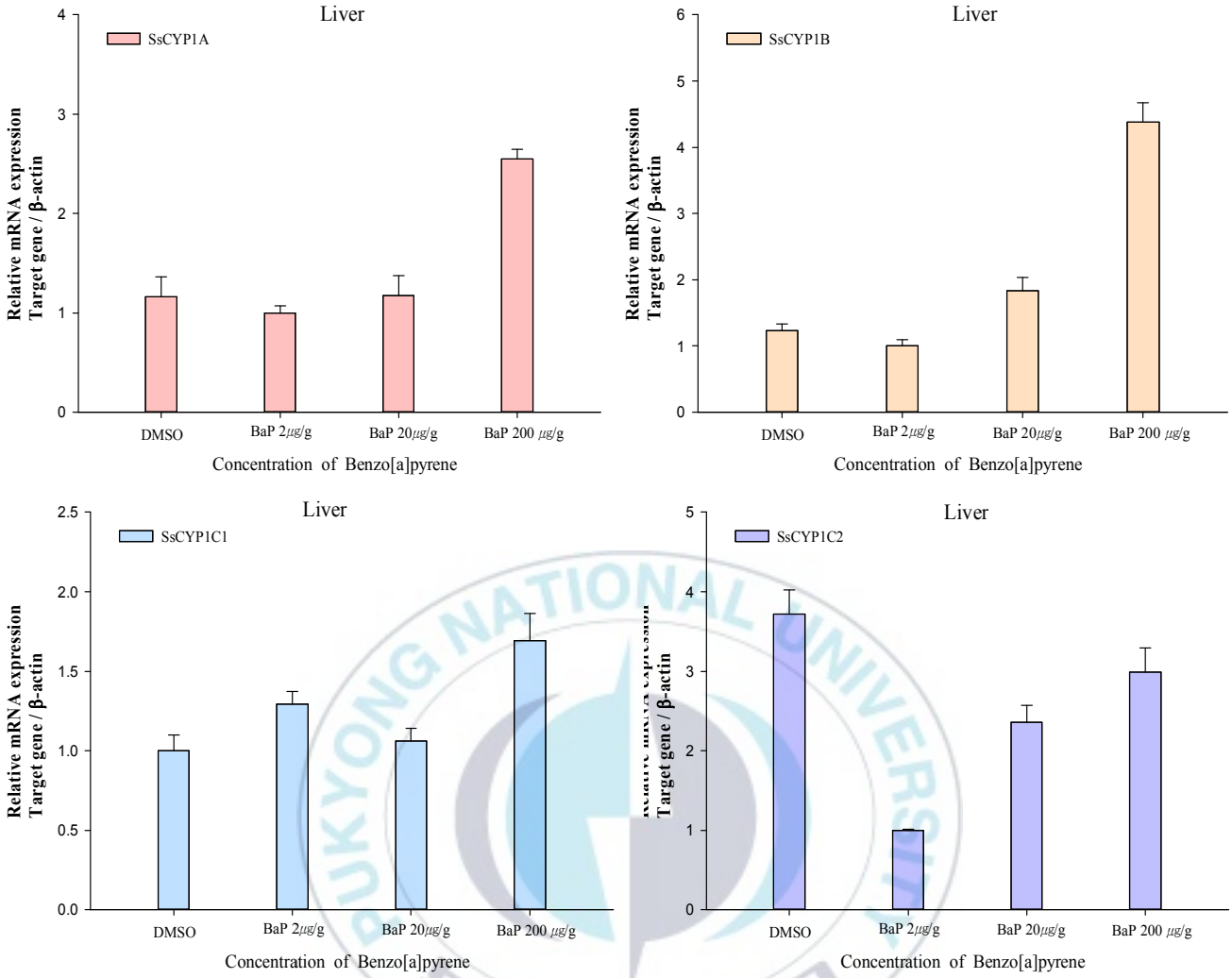


Fig 1.9 Relative transcriptional induction of SsCYP1A, 1B, 1C1, 1C2 in liver of B[a]P 0, 2, 20, 200 ug/g exposed *Sebastes schlegelii*. β-actin gene expression was determined by real-time PCR. Gene expression is presented as relative levels.

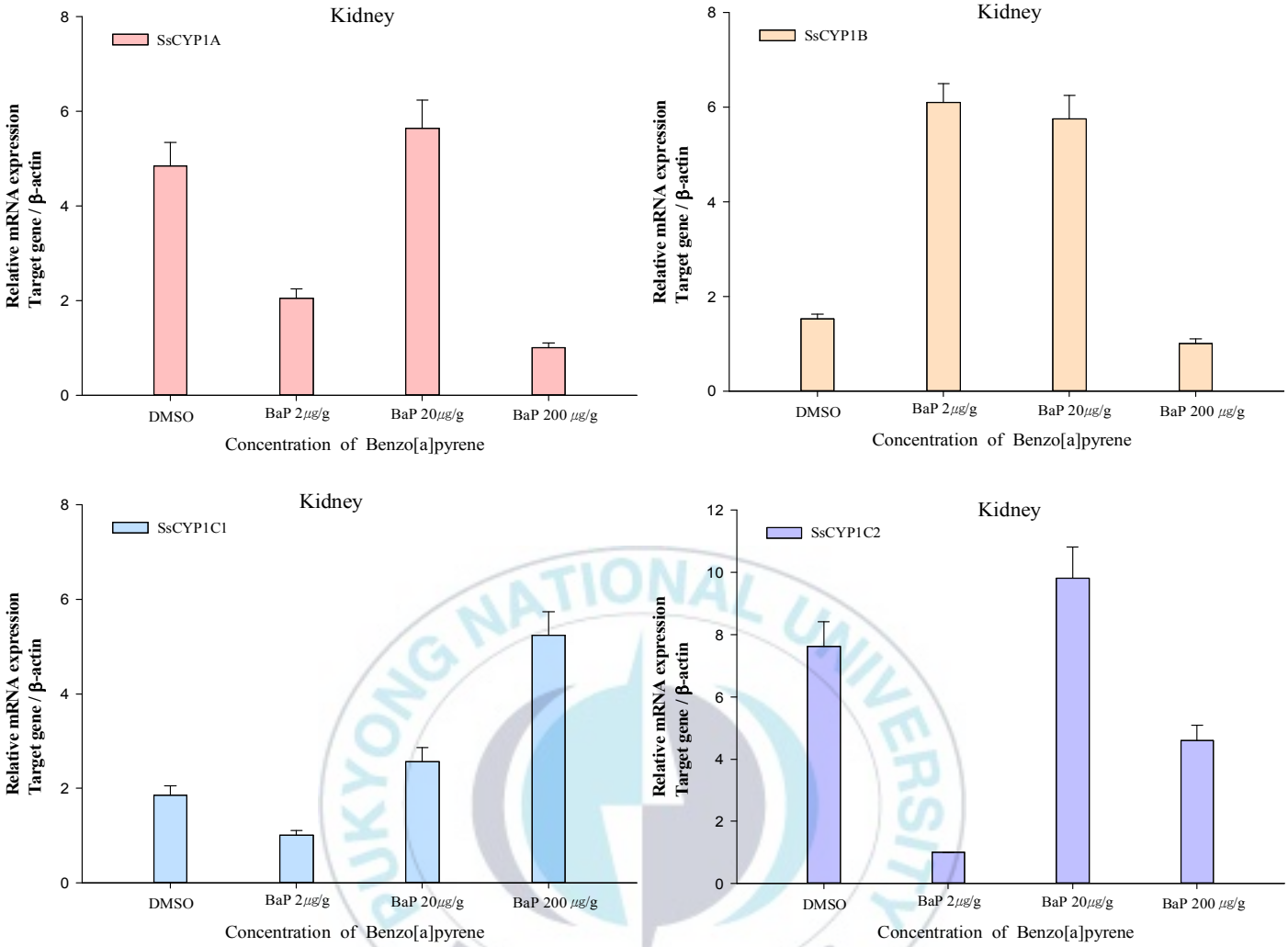


Fig 1.10 Relative transcriptional induction of SsCYP1A, 1B, 1C1, 1C2 in kidney of B[a]P 0, 2, 20, 200 ug/g exposed *Sebastes schlegelii*. β-actin gene expression was determined by real-time PCR. Gene expression is presented as relative levels.

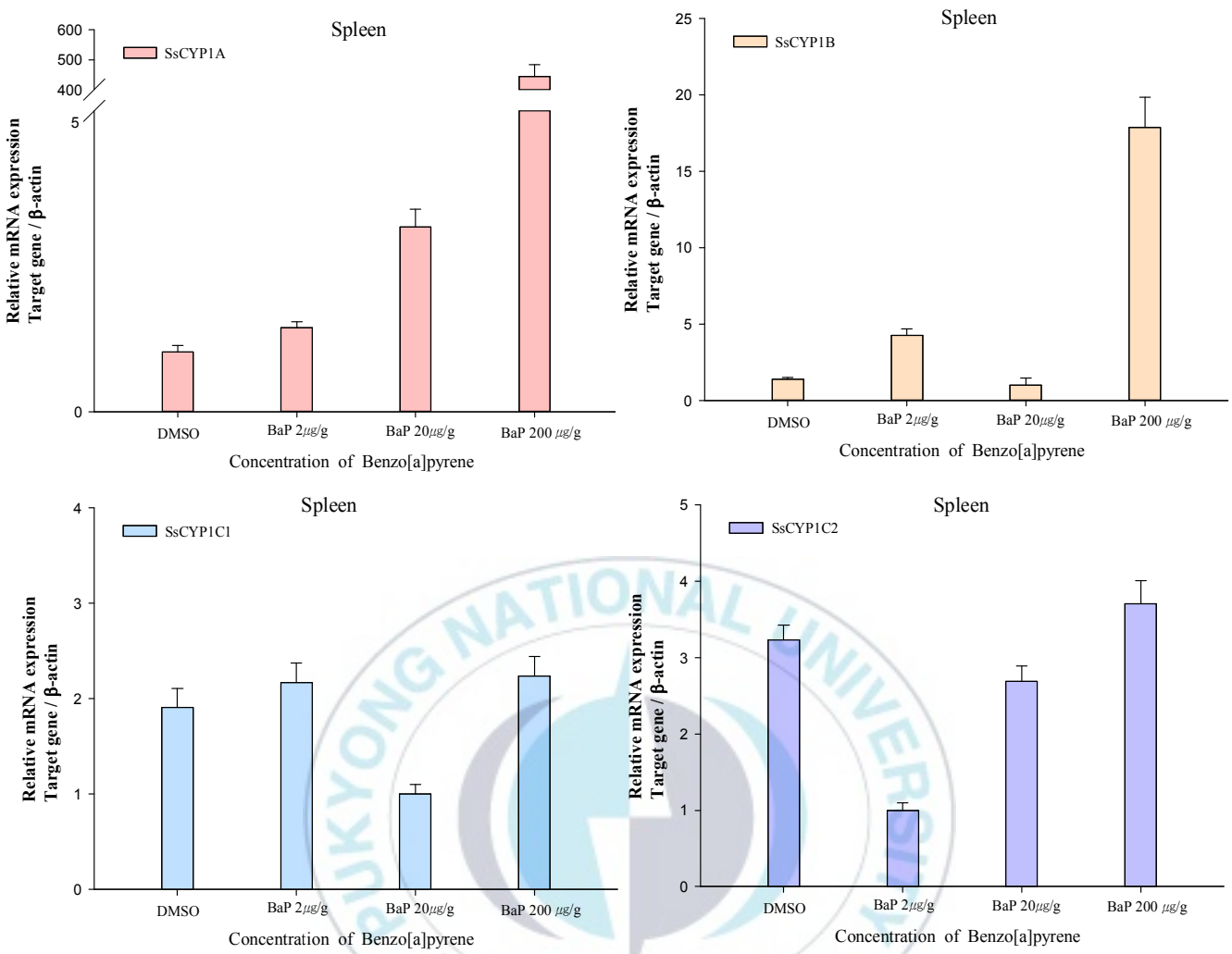


Fig 1.11 Relative transcriptional induction of SsCYP1A, 1B, 1C1, 1C2 in spleen of B[a]P 0, 2, 20, 200 ug/g exposed *Sebastes schlegelii*. β-actin gene expression was determined by real-time PCR. Gene expression is presented as relative levels.

### 1.3.7 CYP1 induction by B[a]P in hepatic microsome

Relative levels of microsomal CYP1A protein levels and EROD activity in liver were determined for *S. schlegelii* injected with B[a]P 2, 20, 200 μg/g bw at 48h post exposure. Hepatic microsomal CYP1A protein compared to control significantly increased following the B[a]P injection concentration using ELISA (Fig 1.12). Exposure to B[a]P significantly induced EROD activity compared to control (Fig 1.13). B[a]P markedly elevated CYP1A protein levels at absorbance 450nm ~ 5.6 fold to compared to control DMSO, whereas the marked elevation of EROD activity was elevated ~5 fold to compared to control at high dose of B[a]P 200 μg/g bw. Western blot analysis showed the presence of a predicted size band of CYP1A protein (about 60kDa) (Fig 1.14). The expression of band signal was increased in B[a]P exposed fish compared with DMSO microsome.

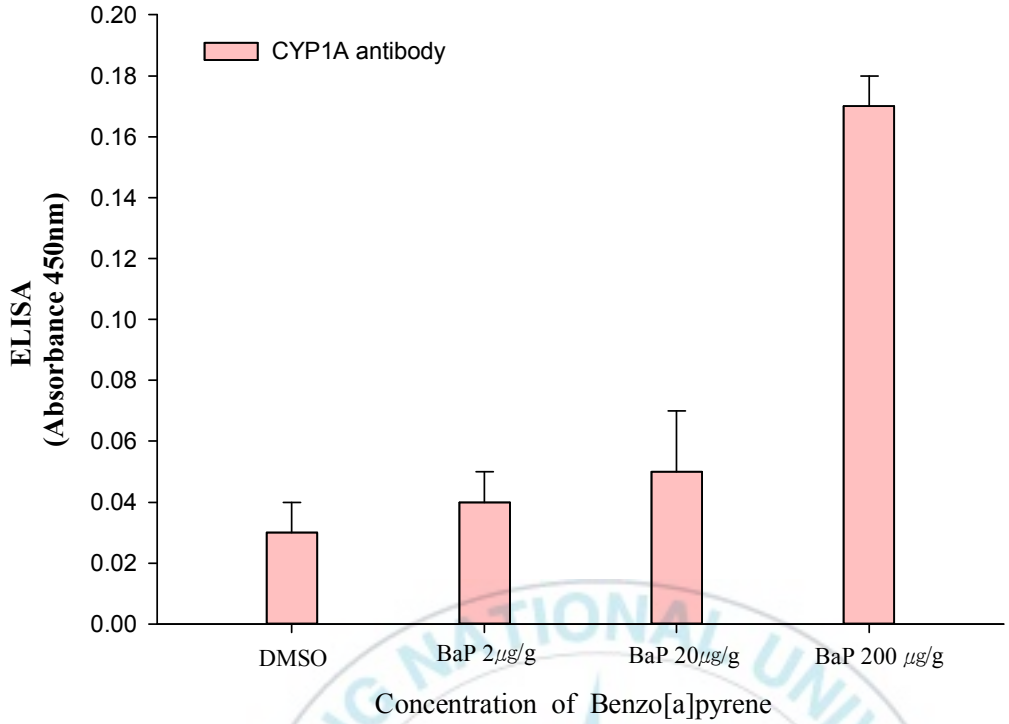


Fig 1.12 Relative levels of hepatic microsomal CYP1A activity were determined by an ELISA and values represent the mean absorbance at 450nm

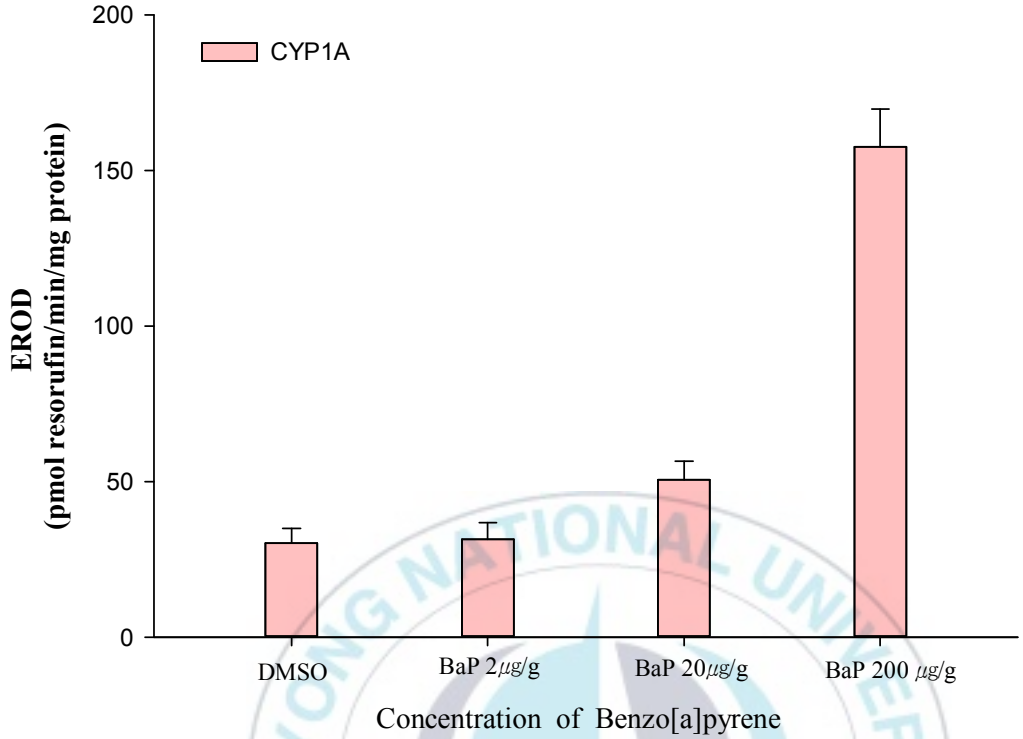


Fig 1.13 Relative levels of hepatic microsomal CYP1A activity were determined by an EROD microtiter assay, and values represent the mean picomoles of resorufin/min per mg protein

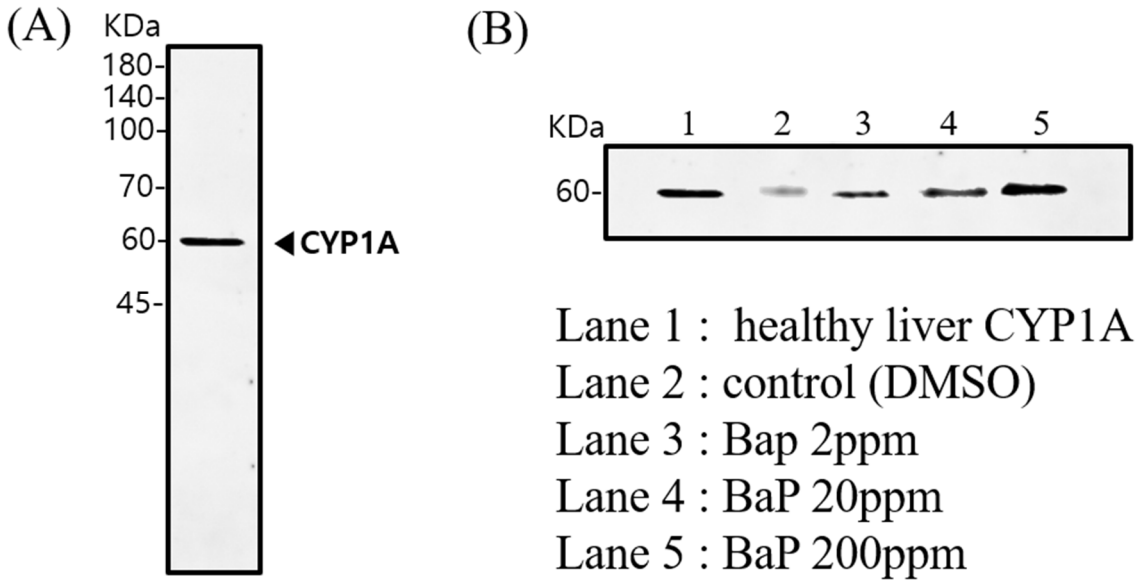


Fig 1.14 Effects of IP exposure to Benzo[a]pyrene (B[a]P) on hepatic microsomal CYP1A expression from *S. schlegelii*. Forty eight hours following IP injection with either vehicle (DMSO) or B[a]P at 2, 20, and 200 μg/g BW. (A) Western blot of *S. schlegelii* liver microsomal fraction (30 μg protein / lane) labeled with CYP1A (monoclonal antibody C10-7) showing prominent band of the predicted size ~60 kDa. (B) Lane 1 is CYP1A protein from healthy liver microsomal fraction. Lane 2 is control (vehicle, DMSO), Lane 3 to 5 are exposure to B[a]P 2, 20 and 200 μg/g BW after 48h post injection.

### 1.3.8 Immunohistochemical localization of CYP1A induction by B[a]P

To determine those particular tissue/cell types associated with elevated CYP1A expression/activity in B[a]P exposed *S. schlegelii* liver, CYP1A protein within liver was localized by immunohistochemistry at 48h following exposure. Also, we analyzed the sections of gill, liver, kidney and intestine stained with H&E from the groups under study (Fig 1.15). Hepatocytes demonstrated both basal and BaP-inducible levels of CYP1A (Fig 1.16). Significantly higher CYP1A IHC Indices were observed in hepatocytes from fish exposed to 200 µg/g bW compared to the vehicle control or 2 and 20 µg/g bW treatment groups

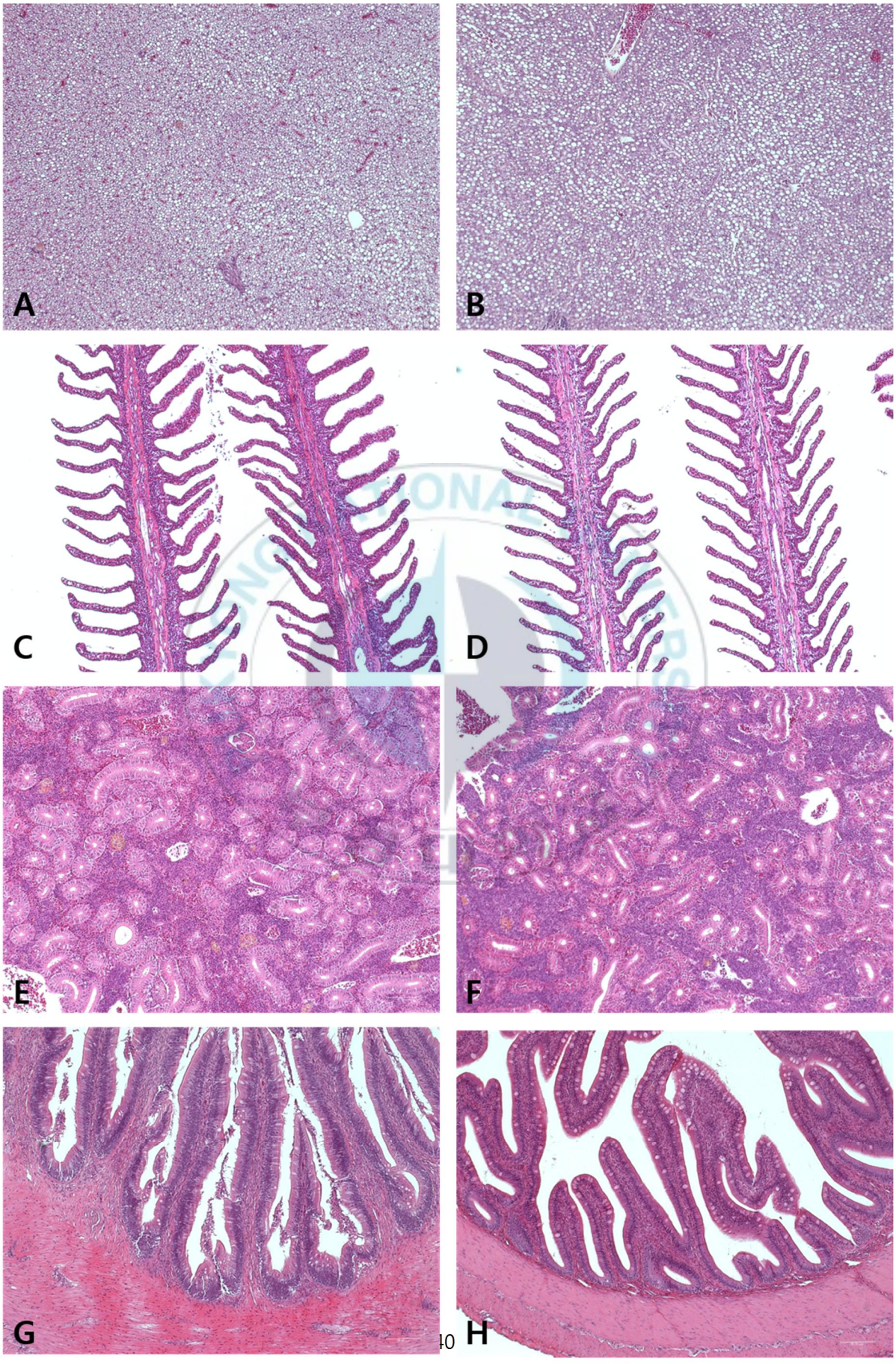
A
B
C
D
E
F
G
H

Fig 1.15 Representative sections of liver (A), gill (C), kidney (E) and intestine (G) in control and liver (B), gill (D), kidney (F) and intestine (H) in B[a]P 200 μg/g bw with H&E.

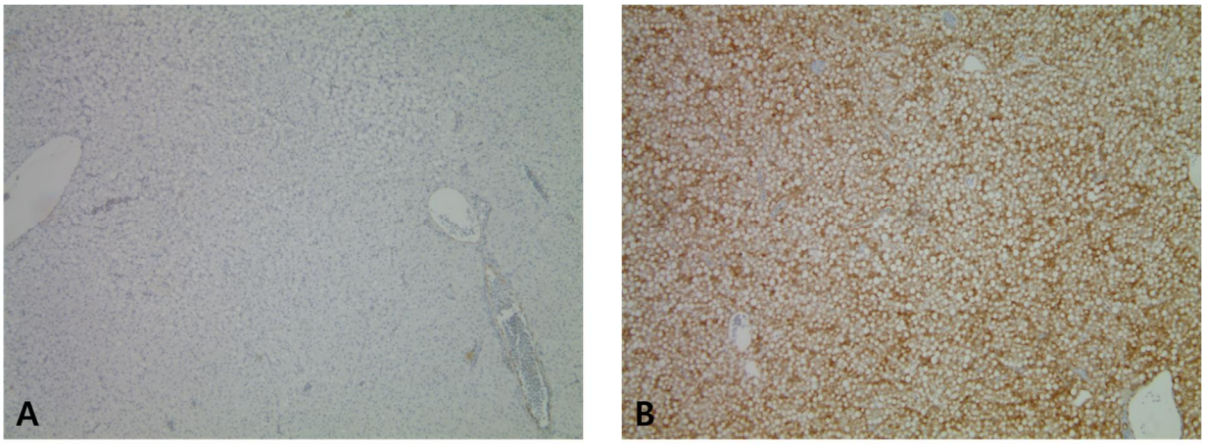


Fig 1.16 Immunohistochemical localization of CYP1A protein in *S. schlegelii* liver (A-control group) (B-B[a]P 200 µg/g bw). Notice the higher expression of CYP1A in the liver from the B[a]P 200 ug/g bw, when compared to the observed in the control group.

## 1.4 Discussion

### 1.4.1 Identification of new CYP1 genes in *S. schlegelii*

Cytochrome P450 family 1 (CYP1) enzymes play crucial role in the metabolism of pharmaceuticals and toxicants especially PAHs. The main metabolism is detoxification, but may in certain cases result in bioactivation, mutagenesis, cancer, and other kinds toxicity. CYP1 induction is generally used as a biomarker for contamination with chemicals activating the AHR.

With the cloning and sequencing of four new CYP1 genes in *S. schlegelii*, we analyzed the comparison of amino acid, phylogenetic tree, and specific tissue expression. These new transcripts were denoted SsCYP1A, SsCYP1B, SsCYP1C1 and SsCYP1C2. The CYP1C genes were only recently described and lack of the functions. CYP1Cs have been found in fish frogs and birds but not in mammal (Zanette et al., 2009). The CYP1C amino acid sequence are more similar to CYP1B amino acid than CYP1A amino acid. And phylogentic tree showed that CYP1B and CYP1Cs amino acid clustered together and more closely related to each other than CYP1A. This results are totally consistent with previous studies that the CYP1Bs and CYP1Cs are sister subfamilies occurring in one monophyletic clade (Goldstone et al., 2007) and that the CYP1A is in another clade. And CYP1B and CYP1Cs diverged from a common ancestor. The phylogenetic analyses also described that the *S. schlegelii* CYP1 sequences are more closely related to the CYP1 sequences in medaka or scup than to those in zebrafish. Since zebrafish is in the superorder Ostarophysi while medaka, scup, and *schlegelii* are in the superorder Acanthopterygill. These two superorders were separated from 290 million years ago, while orders Beloniformes (medaka), scup (Perciformes) and Scorpaeniformes (*schlegelii*), around 153 million years ago (Steinke et al., 2006)

### 1.4.2 SRS in CYP1s sequence

The proline rich region beside amino acids harbouring large side chains (tyrosine;Y and tryptophan; W) could play crucial role in shaping the SRS1 region, especially proline residues structurally interrupt

alpha helices (Drew et al., 2001). SRS2 and SRS3 may be less importance than the final structure of the substrate, but these two substrates make substrate acceptance. Based on the analysis of functional conserved regions, it is likely that SRS1, SRS3, and SRS4 contribute the most to any differences in substrate recognition, because of that the three SRS regions have the largest number of the absolute amino acid differences. SRS4 is composed of the threonine-rich center of the I-helix, which binding oxygen with the heme.

The I-helix contains a conserved threonine residue (at position 326 in Fig 1.2) important for influencing the substrate specificity within the active site and for transferring the oxygen during product formation via a negatively charged residue (Asp/Glu) together with a polar uncharged side-chain (Ser/Thr) residue. SRS1 and SRS4 display striking patterns that showed slowed substitution rates relative to the gene set. These two regions might play a role in deciding the broad type of substrate or cofactor recognition that is a common feature of CYP1C gene family (Godard et al., 2005). Cysteine, at position 463, is in the heme binding site (461-RRCIG-465) that highly conserved the sequence in the teleost CYP1 gene family. But R (at position 462) changed to S in SsCYP1C1. And the E-R-R triad using the Glu (at positon 379) and Arg (at position 382) of the helix K consensus (ExxR) and the Arg in the 374-PDRF-377 consensus. The E-R-R triad is generally concerned that locking the heme pocket into position and to confirm stabilization of the conserved core structure (Hamberger & Bak 2013).

### 1.4.3 CYP1s expression in *S. schlegelii*

When compared to other CYP1s, relatively higher levels of CYP1A were also observed in the organs of abdominal cavity such as liver, heart, and kidney in *S. schlegelii*, and could be associated with the role of these organs in drug metabolism and blood and nutrient processing, e.g., detoxification of endogenous compounds and nutrient-derived AHR agonists (Jönsson et al.,2007). CYP1B also expressed in substantial levels of brain. Similar to the present study, high levels of CYP1B and CYP1D1 expression in brain from adult zebrafish (Goldstone et al., 2009). The basal levels of expression of

CYP1B were higher than CYP1A in rat brain (Desaulniers et al., 2005). Despite the fact that the CYP1B role in the brain function is not unknown, it might be play an important role in vertebrates including fish and mammals.

### 1.4.4 Basal and B[a]P induced CYP1 expression patterns in *S. schlegelii*

CYP1 expression patterns in four tissue (gill, liver, kidney and spleen) exposed to B[a]P suggested that the four CYP1 family genes have tissue specific roles in regulation and possibly different function. Basal levels of CYP1A, CYP1B expression were highest in the liver, and CYP1C1, CYP1C2 expression were highest in the muscle. Exposed to B[a]P at 200 μg/g bw, CYP1A was strongly induced in the gill (about 6 fold over the control), liver (about 2.5 fold over the control) and spleen (about 450 fold over the control). After exposure to B[a]P contaminants, the liver showed a much weaker CYP1A induction response than the gill. These observations might be explained that B[a]P was rapidly eliminated after uptake by the gills. Specially, CYP1A activated carcinogen B[a]P undergoes first-pass effect in the fish gill (Andersson and Pärt, 1989). Induction of CYP1B by B[a]P 200 μg/g bw was observed in gill, liver and spleen. Similarly, zebrafish and killifish showed strong induction of CYP1B in the liver, gill and kidney (Jönsson et al., 2007b). It seems likely that B[a]P are metabolized by induced CYP1 and phase II enzymes, although it didn't experiment in target fish species.

### 1.4.5 CYP1A protein expression response to B[a]P concentration

The results of this study clearly showed that B[a]P exposure to *S. schlegelii* increases in hepatic CYP1A mRNA, protein expression as well as EROD activity. Consistent with our findings, B[a]P 2, 20, 200 μg/g bw at 48h exposure to medaka caused significant 5 fold increases in hepatic CYP1A protein expressions and EROD activity compared to control corn oil. (Carlson et al., 2004). Also the mRNA expression level of CYP1A induced in gill, liver, kidney and spleen. CYP1A has been proposed to play

a role in controlling AHR activation via a negative feed-back loop by metabolizing endogeneous AHR ligans (Chiaro et al., 2007). CYP1A induced to high levels of expression in detoxification tissues like liver, gastrointestinal tract, gill and kidney and CYP1A is induced endothelium cell types in all organs (Smolowitz et al., 1992). As predicted, CYP1A mediated metabolism of B[a]P has been worked in its carcinogenic, mutagentic, and immunotoxic properties in mammalian systems. Many studies have shown that the hepatic CYP450 enzymes activity and 7-ethoxyresorufin O-deethylase induction in vertebrate liver are highly induced by some organic contaminants such as polychlorinated biphenyls (PCBs), dibenzo-p-dioxins (PCDDs), dibenzofurans (PCDFs) and polycyclic aromatic hydrocarbons (PAHs), known as AHR agonists (Yamashita et al., 2000; Koh et al., 2004). Along with the present study results, we thought that CYP1A, CYP1B, CYP1C1 and CYP1C2 have potential to be sensitive biomarkers of exposure to AHR agonist contaminants in *S. schelgelii* and likely other aquatic organisms.

### 1.5 Conclusion

We cloned four CYP1 genes in *S. schlegelii*, SsCYP1A, SsCYP1B, SsCYP1C1 and SsCYP1C2, and demonstrated that they are constitutively expressed in several organs. The observation that the induction of these genes varied in different organs (gill, liver, kidney and spleen) and at different exposure concentration of B[a]P suggest that the induced *S. schlegelii* CYP1 transcript patterns may be useful biomarkers for AHR agonistic environmental pollutants in seawater.

### 1.6 Reference

Arkoosh M.R., Clemons E., Huffman P., Kagley A.N., Casillas E., Adams N., Sanborn H.R., Collier T.K. & Stein J.E. 2001. Increased susceptibility of juvenile chinook salmon to vibriosis after exposure to chlorinated and aromatic compounds found in contaminated urban estuaries. Journal of Aquatic Animal Health 13, 257–268.

Bai S.C., Choi S.M., Kim K.W. & Wang X.J. 2001. Apparent protein and phosphorus digestibilities of five different dietary protein sources in Korean rockfish, *Sebastes schlegeli* (Hilgendorf). Aquaculture research 32, 99–105.

Bugiak B. & Weber L.P. 2009. Hepatic and vascular mRNA expression in adult zebrafish (*Danio rerio*) following exposure to benzo-a-pyrene and 2, 3, 7, 8-tetrachlorodibenzo-p-dioxin. Aquatic toxicology 95, 299–306.

Carlson E.A., Li Y. & Zelikoff J.T. 2002. Exposure of Japanese medaka (*Oryzias latipes*) to benzo [a] pyrene suppresses immune function and host resistance against bacterial challenge. Aquatic Toxicology 56, 289–301.

Carlson E.A., Li Y. & Zelikoff J.T. 2004. Benzo [a] pyrene-induced immunotoxicity in Japanese medaka (*Oryzias latipes*): relationship between lymphoid CYP1A activity and humoral immune suppression. Toxicology and applied pharmacology 201, 40–52.

Drew D.P., Hrmova M., Lunde C., Jacobs A.K., Tester M. & Fincher G.B. 2011. Structural and functional analyses of PpENA1 provide insights into cation binding by type IID P-type ATPases in lower plants and fungi. Biochimica et Biophysica Acta (BBA)-Biomembranes 1808, 1483–1492.

Duncan D.B. 1955. Multiple range and multiple f tests. Biometrics 11, 1–42.

El Nemr A., Said T.O., Khaled A., El-Sikaily A. & Abd-Allah A.M. 2007. The distribution and sources of polycyclic aromatic hydrocarbons in surface sediments along the Egyptian Mediterranean coast. Environmental Monitoring and Assessment 124, 343–359.

Galván N., Teske D.E., Zhou G., Moorthy B., MacWilliams P.S., Czuprynski C.J. & Jefcoate C.R. 2005. Induction of CYP1A1 and CYP1B1 in liver and lung by benzo (a) pyrene and 7, 12-d imethylbenz (a) anthracene do not affect distribution of polycyclic hydrocarbons to target tissue: role of AhR and CYP1B1 in bone marrow cytotoxicity. Toxicology and applied pharmacology 202, 244–257.

Goldstone H.M. & Stegeman J.J. 2006. A revised evolutionary history of the CYP1A subfamily: gene duplication, gene conversion, and positive selection. Journal of molecular evolution 62, 708–717.

Goldstone J.V., Jönsson M.E., Behrendt L., Woodin B.R., Jenny M.J., Nelson D.R. & Stegeman J.J. 2009. Cytochrome P450 1D1: a novel CYP1A-related gene that is not transcriptionally activated by PCB126 or TCDD. Archives of biochemistry and biophysics 482, 7–16

Godard C.A.J., Goldstone J.V., Said M.R., Dickerson R.L., Woodin B.R. & Stegeman J.J. 2005. The new vertebrate CYP1C family: cloning of new subfamily members and phylogenetic analysis. Biochemical and Biophysical Research Communications 331, 1016–1024.

Goksøyr A. 1995. Use of cytochrome P450 1A (CYP1A) in fish as a biomarker of aquatic pollution. In Toxicology in Transition 80-95.

Granberg A.L., Brunström B. & Brandt I. 2000. Cytochrome P450-dependent binding of 7, 12-dimethylbenz [a] anthracene (DMBA) and benzo [a] pyrene (B [a] P) in murine heart, lung, and liver endothelial cells. Archives of toxicology 74, 593-601.

Hall T.A. 1999. BioEdit: a user-friendly biological sequence alignment editor and analysis program for Windows 95/98/NT. Nucleic Acids Symposium Series 41, 95–98.

Hamberger B., & Bak S. 2013. Plant P450s as versatile drivers for evolution of species-specific chemical diversity. Philosophical Transactions of the Royal Society of London B: Biological Sciences, 368, 20120426.

Hankinson O. 1995. The aryl-hydrocarbon receptor complex. Annu Rev Pharmacol Toxicol 35, 307–340

Hawkins S.A., Billiard S.M., Tabash S.P., Brown R.S. & Hodson P.V. 2002. Altering cytochrome P4501A activity affects polycyclic aromatic hydrocarbon metabolism and toxicity in rainbow trout (*Oncorhynchus mykiss*). Environmental Toxicology and Chemistry 21, 1845–1853.

Hose J.E., Hannah J.B., Landolt M.L., Miller B.S., Felton S.P. & Iwaoka W.T. 1981. Uptake of Benzo(a)pyrene by gonadal tissue of flatfish and its effects on subsequent eggs development. Journal of Toxicology and Environmental Health 7, 991–1000.

Jönsson M.E., Orrego R., Woodin B.R., Goldstone J.V. & Stegeman J.J. 2007. Basal and 3, 3′, 4, 4′, 5-pentachlorobiphenyl-induced expression of cytochrome P450 1A, 1B and 1C genes in zebrafish. Toxicology and applied pharmacology 221, 29–41.

Jönsson M.E., Brunström B. & Brandt I. 2009. The zebrafish gill model: Induction of CYP1A, EROD and PAH adduct formation. Aquatic Toxicology 91, 62–70.

Jönsson M.E., Franks D.G., Woodin B.R., Jenny M.J., Garrick R.A., Behrendt L., Hahn M.E. & Stegeman J.J. 2009. The tryptophan photoproduct 6-formylindolo[3, 2-b]carbazole (FICZ) binds multiple AHRs and induces multiple CYP1 genes via AHR2 in zebrafish. Chemico-Biological Interactions 181, 447–454.

Kim J.H., Raisuddin S., Ki J.S., Lee J.S. & Han K.N. 2008. Molecular cloning and betanaphthoflavone-induced expression of a cytochrome P450 1A (CYP1A) gene from an anadromous river pufferfish, *Takifugu obscurus*. Marine Pollution Bulletin 57, 433–440.

Lee S.M., Jeon I.G. & Lee J.Y. 2002. Effects of digestible protein and lipid levels in practical diets on growth, protein utilization and body composition of juvenile rockfish (*Sebastes schlegeli*). Aquaculture 211, 227–239.

Lewis D., Gillam E., Everett S. & Shimada T. 2003. Molecular modelling of human CYP1B1 substrate interactions and investigation of allelic variant effects on metabolism. Chemico-Biological Interactions 145, 281–295.

Nebert D.W. & Karp C.L. 2008. Endogenous functions of the aryl hydrocarbon receptor (AHR): intersection of cytochrome P450 1 (CYP1)-metabolized eicosanoids and AHR biology. Journal of Biological Chemistry 283, 36061–36065.

Nelson D.R., Koymans L., Kamataki T., Stegeman J.J., Feyereisen R., Waxman D.J., ... & Gunsalus I.C. 1996. P450 superfamily: update on new sequences, gene mapping, accession numbers and nomenclature. Pharmacogenetics 6, 1–42.

Nilsen B.M., Berg K. & Goksoyr A. 1998. Induction of cytochrome P450 1A (CYP1A) in fish. A biomarker for environmental pollution. In: Phillips, I.R., Shepard, E.A. (Eds.), Cytochrome P450 Protocols. Methods in Molecular Biology 107, 423–437.

Rahman M.S. & Thomas P. 2012. Effects of hypoxia exposure on cytochrome P4501A (CYP1A) expression in Atlantic croaker: molecular mechanisms of CYP1A down regulation. PLoS ONE 7.

Reynaud S. & Deschaux P. 2006. The effects of polycyclic aromatic hydrocarbons on the immune system of fish: a review. Aquatic Toxicology 77, 229–238.

Rice C.D., Schlenk D., Ainsworth J. & Goksøyr A. 1998. Cross-reactivity of monoclonal antibodies against peptide 277–294 of rainbow trout CYP1A1 with hepatic CYP1A among fish. Marine environmental research 46, 87–91.

Scholz S., Behn I., Honeck H., Hauck C., Braunbeck T. & Segner H. 1997. Development of a monoclonal antibody for ELISA of CYP1A in primary cultures of rainbow trout *Oncorhynchus mykiss* hepatocytes. Biomarkers 2, 287–294.

Scott J., Incardona J.P., Pelkki K., Shepardson S. & Hodson P.V. 2011. AhR2-mediated, CYP1A-independent cardiovascular toxicity in zebrafish (*Danio rerio*) embryos exposed to retene. Aquatic Toxicology 101, 165–174

Shimada T. 2006. Xenobiotic-metabolizing enzymes involved in activation and detoxification of carcinogenic polycyclic aromatic hydrocarbons. Drug Metabolism and Pharmacokinetics 21, 257–276.

Stegeman J.J., Miller M.R. & Hinton D.E. 1989. Cytochrome P450IA1 induction and localization in endothelium of vertebrate (teleost) heart. Molecular pharmacology, 36(5), 723-729.

Wang L., Camus A.C., Dong W., Thornton C. & Willett K.L. 2010. Expression of CYP1C1 and CYP1A in *Fundulus heteroclitus* during PAH-induced carcinogenesis. Aquatic toxicology 99, 439–447.

Xue W. & Warshawsky D. 2005. Metabolic activation of polycyclic and heterocyclic aromatic hydrocarbons and DNA damage: a review. Toxicology and Applied Pharmacology 206, 73–93.

Zanette J., Jenny M.J., Goldstone J.V., Woodin B.R., Watka L.A., Bainy A.C. & Stegeman J.J. 2009. New cytochrome P450 1B1, 1C2 and 1D1 genes in the killifish Fundulus heteroclitus: Basal expression and response of five killifish CYP1s to the AHR agonist PCB126. Aquatic Toxicology 93, 234–243.

# CHAPTER II

## Effects of trichlorfon on biochemical parameters in *Sebastes schlegelii*

**Abstract**

To evaluate the effects of trichlorfon (TCF) on the oxidative stress, neurotoxicity, cortisol level, drug conjugation, and drug metabolism in *Sebastes schlegelii* was exposed to trichlorfon at concentrations of 30 and 150 mg/kg bw at two different temperature (15 and 25 °C). TCF exposure induced significant alterations in antioxidant responses in the gill and liver. The activities of catalase (CAT) and glutathione S-transferase (GST) as well as glutathione (GSH) levels decreased after the TCF exposure depending on water temperature, and then recovered to normal states until 336 hours. Remarkable antioxidant responses were observed in the gill, because the gill seemed to be more sensitive to oxidative stress than the liver based on CAT, GST, and GSH levels. Acetylcholinesterase (AChE) activity was significantly inhibited in the brain at trichlorfon concentration of 30 and 150 mg/kg, indicating neurotoxicity following trichlorfon exposure. As a stress indicator, plasma cortisol was significantly elevated following exposure to trichlorfon depending on water temperature, thereby enhancing stress, leading to hypothalamic-pituitary-interrenal axis activation. And cytochrome P4501A (CYP1A) levels were monitored in liver. CYP1A levels during the first 3h of exposure, followed by a significant decrease. These results suggest that TCF exposure can induce considerable alterations in detoxifying system. Although the responses showed similar trends in both organs, they were more important in liver than in gill. The early inhibitory effect in CAT activity and GSH content produced by TCF may be associated with a high degree of oxidative stress. Early induction of CYP1A, GST and CAT by TCF followed by enzyme inhibition suggests a milder or delayed oxidative stress, revealing organophosphate compounds metabolization. AChE inhibition is a good biomarker for TCF exposure.

## 2.1 Introduction

The use of organophosphorus pesticides (OPPs) such as trichlorfon (TCF) pesticide in aquaculture has become widespread because of their relatively low bioacucumulation and short-term persistence (Rao & Kavitha 2004). The dosage necessary to kill ectoparasites varies from 0.1 to 1 mg/L in the ponds (Chang et al., 2006). However, excessive amounts are often applied in aquaculture management. Residue of TCF in the water have cause problems and TCF is rapidly hydrolyzed to dichlorvos, which is much more toxic and harmful to non-target organisms such as fish, crabs, and shrimps (Soumis et al., 2003). Fishes absorb pesticides through the gill and body surface, resulting in harmful effects. The toxicity of TCF has been studied extensively in both in vivo and in vitro conditions. Xu et al (2009) reported that TCF induced apoptosis with mitochondrial vacuolization and nuclear shrinkage in hepatocyte cultures of *Carassius auratus gibelio* in vitro. And maturing mouse oocytes were interfered with spindleformation by TCF in vitro (Cukurcam et al., 2004). Recent studies have implicated oxidative stress as a possible causative mechanism for the non-target toxicity of organophosphates including TCF (Hai et al., 1997; Li & Zhang 2017)

Oxidative stress occurs when the critical balance between oxidants and antioxidants is disrupted owing to the excessive accumulation of reactive oxygen species (ROS). TCF exposure induced the production of ROS, such as hydrogen peroxide ($H_2O_2$), hydroxyl radical, and superoxide radical, which cause DNA damage, lipid peroxidation (LPO), and protein oxidation resulting in oxidative stress (Feng et al., 2008; Xu et al., 2012). In response, there is alteration in the levels of the antioxidant defenses in an attempt to minimize oxidative damage. Among the major antioxidant enzymes are SOD, which converts superoxide anion radical (O2-) to hydrogen peroxide ($H_2O_2$), and catalase (CAT) which reduce $H_2O_2$ to oxygen and water ((Regoli & Giuliani, 2014).

Cytochrome P450 1A (CYP1A) is a key member of the cytochrome P450 family enzyme. Phase I drug metabolism by the CYPs include oxidation, reduction, and hydrolysis of toxic substance. This class of metabolic enzyme is responsible for the biotransformation of the majority of the drugs. The metabolites

formed in the reactions of phase I are conjugated with phase II substrates by transferases, such as GST, enhancing their excretion.

Some OP insecticides are acetylcholinesterase (AChE) inhibitors that block the cholinergic neurotransmission at synapses of pest invertebrates (Smulders et al., 2003). Inhibition of AChE induces undesirable effects in non-target organisms. Recent studies have shown that trichlorfon can strongly disrupt nerve function at low concentrations via inhibition of AChE activity (Sanchez-Hernandez and Walker, 2000; Chandrasekara and Pathiratne, 2005). In this way, the activity of the brain and the muscle AChE can be a critical biomarker to investigate the possible neurotoxic effects of the TCF.

TCF exposure induces stress and may activate the neuroendocrine pathway, including the hypothalamic-pituitary-interrenal (HPI) axis, which in turn leads to the release of cortisol in aquatic animals (Guimarães and Calil, 2008). Physiological stress is associated with high susceptibility to disease. Information on the relationship between cortisol and TCF is important to understand the mechanism underlying stress effects.

Among the various environment factors, temperature is one of the most critical factors affecting the growth and survival of aquatic organisms. High temperature stress for *S. schlegelii* (optimum feeding temperature 15-19°C) is a potential threat, which have been implicate in chronic stress and disease epidemics, as well as in the occurrence of mortality.

However, there is little data regarding toxicity of the TCF to *S. schlegelii*, specifically about biochemical response after fish exposure to low and high amount of TCF. We found in the literature about TCF effects in *Cyprinus carpio* (Ghanim et al., 2008) and *Oreochromis niloticus* (Guimarães et al., 2007). The major contribution brought by our study was to provide more data such as oxidative stress, biotransformation, neurotoxicity, and stress levels about TCF effects from *S. schlegelii* seawater fish.

In the present study, we aimed to investigate the effect of TCF (30 and 150 mg/L) on antioxidant defense system in the gill and liver of *S. schlegelii* at different two temperatures (15 and 25°C). Specifically, enzymatic antioxidants (SOD and CAT) in the gill and liver, the possible neurotoxic effects (AChE) in the brain and muscle, stress indicator (cortisol), in the plasma, and drug metabolism (CYP1A) in the

liver were measured.

## 2.2 Material and Methods

### 2.2.1 Animals

Five hundred clinically healthy Black rockfish (*Sebastes schlegelii*) with a mean weight of 100 ± 5 g were obtained from a commercial farm in Tongyeong, Korea. All fish were randomly and equally distributed in twenty of 400L aquarium tanks under continuous aeration (n=25 fish per tank). The water was analyzed daily for different quality parameters. They were acclimatized to the laboratory conditions for three weeks and fed daily with drug-free pellet dry feed. To make different water temperature (12 and 22°C.), ten of 12°C group tanks maintained their temperature using a cooler. And the other ten of 22°C group tanks changed the water temperature at a rate of 1°C per day using a heater. Control fish were kept separately in a clean tank under the same conditions. In order to focus the drug residues between TCF and temperature, feeding was withheld for about 3 weeks during the experiment. The water in the tank was changed daily to remove excretory wastes. The experiments of the current study were approved by the Institutional Animal Care and Use Committee of Pukyong National University (Busan, South Korea).

### 2.2.2 Exposures and sampling

All fish were randomly and equally divided into two groups (12 and 22°C). Then each group was further equally divided into two of drug exposure subgroups. First and Second subgroups maintained in 100L tank at TCF concentration of 30 mg kg bw at 12°C and 22 °C, respectively, for 10min. Third and the last fourth subgroups maintained in 100L tank at TCF concentration of 150 mg kg bw at 12°C and 22 °C, respectively, for 10min. After dipping administration, each group was removed from the dipping tank and immediately transferred into clean seawater. The administration was operated by six experienced experimenters and could be completed in 20 min for each subgroup. Subgroups of ten fish were sampled

at 0.5, 1, 3, 6, 12, 24, 48, 96, 168, and 336 h after dipping administration. Blood was collected from the caudal blood vessel using a heparinized 3 mL syringe within 1 min after administration. Also the liver and muscle was collected from each time. To obtain plasma, blood samples were immediately separated by centrifugation at 9,000 rpm for 10 min at 4°C and stored with muscle and liver at -70°C until further analysis.

**2.2.3 Sample collection**

Samples of the gill, liver, brain and muscle (n= 10/group) were used to evaluate the enzymatic activity of TCF. Samples of issues were thawed on ice, weighed, and homogenized in potassium phosphate buffer (0.1M pH 7.0) 1:10 (w/v), and then were centrifuged at 10000 g for 30 min at 4°C. The supernatants were stored at -80°C and used for subsequent assays. Blood was drawn directly through the caudal vein by using disposable syringes with a 26-gauge needle. The syringe and needle were pre-chilled and coated with an anticoagulant (heparin lithium salt, 100 unit mg-1; MP Biomedicals, USA). Blood samples were centrifuged at 400 g for 20 min at 4°C, and the plasma was collected and stored at -20°C until further use.

**2.2.4 Antioxidant responses**

Superoxide dismutase (SOD) activity was measured as the rate of WST-1 reduction using SOD Assay Kit (Dojindo Molecular Technologies, Inc.). One unit of SOD is defined the amount of enzyme required to inhibition the autooxidation of pyrogallic acid (Gao et al., 1998), at 450nm spectrophotometrically. And expressed as unit mg protein$^{-1}$.

The catalase (CAT) activity was measured using a catalase assay kit from Cayman Chemical (Ann Arbor, Ml), according to the manufacturer's protocols. The CAT levels in the samples induced a decrease in H2O2. The absorbance was read at 560 nm and expressed as unit mg protein$^{-1}$.

Glutathion-S-transferase (GST) activity was measured using the method by Habig et al. (1974), with modifications. GST catalyzes the conjugation between 1-chloro-2,4 dinitrobenzene (CDNB) and

glutathione (GSH). The change in optical density associated with the reaction was measured at 340 nm, and the enzyme activity was calculated as nmol min-1 mg protein$^{-1}$.

Reduced glutathione (GSH) was estimated using the method by Beutler and Kelly (1963), and expressed as µmol mg protein-1. These parameters were measured using the Nano Quant Infinite M200 spectrophotometer (Tecan Group Ltd, Männedorf, Switzerland).

**2.2.5 Inhibition of AChE activity**

AChE activity was determined by the method proposed by Ellman et al. (1961). AChE activity was analyzed at 412 nm for 5 min (at intervals of 1 min) in the presence of 1 mM acetylthiocholine as substrate and 0.1 mM 5,5′-dithiobis-2-dinitrobenzoic acid (DTNB). Each AChE activity measurement was performed in duplicate. AChE activity was expressed as nmol min$^{-1}$ mg protein$^{-1}$.

**2.2.6 Plasma cortisol**

Plasma cortisol concentration was measured with a monoclonal antibody enzyme-linked immunosorbent assay (ELISA) quantification kit (Enzo Life Sciences, NY, USA) according to the manufacturer's instructions. The sensitivity of the assay was 56.72 pg mL$^{-1}$ and the inter-assay coefficient of variation (CV) for cortisol was <10%.

**2.2.7 CYP1A expression**

Total RNA was isolated from liver samples using the HiYield Total RNA Mini Kit (RBC Biosciences, Taiwan) according to the manufacturer's instruction. Purified RNA was quantified based on its OD at 260/280 nm by using a UV spectrophotometer (Ultrospec 6300 pro, Amersham Biosciences, Piscataway, NJ, USA). The absorbance ratios of all samples ranged from 1.80 to 2.00, indicating a satisfactory purity of the RNA samples. cDNA was synthesized from 2 µg of total RNA using a cDNA synthesis kit (EnzoLife Sciences Inc., Farmingdale, NY, USA) according to manufacturer instruction. Quantitative real-time polymerase chain reaction (qPCR) for CYP1A gene expression was performed using gene

specific primers (Table 2). Real-time PCR assays were carried out in a quantitative thermal cycler (LightCycler® 480 II, Roche Diagnostics Ltd., Rotkreuz, Switzerland) in a final volume of 20 μL containing 10 μL 2× Master Mix (LightCycler® 480 SYBR Green I Master, Roche Diagnostics, Rotkreuz, Switzerland) and 1 μL cDNA mix. The β-actin reference gene was used as the internal control. Reaction cycling conditions consisted of 5 min at 95°C followed by 45 cycles of denaturation for 10 s at 95°C, annealing for 10 s at 58°C, and extension for 10 s at 72°C. To analyze the mRNA expression levels, the relative quantitative values were expressed in accordance with CT methods (2 -ΔΔCT method).

**2.2.8 Protein determination**

Protein concentration in all tissues was measured by the classical Bradford method with Coomassie Brilliant Blue G-250 (Bradford, 1976), using bovine serum albumin (Sigma, USA) as a standard. The absorbance of the samples was measured at 595nm.

**2.2.9 Statistical analysis**

The experiment was conducted for 2 weeks and performed in triplicate. Statistical analysis of data was performed using the SPSS/PC+ statistical package (SPSS Inc., Chicago, IL, USA) and GraphPad Prism 5.0 (GraphPad Software Inc., San Diego, CA). All data were presented as the mean ± S.E. Significant differences between groups were identified using one-way ANOVA followed by Duncan's test for multiple comparisons (Duncan, 1995). The significance level was set at $P<0.05$.

## 2.3 Results

### 2.3.1 Antioxidant responses

Changes in CAT activity in the gill and liver are shown in Fig 2.1. It was observed that CAT activity in the gill decreased after the start of administration in 30 and 150 mg/kg bw at 15 and 25℃. In the gill, CAT levels declined at 1h or 6h after dipping at 30 mg/kg bw at 15 and 25℃. And it started to recover at 12h both concentrations at 15 and 25℃. 150 mg/kg bw group in the gill, CAT levels declined at 6h and it started to recover at 12h both concentrations at 15 and 25℃. The CAT activity in the liver showed similar patterns in 30 and 150 mg/kg bw at 15 and 25℃. CAT activity declined at 3h after dipping, then started to recover at 12h, maintained the normal states following the time until 336 hours.

Changes in GSH content in the gill and liver are shown in Fig 2.2. It was observed that the GSH levels in the gill and liver decreased and recovered throughout the study when compared with the levels in the control group. In the gill, considerable decrease in GSH levels was observed at 6h following exposure to 30 and 150 mg/kg bw at 15 and 25℃. Similarly, in the liver, the GSH levels in 30 and 150 mg/kg bw at 15 and 25℃ declined at 3h after dipping TCF and it started to recover normal states until 336 hours.

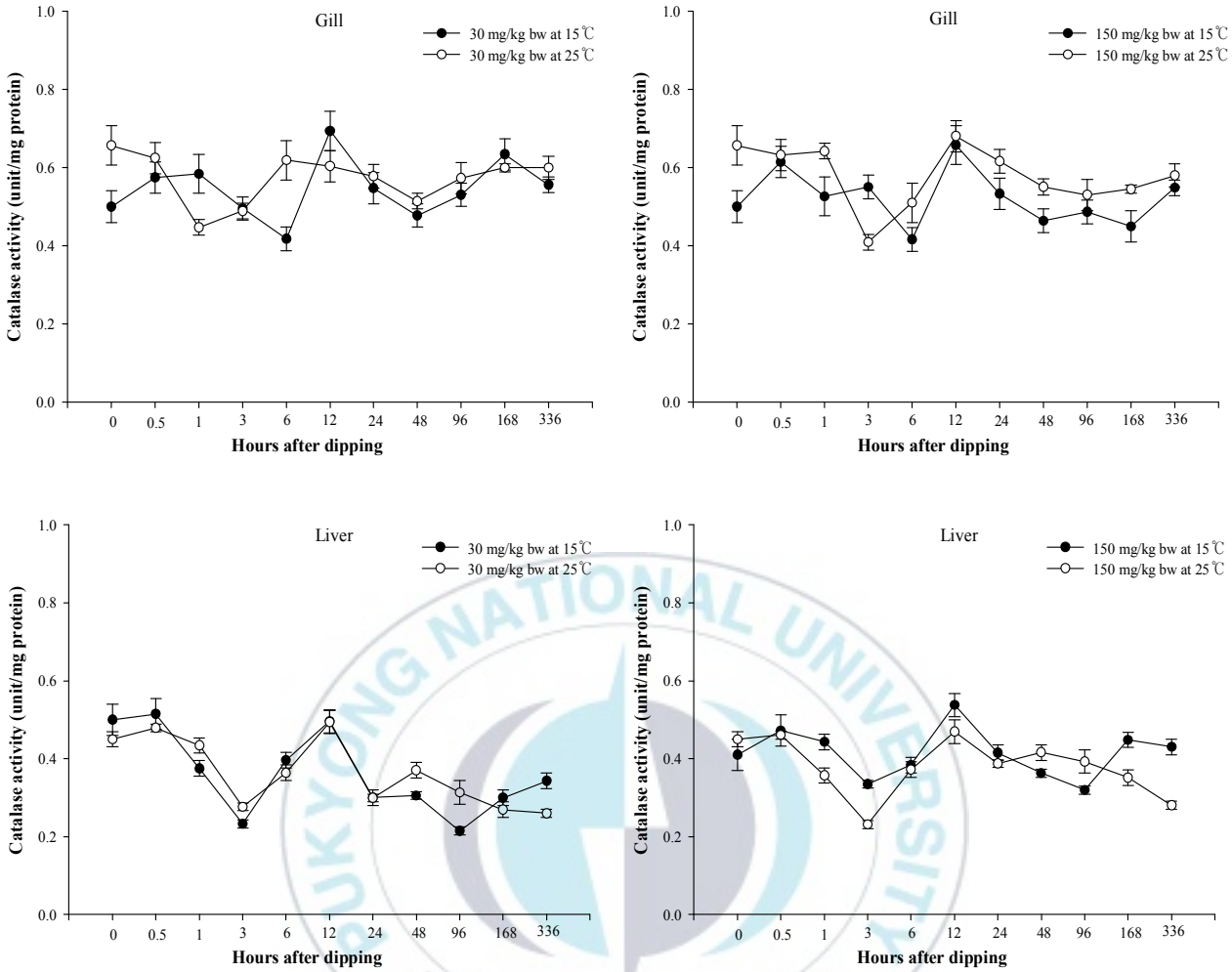


Fig 2.1 Changes of CAT activity in gill and liver of *Sebastes schlegelii* exposed to TCF (30 and 150 mg/kg bw) at different temperatures. Each value represents a mean value ± SD of three replicates (n = 10).

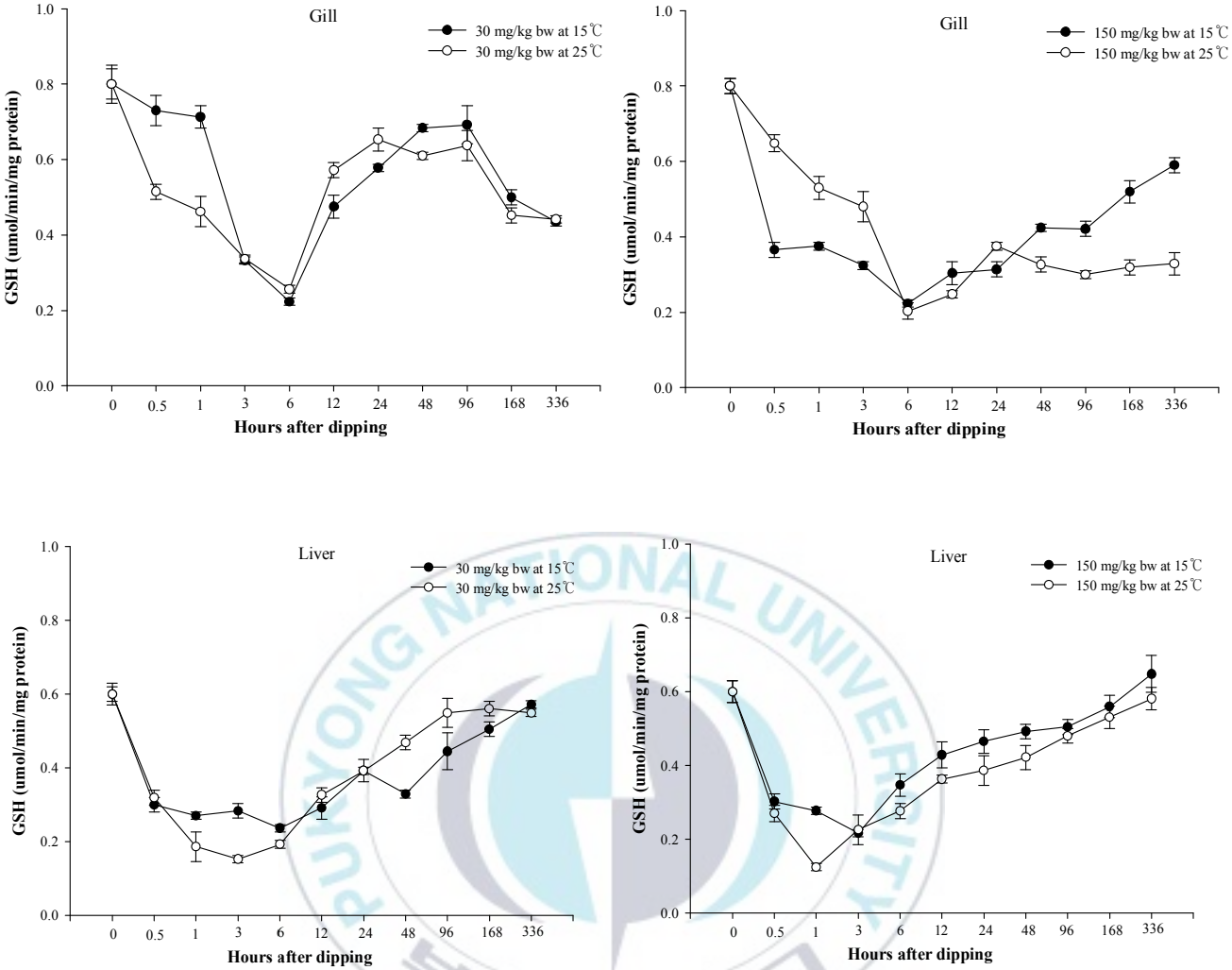


Fig 2.2 Changes of GSH activity in gill and liver of *Sebastes schlegelii* exposed to TCF (30 and 150 mg/kg bw) at different temperatures. Each value represents a mean value ± SD of three replicates (n = 10)

### 2.3.2 Inhibition of AChE activity

Significant inhibition of AChE activities in the brain of *S. schlegelii* was observed with increasing toxicant levels and temperature (Fig 2.3). At the TCF concentration 30 mg/kg bw, AChE activities in the brain were significantly inhibited compared with the activities in the control after administration (decreased to 6.9 fold and 12.3 at 15 and 25℃, respectively). At the TCF concentration 150 mg/kg bw, AChE activities in the brain were significantly inhibited to 19 fold and 6.17 fold at 15 and 25℃, respectively. Then the AChE activities start to maintain a positive state.

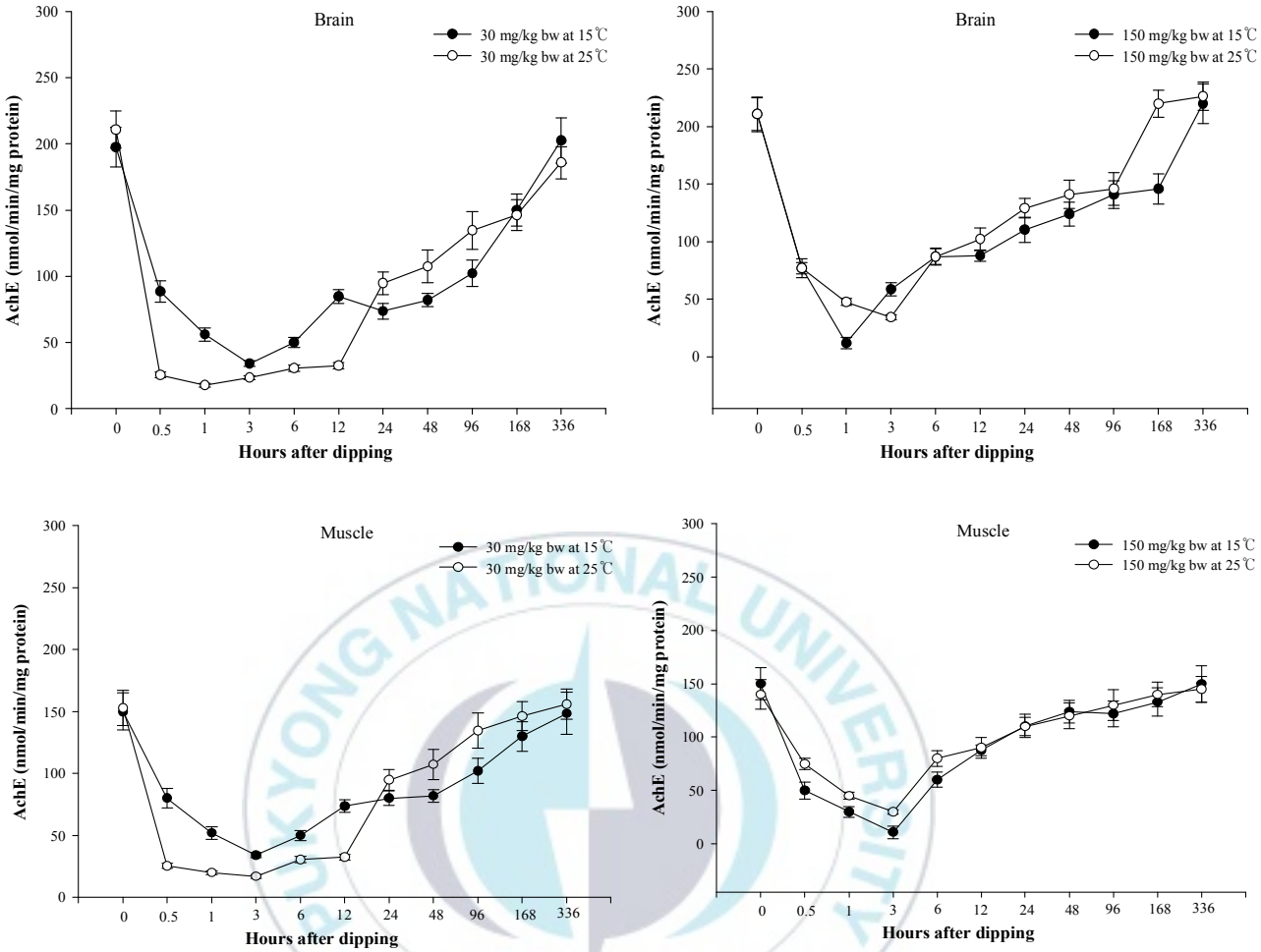


Fig 2.3 Changes of AChE activity in brain of *Sebastes schlegelii* exposed to TCF (30 and 150 mg/kg bw) at different temperatures. Each value represents a mean value ± SD of three replicates (n = 10).

### 2.3.3 Stress indicator

To assess the stress level following TCF exposure at different temperatures, the plasma cortisol levels in *S. schlegelii* were analyzed (Fig 2.4). The plasma cortisol levels increased with increasing toxicant levels and time after administration compared to the levels in control. Cortisol level increased substantially above TCF concentrations of 30 and 150 mg/kg bw. The cortisol showed the highest level at 6h after dipping, then start to decrease to maintain a positive state. And the changes of cortisol level in 25 are much more than 15 .

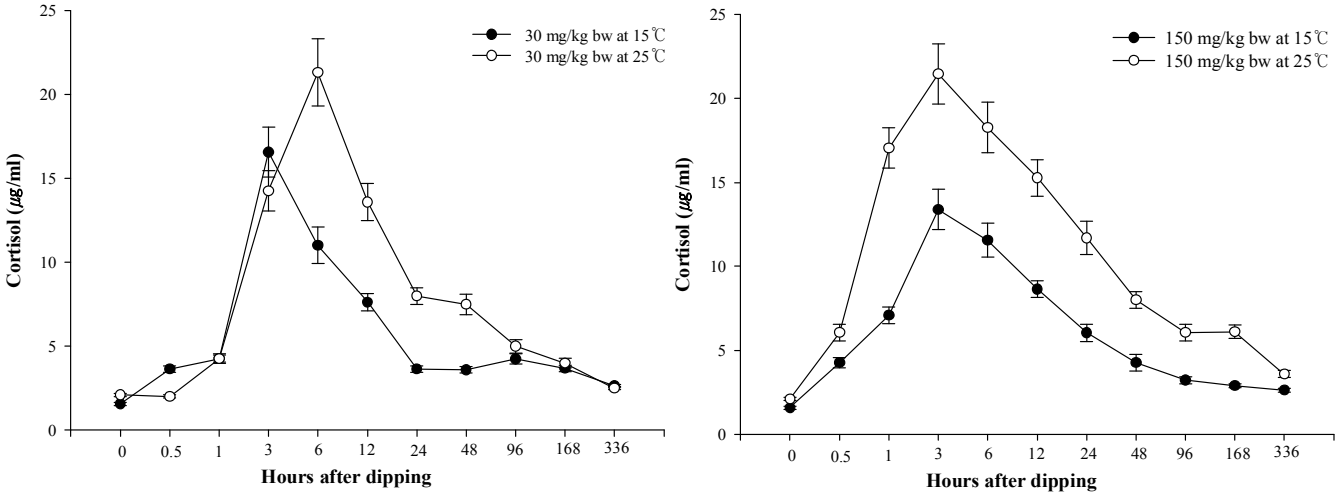


Fig 2.4 Changes of Cortisol levels in serum of *Sebastes schlegelii* exposed to TCF (30 and 150 mg/kg bw) at different temperatures. Each value represents a mean value ± SD of three replicates (n = 10).

### 2.3.4 GST phase II

Changes in GST in the gill and liver are shown in Fig 2.5. It was observed that the GST levels in the gill and liver start to decrease after the start of administration in 30 and 150 mg/kg bw at 15 and 25 . In the gill, GST values declined at 1h or 3h after dipping and started to recover at 6h or 12h both concentrations at 15 and 25 . And the changes of GST values in the gill are much more than the liver. The liver GST values declined at 3h in the 30mg/kg group and at 6h in the 150mg/k group. GST values recover the normal states following the time until 336 hours.

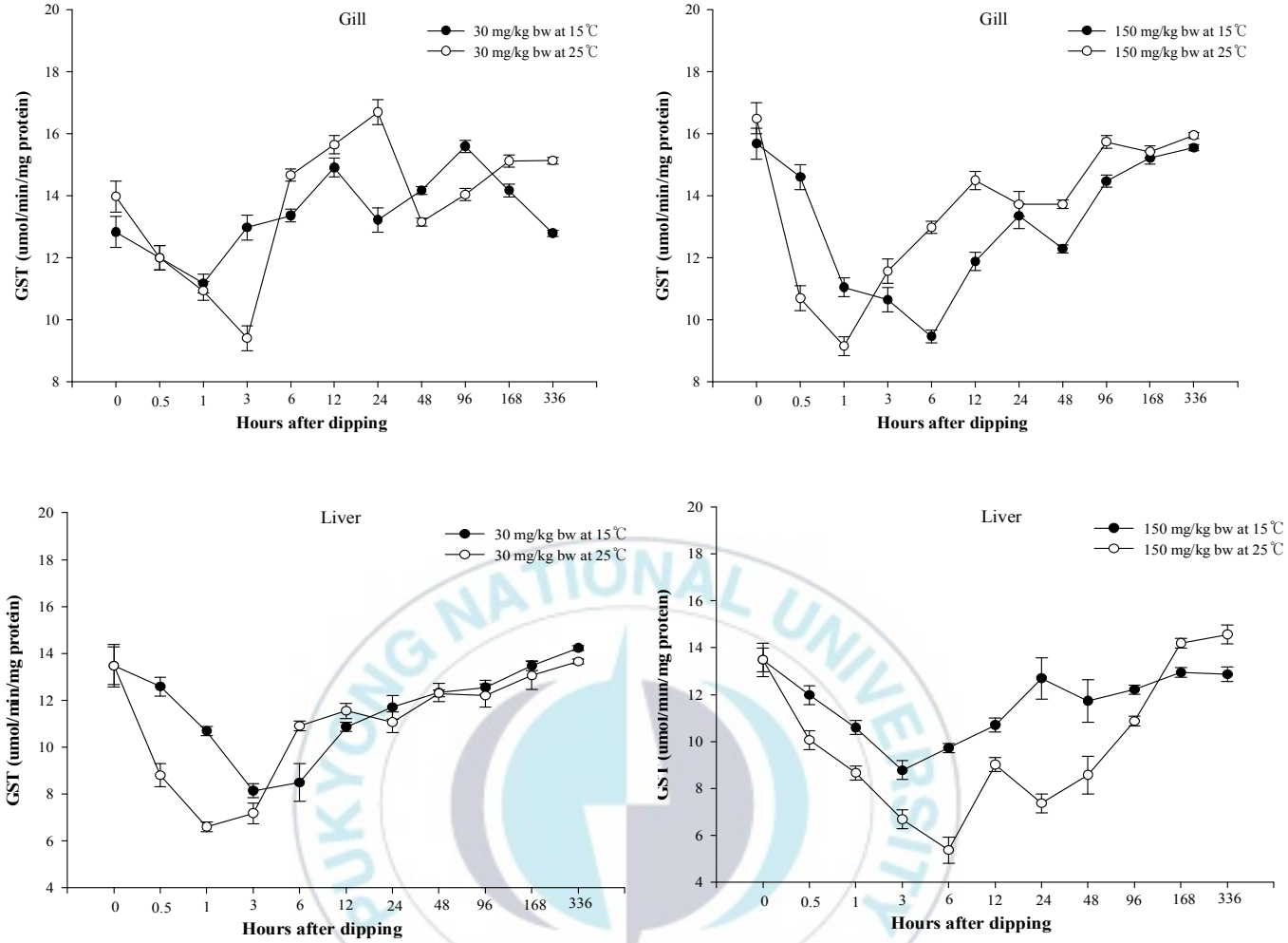


Fig 2.5 Changes of GST activity in gill and liver of *Sebastes schlegelii* exposed to TCF (30 and 150 mg/kg bw) at different temperatures. Each value represents a mean value ± SD of three replicates (n = 10).

### 2.3.5 CYP1A expression

The expression levels in CYP1A gene in the liver of *S. schlegelii* were analyzed by real-time PCR (Fig 2.7). CYP1A expression declined at 0.5h after TCF 30mg/kg dipping. Then the CYP1A expression showed the highest level at 3h (2-2.6 fold compared to control). Similarly, CYP1A expression declined at 1h after TCF 150mg/kg dipping. Then the CYP1A expression showed the highest level at 3h (2-2.5 fold compared to control). CYP1A expression levels recover the normal states following the time until 336 hours.

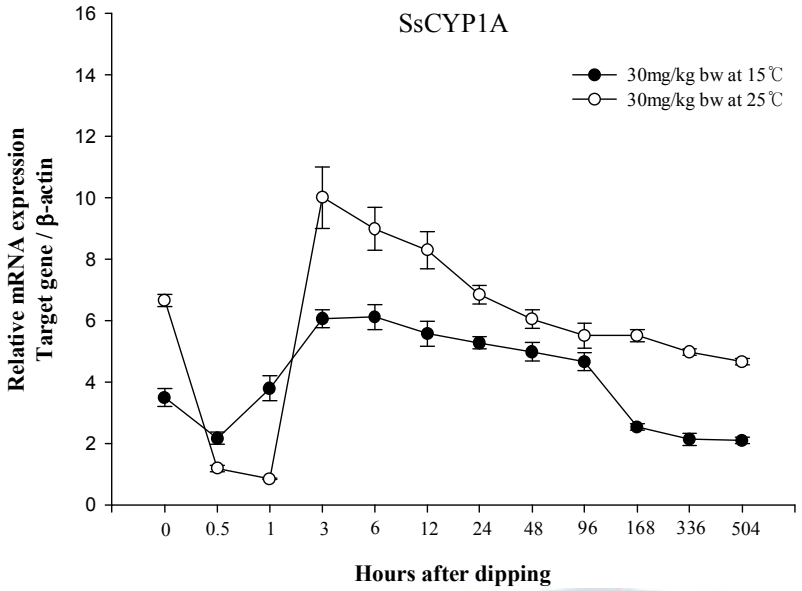


Fig 2.6 CYP1A mRNA expression in liver of *Sebastes schlegelii* exposed to TCF (30 mg/kg bw) at different temperatures. Each value represents a mean value ± SD of three replicates (n = 10).

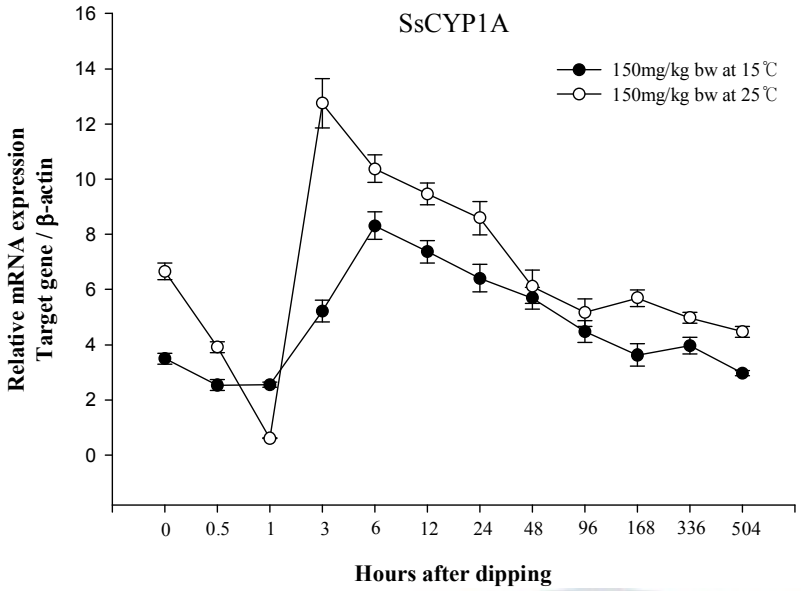


Fig 2.7 CYP1A mRNA expression in liver of *Sebastes schlegelii* exposed to TCF (150 mg/kg bw) at different temperatures. Each value represents a mean value ± SD of three replicates (n = 10).

## 2.4 Discussion

Xenobiotics come into the body and produce active oxygen free radicals through a series of metabolic conversion. If they are not removed clearly, the body balance will be destroyed and cause organisms oxidative damage (Net et al., 2006). The antioxidant defense systems involved a series of antioxidant enzymes and low molecular non-enzymatic antioxidants. They serve as crucial role in biological defense against oxidative stress at a cellular level. The biomarkers of responses were necessary to sub-acute toxicities of TCF to fish and provide further insight into the toxic mechanisms. The present study assessed the activities of main antioxidant enzyme viz., CAT, GST and content of non-enzymatic antioxidant viz., GSH in response to 30min exposure to TCF at 30 and 150 mg/kg bw at 15 and 25℃, respectively.

Many studies pointed out that the antioxidant defense systems could be considerably induced under a certain level of stress at a given time. Under the increasing time and concentration of drugs, that system showed a decrease tendency. In the present study, the antioxidative enzymes activities and non-enzymatic antioxidant content followed a changing factor of being activated at TCF concentration and two different temperatures. Changes levels in the antioxidant defense systems described that a biological response to exposure to sub-lethal concentration of TCF existing a treatment for parasite. A significant inhibition in all the tested tissues (gill and liver0 was induced by TCF at the highest concentration of 150 mg/kg bw, which could indicate that the self-scavenging capacity of antioxidant defense systems was exceeded by over accumulating amount of free radicals and TCF posed impact on the balance of antioxidant defense system and oxidative stress in vivo under this exposure concentration.

CAT is an enzyme located in peroxisomes and facilitates the elimination of the resulting H2O2, which is metabolized to molecular oxygen and water. The elevation of CAT activity could eliminate the resulting H2O2 and get off greater oxidative damage in the body. In our study, CAT activity in *S. schlegelii* fluctuated with the concentration of TCF and time after administration.

GSH is a major sulfhydryl compound with low MW that act as a protective reagent against numerous

toxic compounds through the –SH groups and a hydrogen donor of GPx catalyzing H2O2 or organic peroxides reduction reaction (Moreno et al., 2005). Our results showed that GSH varied with the concentration of TCF and time after administration. The changes of GSH contents in the gill and liver were relatively sensitive. Exposure to 150 mg/kg bw of TCF caused a significant decrease in GSH contents in the exposed organs. It was consistent with the generation of excessive ROS that reacted with and neutralized GSH. This result was in good agreement with Catalgol et al (2007) and Zhang et al (2004), who reported decreased GSH levels following exposure to 2,4-dichlorophenol in the liver in *Carassius auratus*.

Glutathione S-transferases (GST) mediated detoxification an integral part of the Phase I (oxidation) or Phase II (conjugation) system that metabolizes lipophilic drugs and other foreign compounds. This system is the conversion of lipophilic drugs to more polar derivatives in a way that can facilitate their elimination and inactivation. GSTs utilize glutathione (GSH) in a broad range of reactions of cellular metabolism such as conjugation, peroxidase activities, and noncatalytic ligand binding reactions (Waxman, 1990). GST catalyzed reaction involve the direct coupling of GSH conjugation, where they catalyze the nucleophilic attack of a thiolate anion of glutathione reduced (GS-) in the electrophilic center of drugs. Then it neutralized the greatly reactive nucleophilic sites of the chemical substrates and/or increases its water solubility to facilitate its excretion from the cell (Habig et al., 1974). Also GST-based detoxification may occur through the dehydrochlorination reaction, using GS- as a cofactor to remove a hydrogen atom from the substrate leading to the elimination of chlorine (Clark & Shamaan 1984). Although this general reaction may occur nonenzymatically, particularly at high pH (>8 and 9). Many reports have been observed that the implication of dehydrochlorination acitivity of GSTs to different classes of insecticides including organophosphates, pyrethroids and acaricides (Wei et al., 2001; Hemingway et al., 2004) GST might be responsible for catalyzing the conjugation of reduced GSH to an electrophilic carbon from trichlorfon, making trichlorfon more soluble and stable, thereby facilitating its easy excretion from the cell.

AChE activity is the standard biomarker of organophosphate pesticide. In the present study, AChE

activities were significantly reduced by different concentrations with the two different temeperatures at various time with brain homogenate. Our results showed the degree of enzyme inhibition followed a positive correlation with the TCF concentration. Consistent with our data, Okahashi et al (2005) reported that the inhibition of AChE activity occurs when rats intoxicated with different doses of fenitrothion (10, 20, and 60 mg/kg in the diet) for different periods. Inhibition of AchE means that restricted the activity of acetylcholine (ACh) in space and time, caused to increase in ACh content at cholinergic transmission on the muscular synapse. The inhibition of AChE is the representative symptom in organophosphate (OP) intoxication (Yamashita et al., 1997). According to Feng et al. (2008), AChE activity was inhibited at trichlorfon concentration of 0.1 mg L-1 in the muscle of Tilapia nilotica at 25°C. TCF including OP insecticide caused a significant concentration dependent and time make inhibition of AChE activity at all exposure drugs and times due to TCF is a cholinesterase inhibitor. The inhibition of AChE activity let the cellular metabolism decrease, induces deformities of cell membrane, and disturbs metabolic and nervous activity (Suresh et al., 1992).

Cytochrome P450 (CYP) is a hemoprotein, located mainly in the endoplasmic reticulum of various tissues. This enzyme function oxidative metaboslism of a variety of substrate from endogenous compounds to many exogenous compounds such as drugs, carcinogen, and natural products (Porter and Coon, 1991). Among the CYP gene families, CYP1A is known to be induced by polycyclic aromatic hydrocarbons, 3-methylcholanthrene (3-MC), β-naphthoflavone, and 2,3,7,8-tetrachlorodibenzo-p-dioxin (TCDD). In the present study, we observed that TCF and the two different temperature stress induced significant increase in the mRNA expression of CYP1A in the liver. OP compounds may accumulate in the cell membrane, then the CYP1A effectively start to metabolize OP in the liver where the main drug metabolism tissue. The most important CYP isoenzymes are CYP2B, CYP3A, and CYP2C in mammals. A great diversity of CYP450 enzyme in fish has been reported that CYP1A, 2B, 2E1, 2K1, and 3A-type of isoenzyme activities have been recently detected in rainbow trout hepatocytes (Nabb et al., 2006). Therefore, TCF may be metabolized by CYP1A as well as other cytochrome P450 isoenzyme.

Our results confirmed that the gill and liver of fish were most sensitive organs to TCF exposure as alteration on CAT, GSH and GST levels. Furthermore, our results showed that the brain of fish was also susceptible to TCF exposure, which was in high decrease of AChE in the exposed brain in our study.

## 2.5 References


Al-Ghanim K.A., Al-Balawi H.F., Al-Akel A.S., Al-Misned F., Ahmad Z. & Annazri H. 2008. Ethological response and haematological and biochemical profiles of carp (*Cyprinus carpio*) exposed to trichlorfon. Journal of food, agriculture & environment.

Beutler E. & Kelly B.M. 1963. The effect of sodium nitrite on red cell GSH. Cellular and Molecular Life Sciences 19, 96–97.

Bradford M.M. 1976. A rapid and sensitive method for the quantitation of microgram quantities of protein utilizing the principle of protein-dye binding. Analytical Biochemistry 72, 248–254.

Brown S.B., Eales J.G., Evans R.E., Hara T.J. 1984. Interrenal, thyroidal and carbohydrate responses of rainbow trout (Salmo gairdneri) to environmental acidification. Can. Journal of Fisheries and Aquatic Science 41, 36–45.

Chang C.C., Lee P.P., Liu C.H. & Cheng W. 2006. Trichlorfon, an organophosphorus insecticide, depresses the immune responses and resistance to *Lactococcus garvieae* of the giant freshwater prawn Macrobrachium rosenbergii. Fish and Shellfish Immunology 20, 574–585.

Clark A.G. & Shamaan N.A. 1984. Evidence that DDT-dehydrochlorinase from the house fly is a glutathione S-transferase. Pesticide Biochemistry and Physiology 22, 249–261.

Cukurcam S., Sun F., Betzendahl I., Adler I.D. & Eichenlaub-Ritter U. 2004. Trichlorfon predisposes to aneuploidy and interferes with spindleformation in in vitro maturing mouse oocytes. Mutation Research 564, 165–178.

Ellman G.L., Courtney K.D., Andres Jr V.V. & Featherstone R.M. 1961. A new and rapid colorimetric determination of acetylcholinesterase activity. Biochemical Pharmacology 7, 88–95.

Feng T., Li Z.B., Guo X.Q. & Guo J.P. 2008. Effects of trichlorfon and sodium dodecyl sulphate on antioxidant defense system and acetylcholinesterase of Tilapia nilotica in vitro. Pesticide Biochemistry and Physiology 92, 107–113.

Fevolden S.E., Refstie T. & Røed K.H. 1991. Selection for high and low cortisol stress response in Atlantic salmon (*Salmo salar*) and rainbow trout (*Oncorhynchus mykiss*). Aquaculture 95, 53-65.

Gao R., Yuan Z., Zhao Z. & Gao X. 1998. Mechanism of pyrogallol autoxidation and determination of superoxide dismutase enzyme activity. Bioelectrochemistry and Bioenergetics 45, 41–45.

Guimarães A.T.B., De Assis H.S. & Boeger W. 2007. The effect of trichlorfon on acetylcholinesterase

activity and histopathology of cultivated fish *Oreochromis niloticus*. Ecotoxicology and Environmental Safety 68, 57–62.

Habig W.H., Pabst M.J. & Jakoby W.B. 1974. Glutathione S-transferases the first enzymatic step in mercapturic acid formation. Journal of Biological Chemistry 249, 7130–7139.

Hai D.Q., Varga S.I. & Matkovics B. 1997. Organophosphate effects on antioxidant system of carp (*Cyprinus carpio*) and catfish (*Ictalurus nebulosus*). Comparative biochemistry and physiology. Part C, Pharmacology, toxicology & endocrinology 117, 83–88.

Hemingway J., Hawkes N.J., McCarroll L. & Ranson H. 2004. The molecular basis of insecticide resistance in mosquitoes. Insect biochemistry and molecular biology 34, 653–665.

Li B., Ma Y. & Zhang Y.H. 2017. Oxidative stress and hepatotoxicity in the frog, Rana chensinensis, when exposed to low doses of trichlorfon. Journal of Environmental Science and Health, Part B 52, 476–482.

Lin C.H., Kuan W.C., Liao B.K., Deng A.N., Tseng D.Y. & Hwang P.P. 2016. Environmental and cortisol-mediated control of Ca 2+ uptake in tilapia (*Oreochromis mossambicus*). Journal of Comparative Physiology B 186, 323-332.

Moreno I., Pichardo S., Jos A., Gomez-Amores L., Mate A., Vazquez C.M. & Camean A.M. 2005. Antioxidant enzyme activity and lipid peroxidation in liver and kidney of rats exposed to microcystin-LR administered intraperitoneally. Toxicon 45, 395–402.

Nabb D.L., Mingoia R.T., Yang C.H. & Han X. 2006. Comparison of basal level metabolic enzyme activities of freshly isolated hepatocytes from rainbow trout (*Oncorhynchus mykiss*) and rat. Aquatic toxicology 80, 52-59.

Nel A., Xia T., Madler L. & Li N. 2006. Toxic potential of material satthenano level. Science 311, 622–627.

Okahashi N., Sano M., Miyata K., Tamano S., Higuchi H., Kamita Y. & Seki T. 2005. Lack of evidence for endocrine disrupting effects in rats exposed to fenitrothion in utero and from weaning to maturation. Toxicology 206, 17-31.

Porter T.D. & Coon M.J. 1991. Cytochrome P-450: multiplicity of isoforms, substrates, and catalytic and regulatory mechanisms. Journal of Biological Chemistry 266, 13469–13472.

Rao J.V. & P. Kavitha. 2004. Toxicity of azodrin on the morphology and acetylcholinesterase activity of the earthworm *Eisenia foetida*. Environmental Research 96, 323–327.

Regoli F., & Giuliani M.E. 2014. Oxidative pathways of chemical toxicity and oxidative stress biomarkers in marine organisms. Marine Environmental Research 93, 106–117.

Suresh A., Sivaramakrishna B., Victoriamma P.C. & Radhakrishnaiah K. 1992. Comparative study on the inhibition of acetylcholinesterase activity in the freshwater fish *Cyprinus carpio* by mercury and zinc. Biochemistry international 26, 367-375.

Waxman D.J. 1990. Glutathione S-transferases: role in alkylating agent resistance and possible target for modulation chemotherapy—a review. Cancer research 50, 6449–6454.

Wei S.H., Clark A.G. & Syvanen M. 2001. Identification and cloning of a key insecticide-metabolizing glutathione S-transferase (MdGST-6A) from a hyper insecticide-resistant strain of the housefly Musca domestica. Insect biochemistry and molecular biology 31, 1145–1153.

Xu W.N., Liu W.B. & Liu Z.P. 2009. Trichlorfon-induced apoptosis in hepatocyte primary cultures of *Carassius auratus gibelio*. Chemosphere 77, 895–901.

Yamashita M., Yamashita M., Tanaka J. & Ando Y. 1997. Human mortality in organophosphate poisonings. Veterinary and human toxicology 39, 84-85.

# CHAPTER III

## Evaluation of pharmacokinetic effect in trichlorfon from *Sebastes schlegelii*

**Abstract**

This study presents a depletion study for trichlorfon (TCF) in serum, muscle and liver of *Sebastes schlegelii*. The fish were held in seawater at two different temperatures (15 and 25 ). TCF were administered dipping at the concentrations of 30 and 150 mg/kg bw for 30 min. Two different temperatures, two different concentrations were investigated. Ten fish were sampled at each of the days 0.5, 1, 3, 6, 12, 24, 48, 96, 128 and 336 hours after the start of veterinary medicine administration. However, for the calculation of the withdrawal periods, sampling day 1 was set as 24h after the dipping treatment. Fish samples were analyzed for TCF residues by liquid chromatography-mass spectrometry. TCF concentrations declined rapidly from serum, muscle and skin. Also we proposed the maximum residue limit (MRL) of TCF in fish muscle 0.002 μg/kg using the JECFA Tool. Following the proposed MRL, we calculated the withdrawal periods of TCF as 24 and 15 days at 15 and 25 . The investigation of this work is important to protect consumers by controlling the undesirable residues in aquatic organisms.

### 3.1 Introduction

Antibiotics are used to animals for a variety of reasons, including disease treatment, prevention of disease and growth promotion. Overuse and inappropriate use of antibiotics for nonbacterial infections cause drug-resistant bacteria outbreak and residues in food animals. The traces drugs leave in treated products are called 'residues'. It has now been escalated to one of the top health challenges facing the 21st century. To prevent the harmful impact of the antibiotic residues in environment, worldwide government authorities have established maximum residue limits (MRLs) for pharmacologically active substances including antibiotics in food animals as well as in farmed fish. MRL is the maximum amount of pesticide residue (expressed in mg/kg or μg/kg) that is legally tolerated in or on food or feed when pesticides are applied correctly in accordance with Good Agricultural Practice.

MRLs are established by the European Union (EU) and the Food & Agriculture Organization/World Health Organization (FAO)/WHO Codex Alimentarius Commission, which is advised scientifically by the Joint FAO/WHO Expert Committee on Food Additives (JECFA) (FAO/WHO, 2004). EU directives set different MRLs that adapted in each State member for each pesticide within each food group (European Commission 2005a; European Commission, 2005b). JECFA develops recommendations for MRLs of a veterinary drug in appropriate food animal species and tissues on the basis of a permanent ADI (Acceptable Daily Intake) and adequate residue data.

Antibacterial agents like pesticides, fungicides, and herbicides usage in food animal species, including fish, is controlled by guidelines, particularly in European commission, USA, Japan and Korea. MRLS for pharmacologically active antibiotic substance in edible tissues are listed by the Annex I to IV of the Commission Regulation (EU) No. 37/2010 (European Commission, 2010).

Following the importance of perception in MRLs, Ministry of Food and Drug Safety of Korea has set the 27 MRLs for aquatic veterinary drugs. The Ministry implement the system to prohibit the distribution of food including fish that contain agricultural chemicals above certain levels. To ensure that no residues above the MRL exist in the tissues of farmed fish, the appropriate withdrawal time must

be determined for veterinary drugs in each target fish species, at different temperature conditions (Rigos & Troisi, 2005).

There are many ways to antibiotic administration to farmed fish. Different farm circumstances have given rise to several ways to administering antibiotics like injection, dipping (immersion), and incorporation in the feed (i.e. oral administration). Injection and dipping methods are suitable only for intensive aquaculture and not much stressful to fish except handling stress. Especially, dipping is routine use that fish might expose the drugs by outer surface directly relying on uptake, predominantly by the gills and to some extent by imbibition (Horne & Robertson, 1987). Oral method with medicated food pellets are produced by mixing food ingredients with the drugs. The dosage required for treatment with the medicated components depends upon the original level of pharmacologically active ingredient per kg of fish body weight (B.W).

Considerable information is available on the kinetics of the TCF for Crucian carp *Carassius auratus gibelio* (Xu et al., 2012), giant freshwater prawn *Macrobrachium rosenbergii* (Yeh et al., 2005), and Nile tilapia *Oreochromis niloticus* L. (Guimarães et al., 2007). Despite the wide use of TCF against fish parasites in aquaculture, their pharmacokinetic profile has not been extensively studied in seawater fish species such as black rockfish *Sebastes schlegelii*. This species is one of the most abundant marine fish aquacultures in Korea, has been increased recently due to their fast growth characteristic. Also, withdrawal periods after administration of TCF in black rockfish at optimum temperature (15°C) and warn temperature (25°C) have not been calculated.

The EU has set an MRL for the TCF in farmed terrestrial animals at 0.01 mg/kg at 396/2005/EC. The Committee for veterinary Medical Products (CVMP) assessed trichlorfon (metrifonate) in 1999, but concluded that it was not possible to establish MRLs. The JECFA recommended an MRL for bovine milk of 50 μg/kg.

The aim of this work is to present a residue depletion study of TCF in serum, muscle and liver of cultured black rockfish by LC/MS/MS. Previously we reported simultaneous determination of trichlorfon and dichlorvos by LC/MS/MS (Woo et al., 2016). The calculation of MRL and the estimation

of appropriate withdrawal periods of the TCF are assessed, after administration with dipping at concentration of 30 and 150 mg $kg^{-1}$ B.W. at different water temperatures (15 and 25°C). And these data might have important role in correct dosage regime in seawater fish species.

### 3.2 Materials and Methods

#### 3.2.1 Chemicals

High purity (>99%) analytical standards of the aquatic veterinary drugs TCF (C4H8Cl3O4P) were purchased from Sigma Chemical Co. (St. Louis, MO). Trichlorfon used for administration was purchased from Daesung Microbiological Labs Co., Ltd. (Seoul, South Korea). HPLC-grade methanol, n-hexane, acetonitrile, and water were obtained from Merck (Darmstadt, Germany).

#### 3.2.2 Standard solutions

Stock standard solutions of TCF were prepared by dissolving TCF (1g) in MeOH (1mL) and stored at -20°C in the dark. Working standard solutions of various concentrations (2, 5, 10, 50, and 100 μg/L) were prepared by dilution of each of the above stock solutions by HPLC-water with 0.1% formic acid. These solutions were used to spike blank samples and prepare matrix-matched calibration solutions. Stability of these solutions was investigated.

#### 3.2.3 Animals

Five hundred clinically healthy Black rockfish (*Sebastes schlegelii*) with a mean weight of 100 ± 5 g were obtained from a commercial farm in Tongyeong, Korea. All fish were randomly and equally distributed in twenty of 400L aquarium tanks under continuous aeration (n=25 fish per tank). The water was analyzed daily for different quality parameters. They were acclimatized to the laboratory conditions for three weeks and fed daily with drug-free pellet dry feed. To make different water temperature (12 and 22°C), ten of 12°C group tanks maintained their temperature using a cooler. And the other ten of 22°C group tanks changed the water temperature at a rate of 1°C per day using a heater. Control fish

were kept separately in a clean tank under the same conditions. In order to focus the drug residues between TCF and temperature, feeding was withheld for about 3 weeks during the experiment. The water in the tank was changed daily to remove excretory wastes. The experiments of the current study were approved by the Institutional Animal Care and Use Committee of Pukyong National University (Busan, South Korea).

### 3.2.4 Exposures and sampling

All fish were randomly and equally divided into two groups (12 and 22°C). Then each group was further equally divided into two of drug exposure subgroups. First and Second subgroups maintained in 100L tank at TCF concentration of 30 mg kg bw at 12°C and 22°C, respectively, for 10min. Third and the last fourth subgroups maintained in 100L tank at TCF concentration of 150 mg kg b.w at 12°C and 22°C, respectively, for 10min. After dipping administration, each group was removed from the dipping tank and immediately transferred into clean seawater. The administration was operated by six experienced experimenters and could be completed in 20 min for each subgroup. Subgroups of ten fish were sampled at 0.5, 1, 3, 6, 12, 24, 48, 96, 168, and 336 h after dipping administration. Blood was collected from the caudal blood vessel using a heparinized 3 mL syringe within 1 min after administration. Also the liver and muscle was collected from each time. To obtain plasma, blood samples were immediately separated by centrifugation at 9,000 rpm for 10 min at 4°C and stored with muscle and liver at -70°C until further analysis.

### 3.2.5 TCF extraction from samples

TCF extraction and analysis were carried out according to the previously reported method (Woo et al, 2016). Briefly, after thawing at ice, 0.2 mL plasma samples were mixed with 0.5 mL of acetonitrile (ACN) and vortexed for 10 min followed by centrifugation at 9,000 rpm at 4°C for 10 min. The supernatant was filtered using a 0.2 mm membrane (Advantec, Tokyo, Japan), and then transferred to an autosampler vial for LC-MS/MS analysis. To extract the TCF from muscle and liver samples, two

gram of muscle or liver sample was accurately weighted, place in a glass mortar tube, and then added 20 mL of ACN. After these samples were homogenized for 2 min, the tubes were subjected to shaking for 10 min using a vortex mixer, followed by centrifugation at 13,000 rpm at 4°C for 10 min. The supernatant was poured into a 200 mL pear-shaped flask and evaporated to dryness at 40°C using a rotary evaporator (Eyela, Tokyo, Japan). The obtained dry residue was reconstituted two times with 10 mL of acetonitrile-saturated n-hexane, transferred into a test tube, and then shaken for 10 min. The mixed solution was allowed to separate, and the hexane layer was removed. The eluate was collected and re-evaporated to dryness at 40°C using a rotary evaporator. The residue was reconstituted with 1 mL of 50% MeOH and then centrifuged at 12,000 rpm at 4°C for 10 min. The supernatant was filtered using a 0.2 mm membrane (Advantec, Tokyo, Japan) prior to LC-MS/MS analysis within 24 h of preparation.

### 3.2.6 LC-MS/MS analysis

The LC-MS/MS system used in this work consisted of Agilent liquid chromatographic system (Agilent 1290 Infinity), equipped with an auto sampler, degasser, and heater column coupled with an Agilent 6430 Triple Quad LC/MS system (Agilent Technologies, Santa Clara, CA). Instrument control, data acquisition, qualitative and quantitative analysis were performed by Mass Hunter software (ver. A.00.06.32; Agilent Technology). Chromatographic separation was achieved on an Eclipse Plus C18 column (2.1 x 100 mm, 1.8 μm, Agilent Technologies) operating at 40°C. Mobile phases A was HPLC-water with 0.1% (v/v) formic acid and phase B was acetonitrile with 0.1% formic acid (v/v), pumped at the following gradient elution program: 90% eluent A changed to 20% into the first 7 min, maintained this composition until 9.5 min, and then increased to 90% from 10 to 15 min. The flow rate of the mobile phase was 0.3 mL/min, and the injection volume was 10 μL.

Positive Ionization mode in the electrospray ionization (ESI) source of the MS system was used for the detection of the TCF. The ionization conditions were as follows: capillary voltage 4.00 kV; nebulizer gas, N2; nebulizer gas flow rate, 11 L/min; nebulizer pressure, 40.0 psi; gas temperature, 350°C.

The selectivity and the sensitivity were improved using the Multiple reaction monitoring (MRM) mode, with the following precursor to product ion transitions and corresponding parameters: trichlorfon, m/z 259 to 109 with a declustering potential (DP) of 70 V and a collision energy (CE) of 11 eV. The first and most abundant MRM transition was used for quantification, whereas the other transitions were used for qualification (Table 3.1).

### 3.2.7 Statistical analysis and Withdrawal time calculation

The average concentrations of TCF at each time point were calculated, then mean concentrations and time data were subjected to non-compartmental model analysis in the program of PK Solver (Zhang et al., 2010) to get the pharmacokinetics parameters of TCF. All samples of the 30 and 150 mg/kg bw at different temperatures were analyzed in triplicate. Data from days 1, 2, 4, 7, and 14 after the last dose of the treatment were used for the withdrawal-time calculation using the statistical program WT1.4 (Hekman, 2004). To establish the withdrawal time (W.T), a linear regression to the sample data and pltting the natural logarithm (loge) of the residue concentration is recommended (EMEA, 1995a). The withdrawal period was determined as the time when the upper one-sided tolerance limit within a given confidence level (95% or 99%) was below the MRL. If the time point did not make a full day, the withdrawal time was rounded up to the next day.

### 3.3 Results

#### 3.3.1 Performance of the analytical method for TCF quantification

The method developed initially for the determination of TCF in serum, muscle and liver samples were validated according to Woo et al (2016). The results of the validation parameters evaluation are presented in Table 3.2-3.3. These results described that all the requirements of the validation parameters were met. Calibration curves were obtained by analyzing the peak area of the analytes in the chromatograms. A mixture of TCF standards was serially diluted to obtain samples in the range from 0.1 to 100 μg $L^{-1}$, which were analyzed using the optimized method. The equation of the TCF calibration curve in serum was y = 335.67x + 196.63 (y: peak area, x: TCF concentration, n = 5) with a coefficient of determination $r^2$ = 0.999, and the equation of the TCF calibration curve in muscle was y = 200.06x + 682.52 (y: peak area, x: TCF concentration, n = 5) with a coefficient of determination $r^2$ = 0.98. And the liver equation was y = 200.06x + 192.97 (y: peak area, x: TCF concentration, n = 5) with a coefficient of determination $r^2$ = 0.998. These results show that good linearity was observed for TCF.

Korea has not set MRLs for TCF in fish samples; however, the LOD and LOQ were found very low. The LOD and LOQ values for TCF was determined using the minimal accepted S/N values of 3.3 and 10, respectively (Table 3.4). The LOD values of trichlorfon in serum, muscle and liver were 0.2, 0.3, and 0.14 μg $kg^{-1}$, respectively.

The recovery was within the limits established (80-120%), with values ranging from 94 to 102% for serum, 85 to 88% for muscle, 57 to 60% for liver as the % coefficient of variance CV(%) ranged from 1.5 to 3.8% for serum, 1.6 to 2.7% for muscle, 2.9 to 3.7% for liver.

Table 3.1 MS/MS optimal operational conditions for the analysis of trichlorfon

| Compounds | RT(min) | Parent ion (m/z) | MRM transitions (m/z) | DP (V) | CE (eV) | Ionization |
|---|---|---|---|---|---|---|
| Trichlorfon | | 259 | 109[a] | 70 | 11 | ESI+ |
| | | 259 | 221[b] | 70 | 5 | |
| | | 259 | 79[b] | 70 | 9 | |

Table 3.2 Standard curve range, linearity and $r^2$ of TCF

| Compound | Matrices | Standard curve range (μg/kg) | Linearity | $r^2$ |
|---|---|---|---|---|
| TCF | Serum | 2.5-50 | y =335.67x + 196.63 | 0.999 |
| | Muscle | | y = 200.06x + 682.52 | 0.9805 |
| | Liver | | y = 200.06x + 192.97 | 0.998 |

Table 3.3 Recovery rate and coefficient of TCF in spiked *Sebastes schlegelii* samples

| Substance | Species | Matrix | Matrix curve($r^2$) | Spiked Conc(μg/kg) | Recovery rate(%) | CV(%) |
|---|---|---|---|---|---|---|
| TCF | *Sebastes schlegelii* | Serum | >0.999 | 5 | 94±2.1 | 2.5 |
| | | | | 10 | 98±3.5 | 3.8 |
| | | | | 100 | 102±1.1 | 1.5 |
| | | Muscle | >0.999 | 5 | 85±2.5 | 2.6 |
| | | | | 10 | 88±2.6 | 2.7 |
| | | | | 100 | 88±1.5 | 1.6 |
| | | Liver | >0.990 | 5 | 57±3.6 | 3.7 |
| | | | | 10 | 58±3.5 | 3.6 |
| | | | | 100 | 60±2.9 | 2.9 |

Table 3.4 LODs and LOQs of trichlorfon in spiked *Sebastes schlegelii* samples

| Compound | Serum | | Muscle | | Liver | |
|---|---|---|---|---|---|---|
| | LOD | LOQ | LOD | LOQ | LOD | LOQ |
| TCF | 0.20 | 0.61 | 0.31 | 0.94 | 0.14 | 0.42 |

### 3.3.2 Depletion of TCF from samples

The mean concentrations of TCF against time in serum of ten *S. schlegelii* at each time point, are presented in Fig 3.1-3.4 & Table 3.5-3.8 during the administration of the TCF 30 and 150 mg/kg bw at 15 and 25°C. Following the 30 mg/kg bw, the serum concentration-time profile raised a to a peak 98.76 ㎍/㎖ ($C_{max}$) at 1h ($T_{max}$), elimination half-time ($T_{1/2}$) of 6.1 h at 15°C and 479.63 ㎍/㎖ ($C_{max}$) at 0.5h ($T_{max}$), elimination half-time ($T_{1/2}$) of 6.86 h at 25°C. Following the 150 mg/kg bw, the serum concentration-time profile raised a to a peak 253.42 ㎍/㎖ ($C_{max}$) at 1h ($T_{max}$), elimination half-time ($T_{1/2}$) of 7.34 h at 15°C and 301.49 ㎍/㎖ ($C_{max}$) at 1h ($T_{max}$), elimination half-time ($T_{1/2}$) of 4.54 h at 25°C. Following the 30 mg/kg bw, the muscle concentration-time profile raised a to a peak 607.23 ㎍/㎖ ($C_{max}$) at 3h ($T_{max}$), elimination half-time ($T_{1/2}$) of 35.3 h at 15°C and 1695.2 ㎍/㎖ ($C_{max}$) at 0.5h ($T_{max}$), elimination half-time ($T_{1/2}$) of 25.14 h at 25°C. Following the 150 mg/kg bw, the muscle concentration-time profile raised a to a peak 1248.47 ㎍/㎖ ($C_{max}$) at 3h ($T_{max}$), elimination half-time ($T_{1/2}$) of 20.99 h at 15°C and 1264.63 ㎍/㎖ ($C_{max}$) at 3h ($T_{max}$), elimination half-time ($T_{1/2}$) of 19.2 h at 25°C. Following the 30 mg/kg bw, the liver concentration-time profile raised a to a peak 632.02 ㎍/㎖ ($C_{max}$) at 1h ($T_{max}$), elimination half-time ($T_{1/2}$) of 15.36 h at 15°C and 1742.92 ㎍/㎖ ($C_{max}$) at 1h ($T_{max}$), elimination half-time ($T_{1/2}$) of 46.34 h at 25°C. Following the 150 mg/kg bw, the serum concentration-time profile raised a to a peak 745.52 ㎍/㎖ ($C_{max}$) at 1h ($T_{max}$), elimination half-time ($T_{1/2}$) of 51.45 h at 15°C and 923.03 ㎍/㎖ ($C_{max}$) at 0.5h ($T_{max}$), elimination half-time ($T_{1/2}$) of 38.16 h at 25°C (Table 3.9-11).

Table 3.5 Concentration of TCF residues in *Sebastes schlegelii* tissues after post dipping

| *Sebastes schlegelii* | After post dipping (hour) | Serum (μg/kg) | Muscle (μg/kg) | Liver (μg/kg) |
|---|---|---|---|---|
| 30 mg/kg bw at 15℃ for 30min | 0.5 | 77.605±2.295 | 194.365±4.278 | 183.193±15.595 |
| | 1 | 98.764±0.933 | 401.786±12.202 | 632.029±31.339 |
| | 3 | 82.978±3.228 | 606.861±20.304 | 350.113±4.936 |
| | 6 | 52.489±0.95 | 272.829±14.478 | 154.254±5.213 |
| | 12 | 39.258±2.688 | 116.012±6.616 | 101.89±2.618 |
| | 24 | 36.958±1.063 | 71.175±4.257 | 45.754±1.976 |
| | 48 | 7.166±0.24 | 74.142±2.589 | 17.091±2.509 |
| | 96 | ND | 21.183±2.031 | 1.813±0.323 |
| | 168 | ND | 6.969±0.709 | ND |
| | 336 | ND | ND | ND |

Table 3.6 Concentration of TCF residues in *Sebastes schlegelii* tissues after post dipping

| *Sebastes schlegelii* | After post dipping (hour) | Serum (μg/kg) | Muscle (μg/kg) | Liver (μg/kg) |
|---|---|---|---|---|
| 30 mg/kg bw at 25℃ for 30min | 0.5 | 479.637±12.733 | 1815.151±84.299 | 1144.652±87.504 |
| | 1 | 159.633±22.009 | 1000.404±12.275 | 1742.923±46.02 |
| | 3 | 69.496±2.939 | 488.747±21.786 | 522.952±19.793 |
| | 6 | 62.652±2.712 | 301.604±8.21 | 269.053±16.221 |
| | 12 | 26.576±2.433 | 233.961±3.021 | 123.1±13.23 |
| | 24 | 5.398±1.014 | 103.795±4.58 | 61.42±4.187 |
| | 48 | 0.862±0.629 | 52.963±2.349 | 20.514±3.106 |
| | 96 | ND | 15.527±1.38 | 6.765±1.106 |
| | 168 | ND | 0.942±0.404 | 3.246±0.151 |
| | 336 | ND | ND | ND |

Table 3.7 Concentration of TCF residues in *Sebastes schlegelii* tissues after post dipping

| *Sebastes schlegelii* | After post dipping (hour) | Serum (μg/kg) | Muscle (μg/kg) | Liver (μg/kg) |
|---|---|---|---|---|
| 150 mg/kg bw at 15℃ for 30min | 0.5 | 206.524±2.733 | 941.775±14.494 | 667.432±36.77 |
| | 1 | 235.427±14.296 | 1258.843±41.667 | 746.521±29.08 |
| | 3 | 173.068±2.061 | 1325.963±40.754 | 620.421±10.206 |
| | 6 | 156.199±2.422 | 455.373±20.802 | 532.253±6.058 |
| | 12 | 53.698±2.77 | 335.866±11.118 | 432.707±11.055 |
| | 24 | 41.234±1.475 | 157.904±9.846 | 383.082±13.702 |
| | 48 | 2.308±0.242 | 85.528±10.227 | 304.024±8.311 |
| | 96 | ND | 23.510±1.771 | 127.263±9.025 |
| | 128 | ND | 7.083±0.244 | 30.96±2.015 |
| | 336 | ND | ND | 7.656±3.013 |

Table 3.8 Concentration of TCF residues in *Sebastes schlegelii* tissues after post dipping

| *Sebastes schlegelii* | After post dipping (hour) | Serum (μg/kg) | Muscle (μg/kg) | Liver (μg/kg) |
|---|---|---|---|---|
| 150 mg/kg bw at 25℃ for 30min | 0.5 | 266.69±9.034 | 716.470±10.165 | 923.033±88.286 |
| | 1 | 301.495±7.38 | 1014.394±7.898 | 650.243±6.332 |
| | 3 | 190.461±3.803 | 1298.366±35.326 | 386.956±3.65 |
| | 6 | 97.13±0.961 | 318.832±5.816 | 199.51±14.257 |
| | 12 | 65.09±2.027 | 244.963±4.327 | 123.77±6.251 |
| | 24 | 5.572±0.94 | 94.029±2.043 | 86.088±1.228 |
| | 48 | ND | 53.173±2.326 | 58.142±2.091 |
| | 96 | ND | 23.515±1.811 | 32.28±0.44 |
| | 168 | ND | 13.574±0.309 | 6.339±0.528 |
| | 336 | ND | ND | ND |

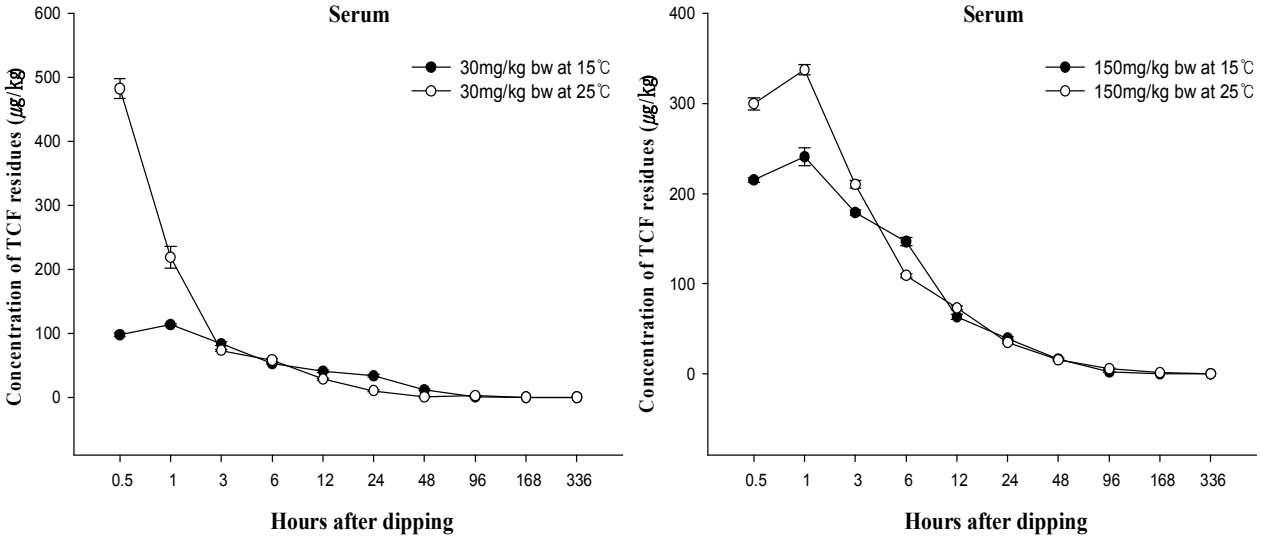


Fig 3.1 Depletion of TCF from *S. schlegelii* serum after the administration of 30 and 150 mg/kg bw at 15 and 25°C

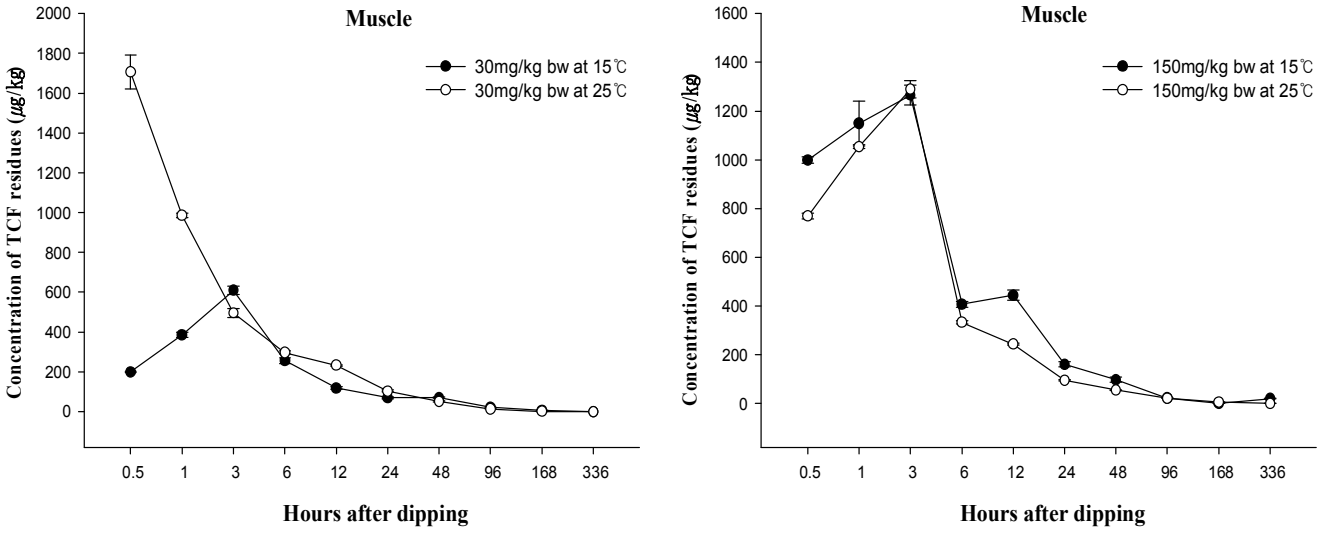


Fig 3.2 Depletion of TCF from *S. schlegelii* muscle after the administration of 30 and 150 mg/kg bw at 15 and 25°C.

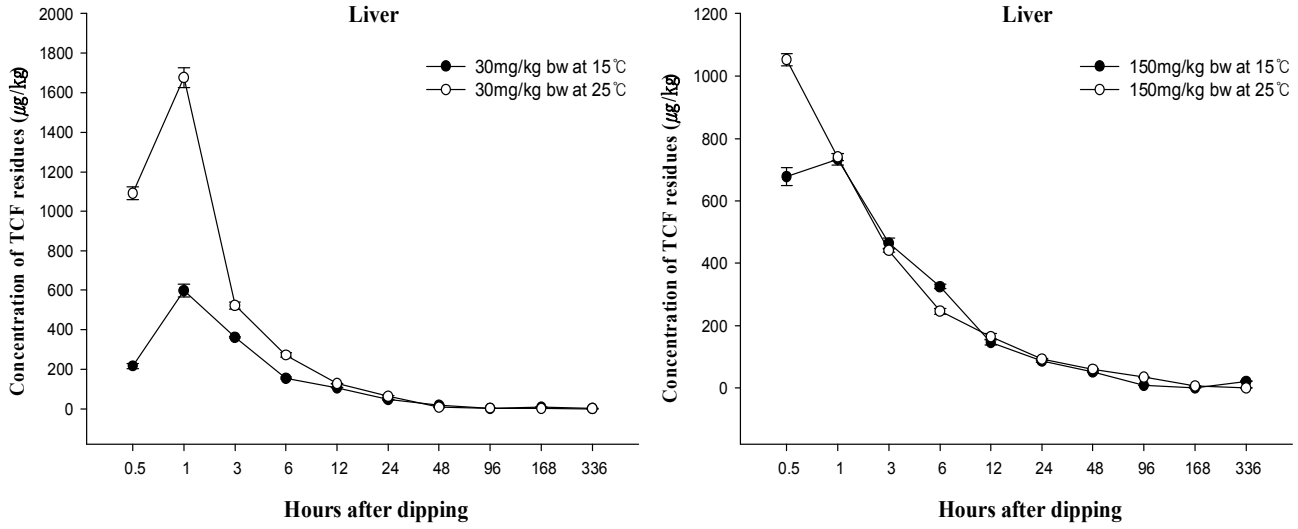


Fig 3.3 Depletion of TCF from *S. schlegelii* liver after the administration of 30 and 150 mg/kg bw at 15 and 25°C.

Table 3.9 Pharmacokinetic parameters of TCF in serum from *Sebastes schlegelii* after dipping concentration of 30 and 150 mg/kg at different temperatures (15 and 25°C)

| Parameters | Unit | 30ppm | | 150ppm | |
|---|---|---|---|---|---|
| | | 15 | 25 | 15 | 25 |
| $C_{max}$ | μg/mℓ | 98.76 | 479.63 | 253.42 | 301.49 |
| $T_{max}$ | h | 1 | 0.5 | 1 | 1 |
| $\lambda_z$ | 1/h | 0.113 | 0.1 | 0.09 | 0.152 |
| $t_{1/2}$ | h | 6.10 | 6.86 | 7.34 | 4.54 |
| $AUC_{0-t}$ | μg/mℓ*h | 1882.75 | 1241.72 | 2786.30 | 2112.24 |
| $AUC_{0-\infty}$ | μg/mℓ*h | 1882.86 | 1250.26 | 2810.75 | 2113.71 |
| $AUMC_{0-\infty}$ | μg/mℓ*$h^2$ | 34812.58 | 8725.31 | 32235.85 | 14140.40 |
| $MRT_{0-\infty}$ | h | 18.489 | 6.978 | 11.468 | 6.689 |
| $V_z$ | mℓ/g | 0.14 | 0.237 | 0.56 | 0.464 |
| Cl | mℓ/g/h | 0.015 | 0.023 | 0.05 | 0.07 |

Table 3.10 Pharmacokinetic parameters of TCF in muscle from *Sebastes schlegelii* after dipping concentration of 30 and 150 mg/kg at different temperatures (15 and 25℃)

| Parameters | Unit | 30ppm | | 150ppm | |
|---|---|---|---|---|---|
| | | 15 | 25 | 15 | 25 |
| $C_{max}$ | μg/mℓ | 607.23 | 1695.20 | 1248.47 | 1264.63 |
| $T_{max}$ | h | 3 | 0.5 | 3 | 3 |
| $\lambda_z$ | 1/h | 0.019 | 0.027 | 0.033 | 0.036 |
| $t_{1/2}$ | h | 35.30 | 25.14 | 20.99 | 19.2 |
| $AUC_{0-t}$ | μg/mℓ*h | 9644.11 | 11357.12 | 18472.95 | 13340.88 |
| $AUC_{0-\infty}$ | μg/mℓ*h | 9974.35 | 11426.09 | 18530.23 | 13357.86 |
| $AUMC_{0-\infty}$ | μg/mℓ*$h^2$ | 413936.14 | 278884.96 | 462635.89 | 308460 |
| $MRT_{0-\infty}$ | h | 41.5 | 24.40 | 24.96 | 23.09 |
| $V_z$ | mℓ/g | 0.153 | 0.095 | 0.245 | 0.311 |
| Cl | mℓ/g/h | 0.003 | 0.002 | 0.008 | 0.011 |

Table 3.11 Pharmacokinetic parameters of TCF in liver from *Sebastes schlegelii* after dipping concentration of 30 and 150 mg/kg at different temperatures (15 and 25°C)

| Parameters | Unit | 30ppm | | 150ppm | |
|---|---|---|---|---|---|
| | | 15 | 25 | 15 | 25 |
| $C_{max}$ | μg/mℓ | 632.02 | 1742.92 | 746.52 | 923.03 |
| $T_{max}$ | h | 1 | 1 | 1 | 0.5 |
| $\lambda_z$ | 1/h | 0.045 | 0.014 | 0.0134 | 0.018 |
| $t_{1/2}$ | h | 15.365 | 46.34 | 51.45 | 38.16 |
| $AUC_{0-t}$ | μg/mℓ*h | 4850.42 | 8743.81 | 38941.84 | 10061.13 |
| $AUC_{0-\infty}$ | μg/mℓ*h | 4890.61 | 8960.85 | 39510.20 | 10410.14 |
| $AUMC_{0-\infty}$ | μg/mℓ*$h^2$ | 76856.11 | 198498.63 | 2564135.42 | 462479.54 |
| $MRT_{0-\infty}$ | h | 15.715 | 22.151 | 64.89 | 44.425 |
| $V_z$ | mℓ/g | 0.135 | 0.223 | 0.281 | 0.793 |
| Cl | mℓ/g/h | 0.006 | 0.003 | 0.003 | 0.014 |

### 3.3.3 Withdrawal time calculation

The withdrawal period was estimated for the sum of the TCF concentrations considering a 95% and 99% confidence. The data were linerarized by plotting the TCF residues concentration as a function of a time, as shown in Fig.3.5 & 3.6. The obtained figure confirmed the log-normal distribution profile. The depletion regression line and the line of upper confidence (95%), the small circles in vertical direction indicate the observed TCF concentrations, the horizontal line represents the proposed MRL level, and the two vertical lines indicated the withdrawal period. Following the 30 mg/kg bw, the muscle sample were calculated as 23.97 days at 15°C and 14.879 days at 25°C. Following the 150 mg/kg bw, the muscle sample were calculated as 15.21 days at 15°C and 13.54 days at 25°C.

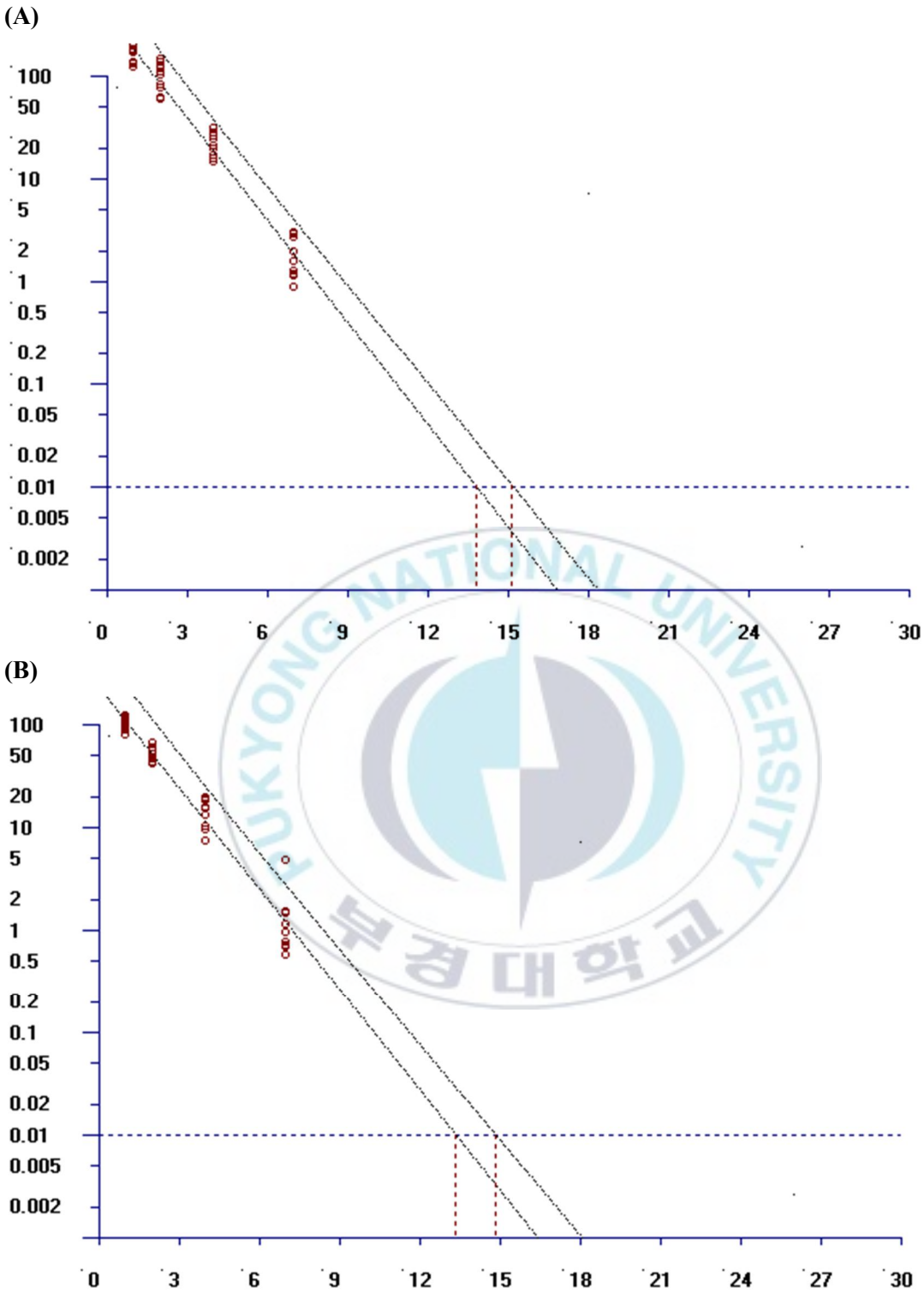


Fig 3.5 Plot of withdrawal period calculation of TCF for *Sebastes schlegelii* muscle at 30 mg/kg at 15 (A) and 25°C (B). The depletion regression line and the line of upper confidence (95%) are presented [~~~~], the small circles in vertical direction [°°°°] indicate the observed TCF concentrations, the horizontal line [----] represents the proposed MRL level and the two vertical lines [----] indicates the withdrawal period

**(A)**

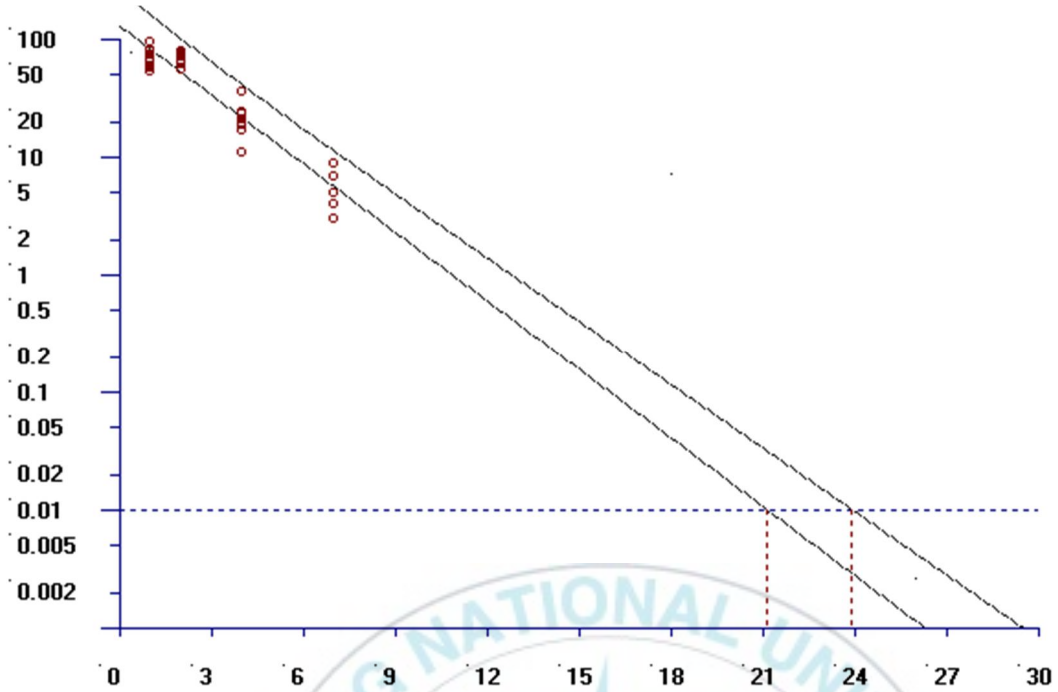


**(B)**

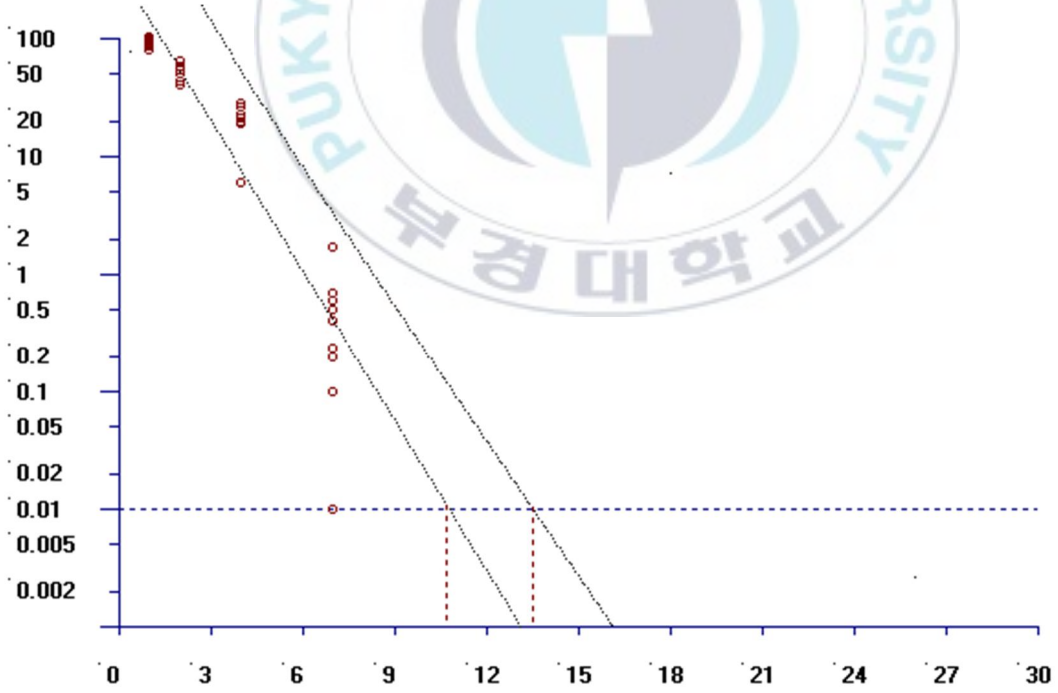


Fig 3.6 Plot of withdrawal period calculation of TCF for *Sebastes schlegelii* muscle at 150 mg/kg at 15 (A) and 25°C (B) The depletion regression line and the line of upper confidence (95%) are presented [~~~~], the small circles in vertical direction [°°°°] indicate the observed TCF concentrations, the horizontal line [----] represents the proposed MRL level and the two vertical lines [----] indicates the withdrawal period

### 3.4 Discussion

There is few number of investigations for TCF depletion in farmed fish. TCF has been authorized by the National Institute of Fisheries Science (NIFS) in Korea. Although it has been widely used during the last years in Korea aquaculture, there has been no report concerning the depletion study and withdrawal period estimation of this antibiotics after dipping administration in seawater fish species such as black rockfish. This gap in knowledge was one of the motivating factor for the conduct of our study.

According to the EU, TCF is not included in the Annex I positive list to Directive 91/414 EEC since September 2006. Consequently, TCF is no longer sold and used across Europe. TCF is banned in EU (Regulation (EC) 689/2008). Norway has been discontinued license since 1996 and Japan is prohibited for sea water applications. The compound had also see use in Chile, but has been displaced by more recently developed drugs. But product as active commencement is used in fish cultures in Brazil, indiscriminately, in high concentrations, and without specialized technical method. The lack of knowledge of pesticides may result in a serious problems related to environment.

We proposed the MRL using the JECFA Tool. We suggest the MRL for TCF as 2 μg/kg throughout the 30 and 150 mg/kg bw at two different temperatures. We get the very low MRL, so we adjust the MRL for fish as 20ug/kg which apply to aquatic organism many countries.

During our investigation in *S. schlegelii*, the leading species in Korea aquaculture, TCF is muscle and liver reached their maximum values on day 1 to 3hours and declined rapidly below their MRLs on day 14 days. On day 15, the concentrations of drug residues reached their LOQ levels. The kinetic profile of TCF was similar in serum, muscle and liver. The calculation model for the statistical determination of the withdrawal periods is based on accepted pharmacokinetic principles. According to the pharmacokinetic compartment model, the relationship between drug concentration and time through all phases of absorption, distribution, and elimination is usually described by multi-exponential mathematical terms. However, the terminal elimination of a TCF from muscle, or residue depletion, follows a non-compartment model in most cases and is sufficiently described by one exponential term.

Therefore, the depletion curve for TCF was analyzed assuming the non-compartment model of elimination kinetics.

In the present study, ten fish were evaluated for each withdrawal periods. The dispersion of the results among fish from the same withdrawal periods is influenced by the number of fish used in our experiment and by the administration route used to provide the prescription. When all the fish in a determined group are exposed to TCF, there is natural intakes among the individuals, which promotes similar intakes among them.

The FDA (2006) proposes excluding from the calculation any observed data residue that is below the limit of detection (LOD). However, this approach prejudices the regression line. To avoid prejudicing the slope and intercept, each data point of the regression line should derive from the equal number of repeated sample values. Therefore, it is advised to set the data that are below the LOD or LOQ to one-half of the respective limit (EMEA, 1995).

The first attempt for the withdrawal period estimation of TCF in farmed fish was reported by Brandal and Egidius (1979). The authors investigated the depletion of TCF from muscle of salmonids, no chemical residue were found in tissue 12 days after the treatment. For treatment with TCF, a 21 withdrawal period is advised, before consumption.

In aqueous solution, TCF is transformed in dichlorvos (DDVP), which is a powerful cholinesterase inhibitor. The DDVP is currently used in the UK, Ireland and Chile. The reported withdrawal period for DDVP ranged from 4 (UK) to 14d (Norway) (Roth, 2000).

We investigated the depletion of TCF in seawater fish. Two trials were carried out at two different water temperatures (15 and 25°C). In both trials, the fish were administered 30 and 150 mg/kg bw for 30min. No detectable concentrations of the TCF remained in muscle 21days after treatment. Nevertheless, metabolites of the antibiotics were not investigated.

No studies have been performed for TCF depletion in *Sebastes schlegelii*. It is difficult to compare experimental data because procedures such as distribution, depletion, elimination, and metabolism of the TCF depend on the experimental conditions (e.g., water temperature, tank, pH, feed, size), the

dosage regimen (treatment period and medication route), and fish species, and fish body weight. There are so many factors to extrapolate kinetic information from seawater and/or freshwater species to cold/warm fish species could make wrong results.

The high temperature is one of the major reasons that could explain the longer withdrawal periods. It is well known that high temperature makes increase xenobiotic metabolism and elimination rates, because of the increase in bile excretion rates (Curtis et al., 1986), membrane dynamics (Miranda & Hazel, 2002) and increased rate activity of xenobiotic detoxification enzymes (Kleinow et al., 1987). Especially, a major part of these differences could be contribute to the different dosage administration, as well as the different fish species, and different fish size.

Evaluating the data from our study, we would suggest a withdrawal period of 24 days for the TCF in *S. schlegelii* muscle tissues after administration dipping. This suggestion might be helped to farmers when the using the TCF to control sea-lice, applied to protect human health.

### 3.5 References


Burridge L., Weis J.S., Cabello F., Pizarro J. & Bostick K. 2010. Chemical use in salmon aquaculture: a review of current practices and possible environmental effects. Aquaculture 306, 7–23

Brandal P.O. & Egidius E. 1979. Treatment of salmon lice (Lepeophtheirus salmonis Krøyer, 1838) with Neguvon®—description of method and equipment. Aquaculture 18, 183-188.

Chang Y.S. & Heo G.J. 2008. Acute and Subacute Toxicity of Trichlorfon in Blacktetra (*Gymnocorymbus ternetzi*). Journal of Biomedical Research 9, 43–48.

Curtis L.R., Kemp C.J. & Svec A.V. 1986. Biliary excretion of $^{14}$C-taurocholate by rainbow trout is stimulated at warmer acclimation temperature. Comparative Biochemistry and Physiology C 84, 87–90.

EMEA, European Agency for the Evaluation of Medicinal Products Veterinary Medicines Evaluation Unit. 1995. Committee for veterinary medicinal products. Note for guidance: approach towards harmonization of withdrawal periods, EMEA / CVMP / 036 / 95. Available athttp://www.emea.europa.eu/pdfs/vet/swp/003695en.pdf (active as of March 01, 2010).

EMEA, The European Agency for the Evaluation of Medicinal Products, Veterinary Medicines Evaluation Unit. 1995a. Note for Guidance: Approach towards harmonization of withdrawal periods. EMEA/CVMP'/036/95 FINAL.

Eraslan G., Kanbur M., Silici S. & Karabacak M. 2010. Beneficial effect of pine honey on trichlorfon induced some biochemical alterations in mice. Ecotoxicology and Environmental Safety 73, 1084–1091.

European Commission. 2005a. Pesticide residue. <http://europa.eu.int/comm./food/fs/ph-ps/pest/index-en.htm> Accessed 20.10.2005.

European Commission. 2005b. Monitoring of pesticide residues in products of plant origin in the European Union, Norway and Iceland. Report 2001. <http://europa.eu.int/comm./food/fvo/specialreports/pesticides-index-en.htm> Accessed 30.10.2007.

FAO/WHO 2004, 2004 FAO/WHO. 2004.<http://www.codexalimentarius.net> Accessed 30.10.2007.

FDA. 2000. FDA Task Force on Antimicrobial Resistance: key recommendations and report, Washington, DC. FDA, Washington, DC. http://www .fda.gov/downloads/ForConsumers/ConsumerUpdates/UCM143458.pdf.

Guimarães A.T.B., De Assis H.S. & Boeger W. 2007. The effect of trichlorfon on acetylcholinesterase

activity and histopathology of cultivated fish Oreochromis niloticus. Ecotoxicology and Environmental Safety 68, 57–62.

Hekman P. 2004. Withdrawal-Time Calculation Program-WT1.4. BRD Agency for the Registration of Veterinary Medicinal Products, Wageningen, The Netherlands 1-8.

Horne M.T. & Robertson D.A. 1987. Economics of vaccination against enteric redmouth disease of salmonids. Aquaculture Research 18, 131–137.

Kleinow K.M., Melancon M.J. & Lech J.J. 1987. Biotransformation and induction: implications for toxicity, bioaccumulation and monitoring of environmental xenobiotics in fish. Environmental Health Perspectives 71, 105–119.

Mattson N.S., Egidius E. & Solbakken J.E. 1988. Uptake and elimination of (methyl-14C) trichlorfon in blue mussel (*Mytilus edulis*) and European oyster (*Ostrea edulis*)—impact of NeguvonR disposal on mollusc farming. Aquaculture 71, 9-14.

Mehl A., Schanke T.M., Torvik A. & Fonnum F. 2007. The effect of trichlorfon and methylazoxymethanol on the development of guinea pig cerebellum. Toxicology and applied pharmacology 219, 128-135.

Miranda E.J. & Hazel J.R. 2002. The effect of acclimation temperature on the fusion kinetics of lipid vesicles derived from endoplasmic reticulum membranes of rainbow trout (*Oncorhynhus mykiss*) liver. Comparative Biochemistry and Physiology A 131, 275–286.

National Institute of Fisheries Science (NIFS): Catalog of aquaculture drugs in 2016, pp 101~102, NIFS, Ministry of Oceans and Fisheries, 2016. https://www.nifs.go.kr/adms/index.ad

Rigos G. & Troisi G.M. 2005. Antibacterial agents in Mediterranean finfish farming: a synopsis of drug pharmacokinetics in important euryhaline fish species and possible environmental implications. Reviews in Fish Biology and Fisheries 15, 53–73.

Roth M. 2000. The availability and use of chemotherapeutic sea lice control products. Contributions to Zoology 69, 109-118.

Schaperclaus W. 1992. Therapy of fish disease. In: Fish Diseases. AA Balkema/Rotterdam, Netherlands, 210–296.

Sievers G., Palacios P., Inostroza R. & Dolz H. 1995. Evaluation of the toxicity of 8 insecticides in *Salmo salar* and the in vitro effects against the isopode parasite, *Ceratothoa gaudichaudii*, Aquaculture 134, 9–16.

Xu W., Liu W., Shao X., Jiang G. & Li X. 2012. Effect of trichlorfon on hepatic lipid accumulation in crucian carp *Carassius auratus gibelio*. Journal of aquatic animal health 24, 185–194.

Yeh S.P., Sung T.G., Chang C.C., Cheng W. & Kuo C.M. 2005. Effects of an organophosphorus insecticide, trichlorfon, on hematological parameters of the giant freshwater prawn, *Macrobrachium rosenbergii* (de Man). Aquaculture 243, 383–392.

Zhang Y., Huo M., Zhou J. & Xie S. 2010. PKSolver: An add-in program for pharmacokinetic and pharmacodynamic data analysis in Microsoft Excel. Computer methods and programs in biomedicine, 99, 306-314.

# Conclusion

Cytochrome P450 (CYP) is the important protein of the superfamily containing heme as a cofactor and metabolized the number of the endogeneous and exogeneous chemicals. Also, CYP450 enzyme associated with the phase I metabolism of the drugs and other chemicals. The purpose of this study is to determine the drug metabolism system associated with the exposure of benzo[a]pyrene and trichlorfon in rockfish (*Sebastes schlgelii*) and to clone the sequence of CYP1 family (CYP1A, CYP1B, CYP1C1, CYP1C2). CYP1A showed the highest expressed in liver, heart, kidney, CYP1B in gill, CYP1C1 and CYP1C2 showed generally similar patterns of expression levels among tissues, especially, in the muscle. B[a]P induced the high expression of CYP1 family genes in all 4 tissues (gill, liver, kidney, and spleen). Hepatic microsomal CYP1A protein levels increased following the exposure of B[a]P concentration using ELISA and EROD assay which is supported by the results of the IHC. Exposure of B[a]P induced the expression levels of CYP1 family, especially, the microsomal CYP1A protein significantly increased compared to the vehicle control.

To control planktonic invertebrates and parasites, five pesticides can use in aquaculture from Korea., Trichlorfon (TCF) is the organophosphorus pesticides that is used to eradicate ectoparaistes such as anchorworms, lice, gill flukes and copepods in a wide range of fish species. But the MRL and withdrawal periods after administration of TCF have not been established in fish. Therefore, we determined TCF residues in serum, muscle and liver using LC-MS/MS and the kinetic profiles of $C_{max}$, $T_{max}$, $T_{1/2}$ were analyzed by fitting to a non-compartmental model with PKsolver program. We calculated the MRL and withdrawal period of TCF by JECFA tool and WT 1.4. To evaluate the effects of TCF (30 and 150 mg/kg bw) in *Sebastes schlegelii*, we studied the oxidative stress, neurotoxicity, cortisol level, drug conjugation, and drug metabolism including phase I & phase II at two different temperatures (15 and 25°C). We suggested the 0.01 mg/kg of MRL and 21 withdrawal periods for TCF in *S. schlegelii* muscle tissues from the calculation of TCF residue data. This suggestion might be helped to farmers when the using the TCF to control sea-lice, applied to protect human health

# Acknowledgements

정말 많은 노력과 인내가 담겨있는 논문입니다. 많이 힘들었고, 울었고, 버텼고, 이겨냈습니다.

철모르는 학부 시절, 3학년 2학기(2012년)에 약을 배우고 싶다는 생각에 약리방에 들어오게 되었고, 잠깐 미국으로 다녀오기도 했습니다. 아마 그때 다른 길을 선택했다면, 저는 지금 이 학위논문을 쓰지 못했을 것입니다. 석사2년과 박사3년, 총 5년의 시간 동안 즐거운 시간도 있었지만, 힘든시간이 상대적으로 더 많았습니다. 아무도 없는 실험실에서 혼자 실험하고, 혼자 헤매고, 혼자 답을 찾고, 혼자 실험준비를 하였습니다. 예상치못한 강의준비와 논문투고 등 많은 일이 있었지만, 저를 여기까지 있게 해주신 많은 분들 덕분에 본 논문이 나오게 되었습니다.

스스로의 힘으로 이룬 학위가 아님을 잘 알기에 한분 한분 고마운 분들께 직접 찾아가 고맙다는 말씀 전해드리겠습니다. 그리고 고마운 마음을 말로 다 표현할 수 없지만 작은 지면을 통해 마지막으로 감사의 인사를 드리고자 합니다.

학부시절부터 대학원생활동안 저를 지탱해주신 지도교수 정준기 교수님과 멋진 제2의 지도교수 이형호 교수님 두분께 깊은 감사의 인사를 드립니다. 앞으로 더 발전된 모습으로 이 은혜를 갚아나갈게요. 정말 진심으로 감사드립니다.

그리고 저에게 핵심적이고 사실적인 조언을 해주셨던 김기홍교수님, 김도형교수님, 실험잘되가냐고 늘 물어보시는 정현도 교수님께도 감사의 인사드립니다. 또한 바쁘신 와중에 논문 심사를 위해 힘써주시고 시간 내주신 군산대학교 박관하 교수님께도 심심한 감사의 말씀 올립니다.

약리방선배님들.. 먼저 김무상박사님. 항상 윗방과 우리방부터 생각해주시고 많이 가르켜주셔서 감사합니다. 박사님 같은 분이 저의 선배님으로 계셨기에, 정말 행운이라고 생각합니다. 그리고 약리방 1호 서정수박사님. 박사님 덕분에 수산용의약품에 대해서 알게됐고, 덕분에 약리학 전공으

로 올 수 있게 되었습니다. 약리방 2호 김나영박사님. 저의 영원한 멘토이자 병리연구과의 바리스타! 앞으로도 잘 부탁드립니다. 많이 배우겠습니다. 그리고 까칠하지만 츤데레인 용자님, 워킹맘 혜인이언니, 저 쓰라고 용돈 챙겨주신 미정이언니.. 오빠와 언니들이 있었던 그 시절이 저에게 약리방 황금기였습니다. 다신 못 올 순간이겠죠. 그립네요. 오싸 오현석선배, 약리방 고정 손님 영림선배도 너무 고마워요.  모두 다 선배님들 덕분에 본 논문이 나올 수 있었습니다. 앞으로도 초심을 잃지않는 연구사가 되겠습니다.

저의 첫 직장인 국립수산과학원 병리연구과 연구사 선배님들, 조미영연구관님, 김명석 연구관님, 정승희 과장님께 감사의 인사드립니다. 앞으로 질병free, 건강한 양식수산물을 국민에게 공급하는 깊은 연구를 하겠습니다.

우리 약리방 캡스톤 zi존약리. 준우는 예방방가서 열심히 할거야. 상진이는 하고 싶은게 많다고 했는데 나중이 더 기대된다.  그리고 현호, 승현, 주안이 너네들이 누나방 두드리는 그 순간을 절때 잊지못하겠네. 너네들 덕분에 내가 믿고 나올 수 있었어. 고맙다. 내가 많이 도와줄게! 다들 멋진 인생을 살길 바래. 생공 준영이도 너무 고맙고, 너가 있어 윗방이 든든하네! 고혜진박사님, 김찬희박사님 감사합니다! 착한 혜영이언니, 언니는 더 잘되실거에요! 응원합니다

궁금한거 있으면 친절히 알려주신 기방 민선이언니, 준성이오빠, 정인이.. 병리조직 전문가이신 병리방 보성이오빠,경식이,지원이.. 힘내라고 늘 응원해준 진단방 준규오빠, 늘 밝게 인사해준 우주오빠, 먼저 박사졸업하신 영철이오빠, 유일하게 말터놓을 수 있는 수권방 태준이오빠, 과학원에 잠깐 실험하러 갔을때 많이 도와준 예방방 원경이오빠.. 모든 실험실 방장님들과 대학원생 후배님들 진심으로 응원하고 사랑합니다. 모두 다 꽃길만 걷길 바랄게요

우리 10동기들..짱친 하정훈 주문관님(feat. 김이슬 주무관님) 앞으로 공직생활 잘 부탁합니다. 더 이뻐진 소미, 곧 약국차릴 가은이, 이쁜 신혼생활중인 경은이, 인천공항 검역담당 수진이, 인천에

서 물고기키우고 있는 황인기 연구사님, 서울에서 열심히 일하고 있는 준성이오빠, 인천에서 연구하고 있는 경식이, 그리고 현호, 권총, 영현이, 영록이.. 우리가 1학년때 만난게 얼마 전 같은데 벌써 9년차네. 다들 좋은 자리에 있어서 다행이고 날 응원하고 실험실에 한번씩 놀러와줘서 너무 고마웠어. 잊지못할거야.

엄마 아빠! 항상 뒤에서 믿고 지켜봐 주셔서 여기까지 왔습니다. 사랑하고 정말정말 감사해요. 믿고 지켜봐 주신 만큼 앞으로 더 열심히 살겠습니다. 사랑하는 내 동생, 지금은 아직 목표가 없어 방황중이지만 어떤 일이든 묵묵히 하는 성격이니 방향만 잡는다면 잘해나갈 거라 믿는다. 더 많은 경험하고 얼른 목표를 세웠으면 좋겠구나.

마지막으로 내 짝 신후오빠에게 ,, 6년동안 내 옆을 지켜줘서 고마워. 혼자 실험할 때 위험하다고 옆에서 지켜주고, 걱정해주고, 물고기도 함께 해부해주고, 여기에 적기에 너무많다 ㅋㅋ..진짜 든든한 나의 버팀목이 되어줘서 고마워. 오빠 덕분에 여기까지 왔어. 오빠가 아니었으면, 박사학위도, 연구사도 되지 못했어. 진심으로 너무 고맙고 앞으로도 잘 부탁해. 나의 소울메이트

정말 이 모든 분들이 저를 응원하고 도와주지 않았다면 제가 논문을 쓸 수 있었을까 다시 한번 생각합니다. 끝으로 진심으로 저를 아껴주신 모든 분들께 감사의 인사 드리며 저의 노력이 담긴 이 논문을 바칩니다.

2019.01.01

새해를 바라보며.